

TOUGHENING OF POLYLACTIDE BY BLENDING WITH VARIOUS
ELASTOMERIC MATERIALS

A THESIS SUBMITTED TO
THE GRADUATE SCHOOL OF NATURAL AND APPLIED SCIENCES
OF
MIDDLE EAST TECHNICAL UNIVERSITY

BY

YELDA MEYVA

IN PARTIAL FULFILLMENT OF THE REQUIREMENTS
FOR
THE DEGREE OF MASTER OF SCIENCE
IN
POLYMER SCIENCE AND TECHNOLOGY

AUGUST 2014

Approval of the thesis:

**TOUGHENING OF POLYLACTIDE BY BLENDING WITH VARIOUS
ELASTOMERIC MATERIALS**

submitted by **YELDA MEYVA** in partial fulfillment of the requirements for the degree of **Master of Science in of Polymer Science and Technology Department, Middle East Technical University** by,

Prof. Dr. Canan Özgen
Dean, Graduate School of **Natural and Applied Sciences**

Prof. Dr. Teoman Tinçer
Head of Department, **Polymer Science and Technology**

Prof. Dr. Cevdet Kaynak
Supervisor, **Metallurgical and Materials Eng. Dept., METU**

Examining Committee Members:

Prof. Dr. Göknur Bayram
Chemical Engineering Dept., METU

Prof. Dr. Cevdet Kaynak
Metallurgical and Materials Engineering Dept., METU

Assist. Prof. Dr. İrem Erel Göktepe
Chemistry Dept., METU

Assist. Prof. Dr. Y. Eren Kalay
Metallurgical and Materials Engineering Dept., METU

Assist. Prof. Dr. Erhan Bat
Chemical Engineering Dept., METU

DATE: 28.08.2014

I hereby declare that all information in this document has been obtained and presented in accordance with academic rules and ethical conduct. I also declare that, as required by these rules and conduct, I have fully cited and referenced all material and results that are not original to this work.

Name, Last Name : Yelda Meyva

Signature :

ABSTRACT

TOUGHENING OF POLYLACTIDE BY BLENDING WITH VARIOUS ELASTOMERIC MATERIALS

Meyva, Yelda

M. S., Department of Polymer Science and Technology

Supervisor: Prof. Dr. Cevdet Kaynak

August 2014, 102 pages

The purpose of the first part of this thesis was to investigate influences of three different ethylene copolymers on the toughness and other properties of very brittle biopolymer PLA (polylactide). For this aim, PLA was melt blended by twin-screw extruder with various amounts of ethylene vinyl acetate (EVA), ethylene methyl acrylate (EMA) and ethylene-*n*-butyl acrylate-glycidyl methacrylate (EBA-GMA). SEM and DSC analyses indicated that these ethylene copolymers were thermodynamically immiscible with phase separation in the form of 1-5 micron sized round domains in the PLA matrix. Rubber toughening mechanisms of EVA, EMA and EBA-GMA were very effective to improve ductility and toughness of PLA significantly. Depending on the type and content of the ethylene copolymers, the highest increases in % elongation at break, Charpy impact toughness and G_{IC} fracture toughness values of PLA were as much as 160%, 320% and 158%, respectively. Although there were no detrimental effects of using EVA, EMA and EBA-GMA on the thermal properties of PLA, they resulted in certain level of reductions in stiffness, strength and hardness values.

The purpose of the second part of thesis was again to improve toughness of inherently very brittle PLA without sacrificing other mechanical and thermal properties, so that PLA could be used also in engineering applications. For this

purpose, PLA was blended with two different thermoplastic elastomers; TPU (thermoplastic polyurethane) and BioTPE (biomass based thermoplastic polyester) in various amounts. SEM analysis again indicated that TPU and BioTPE were immiscible forming fine and uniform round domains in the PLA matrix. It was revealed that rubber toughening mechanisms of TPU and BioTPE were much more effective, e.g. using only 10 phr of one of them increased Charpy impact toughness of PLA more than 300%, while increases in K_{IC} and G_{IC} fracture toughness values were as much as 35% and 130%, respectively. Other mechanical tests (tension, flexure, hardness) and thermal analyses (DSC, TGA, DMA) indicated that there was no significant detrimental effects of using 10 phr TPU and BioTPE on the other mechanical and thermal properties of PLA.

The purpose of the third part of this thesis was to investigate the effects of using maleic anhydride (MA) compatibilization on the toughness and other properties of PLA blended with TPU and BioTPE. MA grafting on the PLA backbone (PLA-g-MA) was prepared separately by reactive extrusion and added during melt blending of PLA/thermoplastic elastomers. IR spectroscopy revealed that MA graft might interact with the functional groups present in the hard segments of TPU and BioTPE domains via primary chemical interactions, so that higher level of compatibilization could be obtained. SEM studies indicated that PLA-g-MA compatibilization also decreased the size of elastomeric domains leading to higher level of surface area for more interfacial interactions. Toughness tests revealed that Charpy impact toughness and fracture toughness (K_{IC} and G_{IC}) of inherently brittle PLA increased enormously when the blends were compatibilized with PLA-g-MA. For instance, G_{IC} fracture toughness of PLA increased as much as 166%. It was also observed that PLA-g-MA compatibilization resulted in no detrimental effects on the other mechanical and thermal properties of PLA blends.

Key words: Polylactide, Rubber Toughening, Ethylene Copolymers, Thermoplastic Elastomers, Maleic Anhydride Compatibilization

ÖZ

POLİLAKTİTİN ÇEŞİTLİ ELASTOMERİK MALZEMELERLE HARMANLANARAK TOKLAŞTIRILMASI

Meyva, Yelda

Yüksek Lisans, Polimer Bilim ve Teknolojisi Bölümü

Tez Yöneticisi: Prof. Dr. Cevdet Kaynak

Ağustos 2014, 102 sayfa

Bu tez çalışmasının birinci bölümünün amacı üç farklı etilen kopolimerinin oldukça kırılğan bir biyopolimer olan polilaktitin (PLA) tokluk ve diğer özelliklerine etkilerini incelemektir. Bu amaç doğrultusunda, PLA değişik miktarlardaki etilen vinil asetat (EVA), etilen metil akrilat (EMA) ve etilen-*n*-bütil akrilat-glisidil metakrilat (EBA-GMA) ile çift vidalı ekstrüder kullanılarak eriyik halde harmanlanmıştır. SEM ve DSC analizleri bu etilen kopolimerlerinin termodinamik olarak PLA ile karışmadıklarını ve faz ayrışımı yaparak PLA matrisi içerisinde 1-5 mikron boyutlu yuvarlak yapıların oluştuğunu göstermiştir. EVA, EMA ve EBA-GMA'nın kauçuk toklaştırma mekanizmalarının PLA'nın sünekliliğinin ve tokluğunun iyileşmesi için çok etkili olduğu görülmüştür. Kullanılan etilen kopolimerlerin türüne ve miktarına bağlı olarak kırılmadaki % uzama, Charpy darbe tokluğu ve G_{IC} kırılma tokluğu değerlerindeki en yüksek artışlar sırasıyla %160, %320 ve %150 olmuştur. EVA, EMA ve EBA-GMA kullanımının PLA'nın ısı özelliklerine zarar verici bir etkisi olmamasına rağmen esnemezlik, dayanım ve sertlik değerlerinde belirli düzeylerde düşmelere neden olmuştur.

Bu çalışmanın ikinci bölümünün amacı ise PLA'nın mühendislik uygulamalarında da kullanılabilirliğini sağlamak için tokluğunu artırırken, diğer mekanik ve ısı özelliklerinden de ödün vermemektir. Bu amaç doğrultusunda, PLA iki farklı termoplastik elastomer; TPU (termoplastik poliüretan elastomer) ve BioTPE

(biyokütle bazlı termoplastik polyester elastomer) ile harmanlanmıştır. SEM analizi TPU ve BioTPE'nin PLA matrisinde yine mikron boyutlu yuvarlak yapılar oluşturarak PLA ile karışmaz olduklarını göstermiştir. TPU ve BioTPE'nin kauçuk toklaştırma mekanizmalarının ise, çok daha fazla etkili olduğu ortaya çıkmıştır. Örneğin, yalnızca 10 phr TPU ya da BioTPE kullanıldığında PLA'nın K_{IC} ve G_{IC} kırılma tokluğu değerleri sırasıyla %35 ve %130 artarken Charpy darbe tokluğu değeri %300'den fazla artış göstermiştir. Diğer mekanik testler (çekme, eğme, sertlik) ve ısıl analizler (DSC, TGA, DMA) 10 phr TPU ve BioTPE kullanımının PLA'nın diğer mekanik ve ısıl özelliklerine zarar verici bir etkisinin olmadığını göstermiştir.

Bu tez çalışmasının üçüncü bölümünün amacı ise maleik anhidrat (MA) uyumlaştırma işleminin TPU ve BioTPE ile harmanlanan PLA'nın tokluk ve diğer özellikleri üzerindeki etkilerini incelemektir. PLA omurga yapısına MA graft edilme işlemi (PLA-g-MA) reaktif ekstrüzyon yöntemiyle ayrıca yapılmış ve PLA/termoplastik elastomer karışımlarına eriyik karıştırma esnasında eklenmiştir. Kızılötesi spektroskopi çalışmaları MA graftlarının TPU ve BioTPE yapılarındaki sert segmentlerin fonksiyonel gruplarıyla birincil derecede kimyasal etkileşimler nedeniyle yüksek derecede uyumlaştırma sağlanabileceğini göstermiştir. SEM analizi PLA-g-MA uyumlaştırmasının elastomerik fazların boyutlarını azalttığını, böylece artan yüzey alanının ise daha fazla arayüzey etkileşimi sağladığını göstermiştir. Tokluk testleri kırılma PLA'nın K_{IC} ve G_{IC} kırılma tokluğu ve Charpy darbe tokluğu değerlerinin PLA-g-MA uyumlaştırması ile çok daha fazla yükseldiğini göstermiştir. Örneğin, PLA'nın G_{IC} kırılma tokluğu %166'ya kadar artmıştır. Ayrıca, PLA-g-MA uyumlaştırmasının PLA karışımlarının diğer mekanik ve ısıl özelliklerine zarar verici bir etkisi olmadığı da gözlemlenmiştir.

Anahtar Kelimeler: Polilaktit, Kauçuk Toklaştırma, Etilen Kopolimerleri, Termoplastik Elastomerler, Maleik Anhidrat Uyumlaştırması

to my deary family

ACKNOWLEDGEMENTS

I would like to thank to my supervisor Prof. Dr. Cevdet Kaynak for his valuable advice, guidance and, patience at each stage of this thesis, and the opportunity to become a TUBITAK project researcher.

I would like to gratefully acknowledge TUBITAK, the Scientific and Technological Research Council of Turkey, for the grant with the Project number 113M586.

I would like to acknowledge all the technical staff and administrative board of the Metallurgical and Materials Engineering Department for supplying all the research facilities required in this dissertation. I would also like to express my sincere gratitude to METU Wind Energy Center for allowing extensive use of DMA equipment; and to METU Central Laboratory for GPC analyses.

I want to thank my laboratory mates, Ali Rıza Erdoğan, Burcu Sarı, Berk Doğu, Seçil Şankal, and İlker Kaygusuz for their friendship and support. I also want to thank Mertcan Başkan and Mehmet Hazar Şeren for their valuable friendship from the Metallurgical and Materials Engineering Department.

My special thanks go to, Süer Kürklü, Aysu Sağdıç, Ezgi Tekerek Çakıcı, Çiğdem Güngör, Seda Kül, Dilek Adalı Kızılören, Tuğçe Aydil Dalkıran, Derya Silibolatlaz Baykara and Özer Zeybek for helping me get through the hard time, and for all the support and entertainment.

I would like to express my deepest thankfulness to my mother Yasemin Meyva, my father Doğan Meyva and my lovely sister Nesil Meyva. They have been a constant love and encouragement in each step of my life from childhood to adulthood. This dissertation would certainly be not possible without their support.

TABLE OF CONTENTS

ABSTRACT	v
ÖZ	vii
ACKNOWLEDGEMENTS	x
TABLE OF CONTENTS	xi
LIST OF TABLES	xiv
LIST OF FIGURES	xvi
NOMENCLATURE	xix
CHAPTERS	1
1. INTRODUCTION	1
1.1 Polylactide	1
1.2 Ethylene Copolymers	4
1.3 Thermoplastic Elastomers	8
1.4 Maleic Anhydride Compatibilization in Blends.....	11
1.5 Literature Survey	14
1.5.1 Studies on the Blending of PLA with Ethylene Copolymers.....	14
1.5.2 Studies on the Blending of PLA with Thermoplastic Elastomers.....	15
1.5.3 Studies on the Compatibilization of PLA Blends	16
1.6 Aim of the Study	17
2. EXPERIMENTAL WORK	19
2.1 Materials Used.....	19
2.2 Compounding and Shaping of the Specimens.....	22
2.3 Morphological Analysis by Scanning Electron Microscopy.....	22
2.4 Mechanical Tests Performed	23

2.5	Thermal Analyses Conducted.....	23
2.6	Melt Flow Index Determination	24
2.7	Infrared Spectroscopy.....	24
3.	RESULTS AND DISCUSSION.....	25
3.1	Effects of Ethylene Copolymers.....	25
3.1.1	Morphology and Distribution of the Ethylene Copolymer Domains... ..	25
3.1.2	Melt Flow Behavior of the Blends with Ethylene Copolymers	29
3.1.3	Stiffness, Strength and Hardness of the Blends with Ethylene Copolymers	30
3.1.4	Ductility and Toughness of the Blends with Ethylene Copolymers	36
3.1.5	Toughening Mechanisms of the Blends with Ethylene Copolymers ...	38
3.1.6	Thermal Transition Temperatures and Crystallinity of the Blends with Ethylene Copolymers.....	40
3.1.7	Thermal Degradation and Thermomechanical Behavior of the Blends with Ethylene Copolymers.....	43
3.2	Effects of Thermoplastic Elastomers.....	47
3.2.1	Morphology and Distribution of the Thermoplastic Elastomer Domains	47
3.2.2	Melt Flow Behavior of the Blends with Thermoplastic Elastomers	51
3.2.3	Stiffness, Strength and Hardness of the Blends with Thermoplastic Elastomers.....	52
3.2.4	Ductility and Toughness of the Blends with Thermoplastic Elastomers	57
3.2.5	Toughening Mechanisms of the Blends with Thermoplastic Elastomers	58
3.2.6	Thermal Transition Temperatures and Crystallinity of the Blends with Thermoplastic Elastomers.....	60

3.2.7	Thermal Degradation and Thermomechanical Behavior of the Blends... with Thermoplastic Elastomers	63
3.3	Effects of Maleic Anhydride Compatibilization	67
3.3.1	Compatibilization of PLA/Thermoplastic Elastomer Blends with PLA- g-MA	67
3.3.2	Effects of PLA-g-MA on the Morphology of Domains and Melt Flow Index of the Blends	74
3.3.3	Effects of PLA-g-MA on the Mechanical Properties of the Blends	77
3.3.4	Effects of PLA-g-MA on the Thermal Behavior of the Blends	86
4.	CONCLUSIONS	91
	REFERENCES	95

LIST OF TABLES

Table 2.1 Chemical Structure of the Elastomeric Materials Used	21
Table 3.1 Average Domain Sizes Determined by an Image Analysis Software	26
Table 3.2 Melt Flow Index (MFI) Values of the Constituent Materials and Blends with Ethylene Copolymers at 190°C under 2.16 kg.....	29
Table 3.3 Young’s Modulus (E), Flexural Modulus (E_{Flex}), Tensile Strength (σ_{TS}), Flexural Strength (σ_{Flex}) and Hardness (H) Values of the Specimens with Ethylene Copolymers	32
Table 3.4 Tensile Strain at Break (ϵ_f), Unnotched Charpy Impact Toughness (C_U), and Fracture Toughness (K_{IC} and G_{IC}) Values of the Specimens with Ethylene Copolymers	37
Table 3.5 Transition Temperatures (T_g , T_c , T_m), Enthalpies (ΔH_m , ΔH_c) and Crystallinity Percent (X_C) of the Specimens with Ethylene Copolymers During Heating Profile	41
Table 3.6 Thermal Degradation Temperatures ($T_{5\%}$, $T_{10\%}$, $T_{25\%}$) of the Constituent Materials and 5 phr Blends with ethylene copolymers at 5, 10, 25 wt% Mass Losses and their Maximum Mass Loss Rate Peak (T_{max}).....	44
Table 3.7 Storage Modulus (E') Values of PLA and its Blends with 5 phr Ethylene Copolymers at 25° and 50°C.....	44
Table 3.8 Average Domain Sizes Determined by an Image Analysis Software	48
Table 3.9 Melt Flow Index (MFI) Values of the Constituent Materials and Blends with Thermoplastic Elastomers at 220°C under 2.16 kg.....	51
Table 3.10 Young’s Modulus (E), Flexural Modulus (E_{Flex}), Tensile Strength (σ_{TS}), Flexural Strength (σ_{Flex}) and Hardness (H) Values of the Specimens with Thermoplastic Elastomers	54
Table 3.11 Tensile Strain at Break (ϵ_f), Unnotched Charpy Impact Toughness (C_U), and Fracture Toughness (K_{IC} and G_{IC}) Values of the Specimens with Thermoplastic Elastomers	57

Table 3.12 Transition Temperatures (T_g , T_c , T_m), Enthalpies (ΔH_m , ΔH_c) and Crystallinity Percent (X_C) of the Specimens with Thermoplastic Elastomers During Heating Profile	61
Table 3.13 Thermal Degradation Temperatures ($T_{5\%}$, $T_{10\%}$, $T_{25\%}$) of the Specimens with Thermoplastic Elastomers at 5, 10, 25 wt% Mass Losses and Maximum Mass Loss Rate Peak (T_{max}) of the Specimens	63
Table 3.14 Storage Modulus (E') Values of PLA and Blends with 10 phr Thermoplastic Elastomers at 25° and 50°C	64
Table 3.15 Positions and Assignments of Distinctive IR Bands Related to PLA, MA, TPU and TPE	69
Table 3.16 Effects of PLA-g-MA on the Domain Sizes and Melt Flow Index of the Blends.....	76
Table 3.17 Effects of PLA-g-MA on the Young's Modulus (E), Flexural Modulus (E_{Flex}), Tensile Strength (σ_{TS}), Flexural Strength (σ_{Flex}) and Hardness (H) of the Blends.....	79
Table 3.18 Effects of PLA-g-MA on the Tensile Strain at Break (ϵ_f), Unnotched Charpy Impact Toughness (C_U), and Fracture Toughness (K_{IC} and G_{IC}) of the Blends	79
Table 3.19 Effects of PLA-g-MA on the Transition Temperatures (T_g , T_c , T_m), Enthalpies (ΔH_m , ΔH_c) and Crystallinity Percent (X_C) of the Blends During Heating	87
Table 3.20 Effects of PLA-g-MA on the Thermal Degradation Temperatures (T_d) and Storage Modulus (E') Values of the Blends at 25° and 50°C	89

LIST OF FIGURES

Figure 1.1 Two Different Optical Isomers of PLA	1
Figure 1.2 Different Routes to Synthesize PLA	2
Figure 1.3 Petrochemical Route to Lactic Acid	3
Figure 1.4 Examples for the Structure of Block Copolymers	5
Figure 1.5 Chemical Structure of Ethylene Vinyl Acetate (EVA)	6
Figure 1.6 Chemical Structure of Ethylene Methyl Acrylate (EMA)	7
Figure 1.7 Chemical Structure of Ethylene- <i>n</i> -Butyl Acrylate-Glycidyl Methacrylate (EBA-GMA).....	12
Figure 1.8 Hard and Soft Segments of the Thermoplastic Elastomers	9
Figure 1.9 Chemical Structure of Thermoplastic Polyurethane Elastomers (TPU)	10
Figure 1.10 Chemical Structure of Thermoplastic Polyester Elastomers (TPE).....	10
Figure 1.11 The Chemical Structure of the Maleic Anhydride (MA).....	12
Figure 1.12 Schemes for a Proposed Structure of the Copolymer between PP-g-MA and PET	13
Figure 3.1 Smooth SEM Fractograph of Neat PLA and Rough Fractographs of PLA Blends Showing Finely and Uniformly Distributed EVA, EMA and EBA-GMA Domains.....	27
Figure 3.2 SEM Fractographs Showing Interfacial Interactions between PLA Matrix and Domains of EVA, EMA and EBA-GMA with Debonded and Pulled-Out Morphology.....	28
Figure 3.3 Stress-Strain Curves of the Specimens with Ethylene Copolymers Obtained During Tensile and 3-Point Bending (Flexural) Test	33
Figure 3.4 Effects of EVA, EMA and EBA-GMA Content on the Tensile Modulus (E), Flexural Modulus (E_{Flex}) and Hardness (H) of the Specimens.....	34
Figure 3.5 Effects of EVA, EMA and EBA-GMA Content on the Tensile Strength (σ_{TS}) and Flexural Strength (σ_{Flex}) of the Specimens	35

Figure 3.6 Effects of EVA, EMA and EBA-GMA Content on the Ductility (% Strain at Break- ϵ_f), Impact Toughness (Unnotched Charpy- C_U) and Fracture Toughness (K_{IC} and G_{IC}) of the Specimens	39
Figure 3.7 DSC Heating Thermograms of the Specimens with Ethylene Copolymers Obtained After Erasing their Thermal History.....	42
Figure 3.8 Thermogravimetric (TG) and Differential Thermogravimetric (DTG) Curves of PLA and its Blends with 5 phr Ethylene Copolymers.....	45
Figure 3.9 Storage Modulus Curves of PLA and its Blends with 5 phr Ethylene Copolymers Obtained by DMA	46
Figure 3.10 Smooth SEM Fractograph of Neat PLA and Rough Fractographs of PLA Blends Showing Finely and Uniformly Distributed TPU and BioTPE Domains.....	49
Figure 3.11 SEM Fractographs Showing Interfacial Interactions between PLA Matrix and Domains of TPU and BioTPE with Debonded and Pulled-Out Morphology.....	50
Figure 3.12 Stress-Strain Curves of the Specimens with Thermoplastic Elastomers Obtained During Tensile and 3-Point Bending (Flexural) Test.....	53
Figure 3.13 Effects of TPU and BioTPE Content on the Tensile Modulus (E), Flexural Modulus (E_{Flex}) and Hardness (H) of the Specimens.....	55
Figure 3.14 Effects of TPU and BioTPE Content on the Tensile Strength (σ_{TS}) and Flexural Strength (σ_{Flex}) of the Specimens	56
Figure 3.15 Effects of TPU and BioTPE Content on the Ductility (% strain at break- ϵ_f), Impact Toughness (Unnotched Charpy- C_U) and Fracture Toughness (K_{IC} and G_{IC}) of the Specimens	59
Figure 3.16 DSC Heating Thermograms of the Specimens Obtained After Erasing their Thermal History	62
Figure 3.17 Thermogravimetric (TG) and Differential Thermogravimetric (DTG) Curves of the Specimens with Thermoplastic Elastomers.....	65
Figure 3.18 Storage Modulus Curves of PLA and Blends with 10 phr Thermoplastic Elastomers Obtained by DMA	66
Figure 3.19 Grafting of MA onto PLA Backbone by Free Radical Reaction.....	70
Figure 3.20 ATR-FTIR Spectra of PLA and PLA-g-MA	71

Figure 3.21 ATR-FTIR Spectra of PLA/Thermoplastic Elastomer Blends with and without PLA-g-MA Compatibilization	73
Figure 3.22 Very Rough SEM Fractographs of PLA Blends with and without Compatibilization Showing Finely and Uniformly Distributed TPU and BioTPE Domains	75
Figure 3.23 SEM Fractographs Showing Interfacial Interactions (Coalescence, Debonding, Pull-Out) between PLA Matrix and TPU, BioTPE Domains with and without Compatibilization.....	77
Figure 3.24 Stress-Strain Curves of the Blends with and without Compatibilization Obtained During Tensile and 3-Point Bending (Flexural) Tests.....	80
Figure 3.25 Effects of PLA-g-MA on the Elastic Modulus (E and E_{Flex}) of the Blends.....	81
Figure 3.26 Effects of PLA-g-MA on the Strength (σ_{TS} and σ_{Flex}) of the Blends.....	82
Figure 3.27 Effects of PLA-g-MA on the Ductility (% Strain at Break- ϵ_f) and Impact Toughness (Unnotched Charpy- C_U) of the Blends	84
Figure 3.28 Effects of PLA-g-MA on the Fracture Toughness (K_{IC} and G_{IC}) of the Blends.....	85
Figure 3.29 DSC Heating Thermograms of the Blends with and without Compatibilization Obtained after Erasing their Thermal History	88
Figure 3.30 Thermogravimetric Curves of the Blends with and without Compatibilization.....	89
Figure 3.31 Storage Modulus Curves of the Blends with and without Compatibilization Obtained by DMA	90

NOMENCLATURE

σ_{TS}	:	tensile strength
σ_{Flex}	:	flexural strength
ε_f	:	elongation at break, final strain
ΔH_f	:	heat of fusion of the specimens
ΔH_c	:	heat of crystallization
ΔH_m°	:	melting enthalpy of 100% crystalline PLA
C_U	:	Charpy impact toughness
E	:	Young's modulus
E'	:	storage modulus
E_{Flex}	:	flexural modulus
H	:	hardness
G_{Ic}	:	fracture toughness as critical strain energy release rate
K_{Ic}	:	fracture toughness as critical stress intensity factor
ATR-FTIR	:	attenuated total reflectance fourier transform infrared spectroscopy
DSC	:	differential scanning calorimetry
DMA	:	dynamic mechanical analysis
EVA	:	ethylene vinyl acetate
EMA	:	ethylene methyl acrylate
EBA-GMA	:	ethylene- <i>n</i> -butyl acrylate-glycidyl methacrylate
MA	:	maleic anhydride
MFI	:	melt flow index
PLA	:	poly(lactic acid) or polylactide
PLLA	:	L-enantiomer of polylactide
PDLA	:	D-enantiomer of polylactide
PLA-g-MA	:	maleic anhydride grafted polylactide
SEM	:	scanning electron microscopy
TGA	:	thermogravimetric analysis

TPU	:	thermoplastic polyurethane elastomer
TPE	:	thermoplastic polyester elastomer
BioTPE	:	biomass based thermoplastic polyester
$T_{5wt\%}$:	thermal degradation temperature at 5 wt% mass loss
$T_{10wt\%}$:	thermal degradation temperature at 10 wt% mass loss
$T_{25wt\%}$:	thermal degradation temperature at 25 wt% mass loss
T_c	:	cold crystallization temperature
T_g	:	glass transition temperature
T_m	:	melting temperature
T_{max}, T_d	:	thermal degradation temperature of maximum mass loss rate
X_c	:	degree of crystallinity

CHAPTER 1

INTRODUCTION

1.1 Polylactide

Today, non-renewable petroleum or natural gas resources are the basic raw materials for many traditional polymers. Some of them are disposed due to end use contamination while little amount of them are recycled and reused. However, recently the number of researches about compostable polymers produced from renewable resources is on the rise. One of the most popular biopolymer in this respect is poly(lactic acid) or simply called as polylactide (PLA) which is derived from the renewable resources such as corn starch. PLA is typical aliphatic polyester made from α -hydroxy acids. PLA can be presented as two optical D- or L-enantiomers as shown in Figure 1.1.

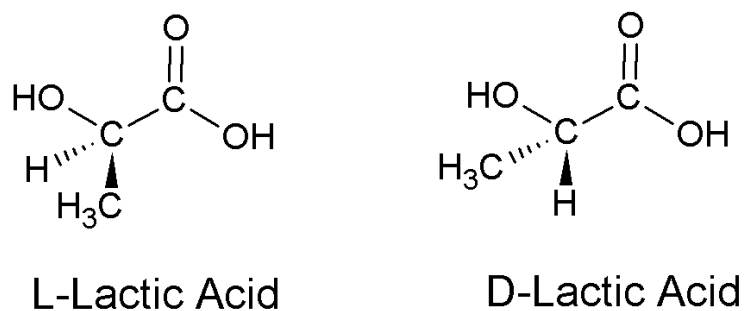


Figure 1.1 Two Different Optical Isomers of PLA

Therefore, depending on the type of its monomer PLA can be named as poly(L-lactic acid) PLLA or poly(D-lactic acid) PDLA or poly(D,L-lactic acid) PDLLA. Thus, PLA having different thermal, barrier and structural properties can be produced. While PLA with less than 1% D-isomer is used for the injection molding process, PLA with 4-8% D-isomer is used for the thermoforming, extrusion, and blow molding processes [1].

Lactic acid was isolated from milk by the Swedish chemist Scheele in 1780, and it is produced commercially in 1781 [2]. Carbohydrate fermentation or chemical syntheses were the ways of the production of the lactic acid, which is known as the building blocks of PLA. However, the fermentation route was the favorite production method. After that, higher molecular weight PLA was produced from many routes such as; azeotropic hydration condensation, direct condensation polymerization and polymerization through lactide formation (Figure 1.2) [1].

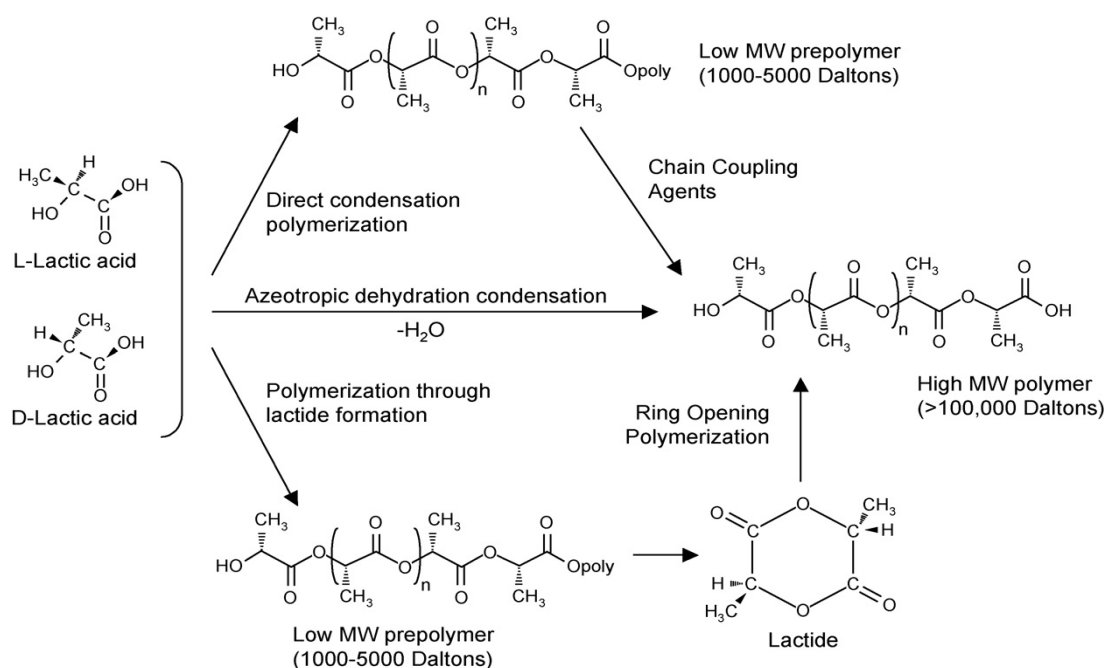


Figure 1.2 Different Routes to Synthesize PLA [1]

Ring opening polymerization of the lactide, which is first confirmed by Carothers in 1932, is the most efficient way of obtaining commercial higher molecular weight PLA while other processes give lower molecular weight, brittle and glassy PLA [1, 2].

In another process, lactic acid and catalysts are azeotropically dehydrated in a refluxing and high-boiling solvent under reduced pressures without using chain extenders in order to obtain higher molecular weight commercial PLA. However, the used catalyst caused many problems such as undesired degradation and catalyst toxicity [2].

In the direct condensation polymerization, lactic acid is used as the raw material and lower molecular weight PLA is produced with an equimolar concentration of hydroxyl and carboxyl end groups. The purpose of the external coupling agents using in the direct condensation polymerization is to increase the molecular weight of the obtained PLA [2].

Besides fermentation reactions, PLA can also be produced via petrochemical route as shown in Figure 1.3. A 50/50 optically inactive mixture of the L- and D- enantiomers belongs to the lactic acid which is produced by petrochemical route. However, PLA having mostly L- enantiomer is the significant point for the PLA production. Therefore, it is not a favorable method for producing the commercial higher molecular weight PLA.

Semicrystalline PLA has glass transition temperature (T_g) and melting temperature (T_m) like the other thermoplastic polymers. T_g of PLA is affected by optical purity and molecular weight. Besides this, T_g value increases with increasing the L- content when D- content is kept constant [1]. T_g and T_m of commercial PLA are around 58°C and 175°C, respectively, while degradation temperature range is 235-255°C [2].

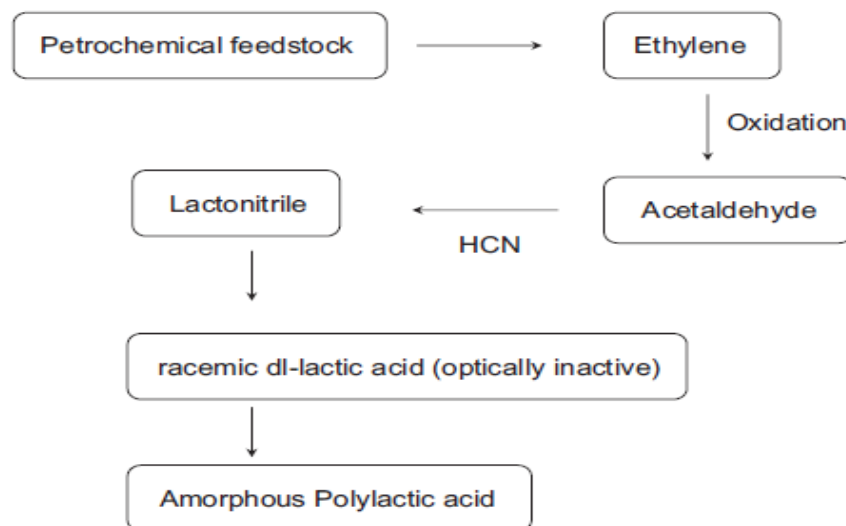


Figure 1.3 Petrochemical Route to Lactic Acid [3]

It is also known that PLA has sensitivity to UV irradiation and humidity leading to chain scission degradation. Therefore, investigations try to measure outdoor performance of PLA to be used for engineering applications [4].

PLA is today generally used in the medical applications like implant devices, tissue scaffolds due to its high cost, low availability and restricted molecular weight. On the other hand, due to the recent developments in the efficient production techniques, PLA is now being considered to be used for many other applications, including automotive industry. Moreover, its future looks bright to solve the waste disposal problem because of its compostable property. It is also appropriate for food packaging applications due to its low toxicity in other words biocompatibility [1].

Compared to traditional petroleum based polymers PLA has sufficient optical and barrier properties including strength, stiffness, and hardness. However, PLA has inherently very brittle nature. Thus, today there are various efforts to improve toughness of PLA, including this thesis. One of the most efficient methods to toughen PLA would be blending with certain elastomeric materials such as “ethylene copolymers” and “thermoplastic elastomers”.

1.2 Ethylene Copolymers

There could be different molecular architectures of copolymers due to different distributions of their comonomers: random, alternating and block copolymers [5]. Especially block copolymers are preferred due to their desired properties. Figure 1.4 shows examples of the molecular architectures that might form with A, B and C monomers. They can exist in the linear, branched or star forms having different properties [6].

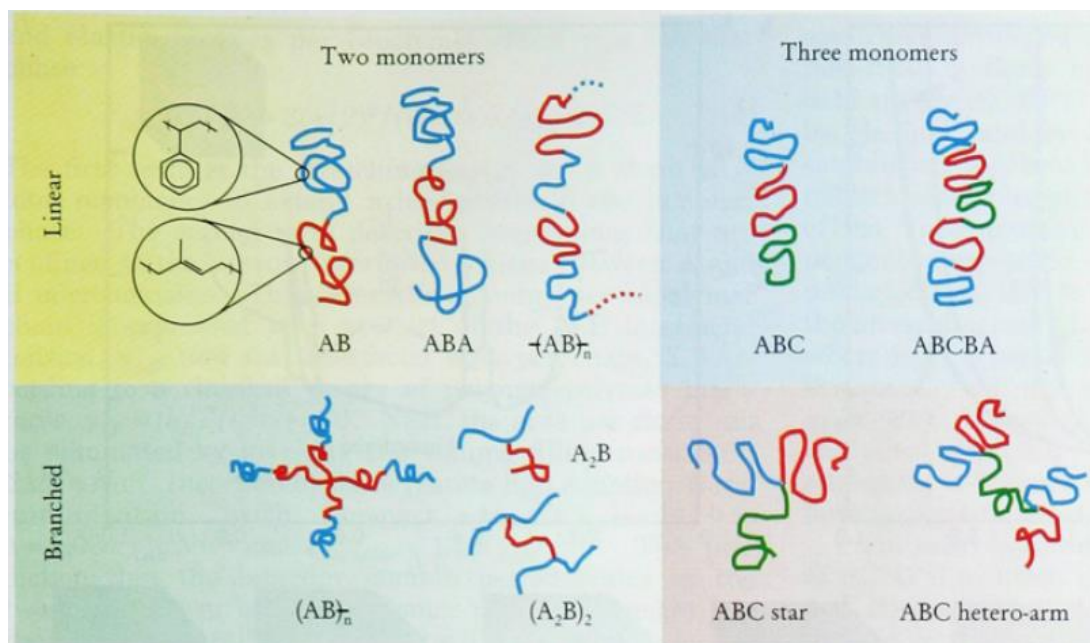


Figure 1.4 Examples for the Structure of Block Copolymers [6]

Copolymers generally synthesized from ethylene and styrene. The addition of polyethylene aromatic groups has been joined together due to its enhanced radiation resistance or electrical break-down resistance. Ziegler-Natta catalysts and free radical processes are used for copolymers with small amount of styrene. In order to copolymerize ethylene and vinyl aromatic groups efficiently, metallocene catalysts are used for metallocene-catalyzed polymerizations in 1990s. In this polymerization, catalyst structure and polymerization conditions are important for the product composition. Copolymerization with the additional monomer is called as terpolymerization. These additional monomers, such as 1, 3- butadiene or propylene, satisfy better crosslinking between the copolymers [5].

One of the most widely used ethylene copolymers is ethylene vinyl acetate copolymer (EVA) (Figure 1.5). It is a low density polyethylene copolymer with excellent low temperature impact properties. Also, the flexibility increases with increasing the vinyl acetate (VA) content. Therefore, they are used especially in packaging and adhesive industry. In addition, they have good processability, high resistance to rupture and uniform shrinkage. The most important disadvantage of EVA is having no stiffness [5]. Depending on the application, industrial grade EVA

copolymers are obtained by using high pressure radical polymerization with various VA contents.

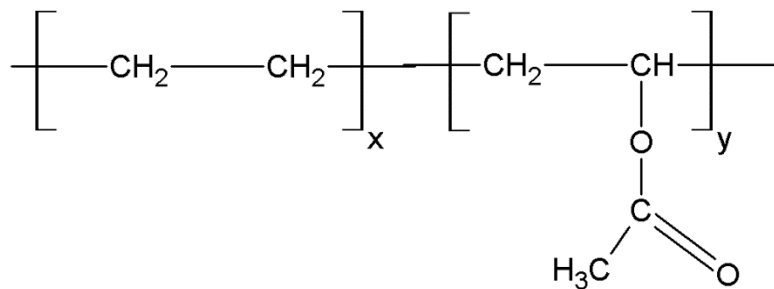


Figure 1.5 Chemical Structure of Ethylene Vinyl Acetate (EVA)

There are also ethylene acrylic copolymers such as ethylene methyl acrylate (EMA) and ethylene-n-butyl acrylate-glycidyl methacrylate (EBA-GMA). Chemical structures of EMA and EBA-GMA are given in Figures 1.6 and 1.7, respectively. These adhesive copolymers include between 3 and 20 wt% acrylic acid. In order to provide heat seal layer for packaging, they are used in extrusion coating [7].

They can be synthesized by the addition copolymerization of ethylene and methyl acrylate with low level of alkenoic acid to satisfy crosslinking between diamines. At the end of the polymerization, a random amorphous terpolymer or a random amorphous dipolymer can be obtained. Methyl acrylate to ethylene ratio is very significant for the fluid resistance and low temperature properties of ethylene acrylic elastomer copolymers. The polarity of the polymer increases by increasing the methyl acrylate amount. T_g of the polymer also increases slightly by increasing the methyl acrylate level [5].

EMA and EBA-GMA have tremendous heat and oil resistance, good weathering resistance, low temperature flexibility, and certain level of mechanical strength. The oxidative crosslinking mechanism might occur at high temperatures leading to embrittlement. However, a temperature level of 190-200°C can be tolerated by ethylene acrylic elastomers. They have also excellent water and glycol resistivity. It is known that ester plasticizers improve the low temperature properties of the ethylene acrylic copolymers. But, the type of the plasticizer should be selected

carefully in order to avoid sacrificed heat resistance. Moreover, ethylene acrylic copolymers have high damping properties between -10 and 160°C, which does not change until six months of aging in air at 150°C [5].

Ethylene acrylic elastomers were sold as 5000 tons in 2000, more than 50% of it in Europe. It is stated that if higher viscosity ethylene acrylic elastomers could be developed, their market can be increased further. Almost 80% of ethylene acrylic elastomers produced is used in the automotive industry and in wire and cable jacketing. Other industrial applications include pipe seals, hydraulic system seals, etc. [5].

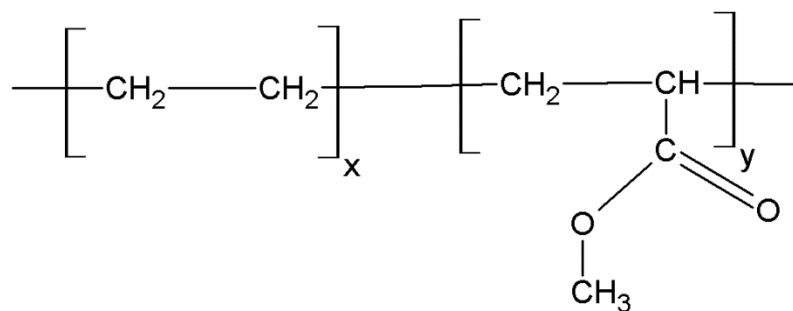


Figure 1.6 Chemical Structure of Ethylene Methyl Acrylate (EMA)

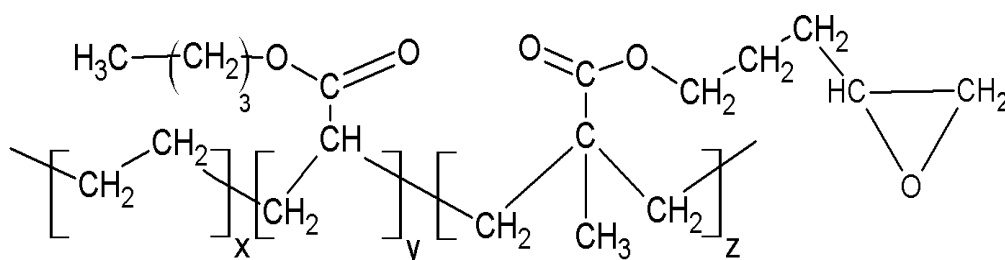


Figure 1.7 Chemical Structure of Ethylene-*n*-Butyl Acrylate-Glycidyl Methacrylate (EBA-GMA)

1.3 Thermoplastic Elastomers

Elastomers have amorphous structure when unstretched and have very elastic character above their T_g . Elastomers can be grouped in two main classes: cross-linked elastomers and thermoplastic elastomers. The preparation of the cross-linked elastomers includes elastomeric polymer with modifying additives and a reactive crosslinking agent. This type of elastomers can be formed to a desired shape via many operations. But, the process in the last step should include decomposition of the crosslinking agent to the free radicals. Then, a three dimensional structure of the elastomeric polymer forms by the reaction of two dimensional chains with the free radicals. Unfortunately, these elastomers cannot be melted and formed again [8].

Thermoplastic elastomers are rather a new class. They have both elastomeric and thermoplastic behavior. The molded components from thermoplastic elastomers can be remelted and reformed. The creep resistance and high temperature resistance properties are not so good due to the un-crosslinked nature of the polymers [8].

Thermoplastic elastomer compounding is achieved by mixing a base polymer and another organic or inorganic substance. Mostly, the used second phase improves the end properties. The base polymer has various densities or molecular weights. They can be a higher viscosity liquid, so they do not need some special processes. Organic additives, such as antioxidants, internal lubricants, release agents, plasticizers, impact modifiers, electrostatic control agents, dyes and organic pigments, may be used. [8].

Thermoplastic elastomers consist of basically two segments in a network structure: hard segment and soft segment as shown in Figure 1.8, “A” represents crystalline domains (hard segment), “B” represents junction of crystalline lamellae, “C” represents noncrystalline (amorphous) segment (soft segment). The applied stress to the thermoplastic elastomer is transformed to the crystalline part via tie molecules. Thus, crystalline part is oriented and the stress transformed to the soft segment. The elastomeric domains absorb the applied stress and give response as a crosslinked elastomer [9].

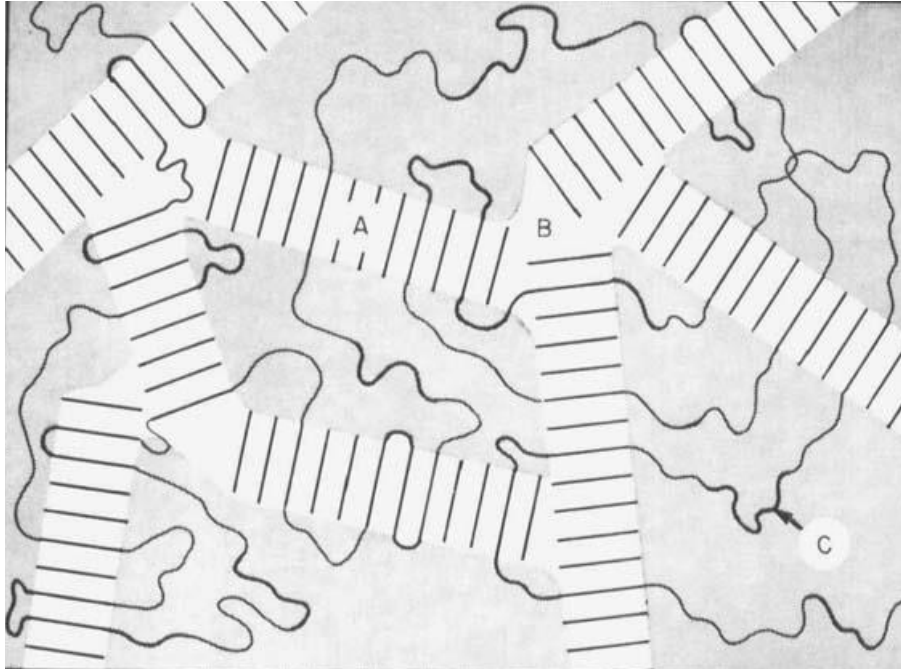


Figure 1.8 Hard and Soft Segments of the Thermoplastic Elastomers [9]

Thermoplastic polyurethane elastomers (TPU) and thermoplastic polyester elastomers (TPE) are two common examples of this class; their chemical structures are given in Figures 1.9 and 1.10, respectively. TPU, being a commercial success, generally made up of three parts; diisocyanates, macroglycols and chain extenders. Diisocyanates are low molecular weight groups that might act as coupling agent for macroglycols in the soft segments and for chain extenders in the hard segments. TPUs have hydrogen bonds between hydrogen groups and carbonyl groups of urethane [10].

Macroglycols are higher molecular weight components than diisocyanates. They are responsible for forming the long, linear and strong TPU chains. TPU elastomers have macroglycol content in the range 50-80 wt% which influences their chemical and physical properties. For instance, chain irregularities of the macroglycols lead to low mechanical properties [10].

Chain extenders, such as glycols, have low molecular weight. Urethane-rich hard segments can be obtained by the strong hydrogen bonds provided with the reaction

between the chain extenders and diisocyanates. Chain extenders also affect the chemical and physical properties of TPUs. For instance, symmetrical and compact chain extenders produce high modulus TPUs [10].

The urethane group in the hard segment of TPU can dissociate into its constituents such as isocyanate as seen in Figure 1.9. This type of dissociation might increase with increasing the temperature. Then, isocyanate groups might react with water or carboxylic acid leading to release of urea groups and carbon dioxide [10].

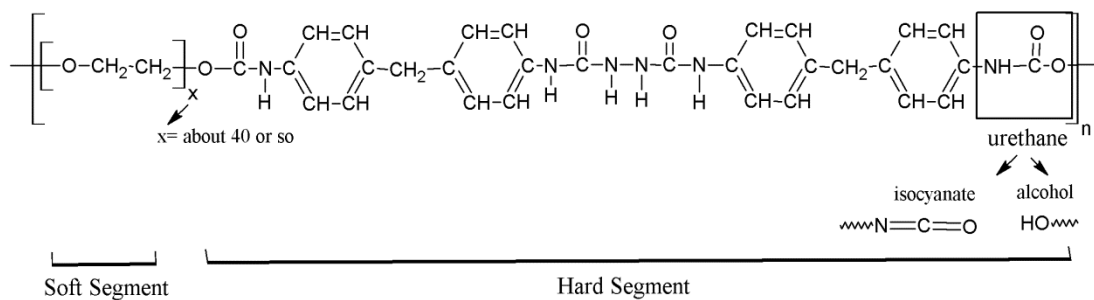


Figure 1.9 Chemical Structure of Thermoplastic Polyurethane Elastomers (TPU)

Another significant thermoplastic elastomer being in the market since 1990s is the thermoplastic polyester elastomers (TPE). As shown in Figure 1.10, TPEs also have hard and soft segments of poly(butylene terephthalate) and poly(tetramethylene ether) glycol, respectively. Soft segment affects the low temperature properties, impact strength, hydrolysis resistance, while hard segment influences the mechanical strength, UV and oxidation resistance, chemical resistance [10].

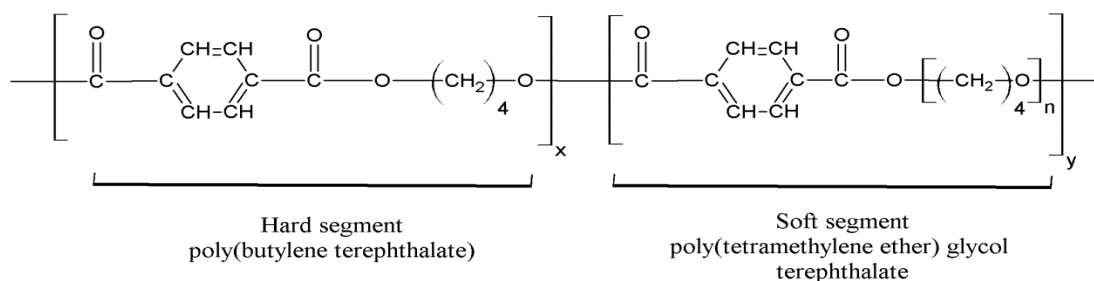


Figure 1.10 Chemical Structure of Thermoplastic Polyester Elastomers (TPE)

The polyester blocks in TPEs generally have regular structures forming crystalline domains which maximize the intermolecular attractions between the hard segments. These crystalline domains also provide physical crosslinking in the amorphous, elastomeric soft segments. TPEs keep their integrity at temperatures under shear forces applied during thermoplastic processing [10].

Most TPEs are synthesized by polycondensation reactions of a poly(ether) diol with a mixture of a phthalate ester and a low molecular weight diol. Thus, TPEs can be classified as segmented polyester-polyether block copolymers. Their hard and soft segments have random distribution with random-length sequences. The crystallizable hard segments are composed of either ethylene phthalate units with ortho, meta, or para substitution in the aromatic dicarboxylic acid unit. Whereas, elastomeric soft segments are composed of phthalate esters of long-chain poly(alkylene oxide) diols. These diols could be poly(oxyethylene) diol or poly(oxypropylene) diol [10].

1.4 Maleic Anhydride Compatibilization in Blends

Polymer blends can be miscible or immiscible. Miscible blends have thermodynamic solubility and are characterized by the presence of one phase and a single glass transition temperature. Their properties can be predicted from the amount weighted average of the properties of the constituents. Immiscible blends have phase separation, exhibiting the glass transition temperatures and/or melting temperatures of each constituent. Their overall behavior depends on the properties of the individual constituents, but also depends significantly on the morphology of the blends and the interfacial interactions between the constituents [11].

Many blends are immiscible and have poor properties compared to their constituents. This problem is due to having no interaction between blend phases. This leads to interfacial tension between the constituents in the blend melt which makes it difficult to deform the dispersed phase of a blend during mixing and to resist phase coalescence during subsequently processing. It also leads to poor interfacial adhesion

in the solid state which usually results in mechanical failure under various types of loading [11].

On the other hand, immiscibility is not always a bad thing. Blends do not have to be miscible to have certain improved properties. Because, morphology and interfacial adhesion can be improved by compatibilization, e.g. by the addition of a suitable block or graft copolymer that might act as interfacial agent. These block or graft copolymers can be made separately and then added to polymer blends. Alternatively, these copolymers can be formed *in situ* during the blend preparation through polymer-polymer grafting reactions using functionalized polymers [11].

Compatibilization to improve blend performance means making the blend constituents less miscible. Compatibilized blends are characterized by the presence of finely dispersed domains, good adhesion between the matrix polymer and the domains, strong resistance to coalescence of domains, and improved properties [11].

Suitable block and graft copolymers should be used as compatibilizers, i.e. the copolymer should contain a segment miscible with the matrix polymer of the blend and another segment forming a chemical bond with the domains. In this respect, one of the most widely used graft copolymer compatibilization method is grafting the base polymer with maleic anhydride (MA). The chemical structure of MA is given in Figure 1.11. Since MA has very reactive functional groups, it is thought to be suitable for many blend systems.

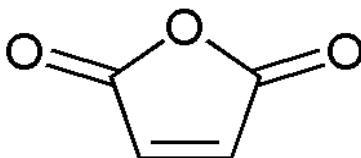


Figure 1.11 Chemical Structure of the Maleic Anhydride (MA)

MA has been used in the industry to promote adhesion and dyeability for many years. MA has been also extensively used in graft copolymer compatibilization of

many polymer blends. For example, MA grafted polypropylene, polyethylene, ethylene propylene rubber, ethylene propylene diene rubber, styrene ethylene butylene styrene copolymer, acrylonitrile butadiene styrene, polysulfone have been used to compatibilize various polymer blends in order to improve their impact toughness, tensile strength, permeability, heat resistance, crystallization, and recycling properties. An example of forming copolymer between MA grafted polypropylene and polyethylene terephthalate is seen in Figure 1.12. [11].

The main reason for the extensive use of MA is the relative ease with which MA can be grafted onto many polymers at normal melt processing temperatures. Therefore, in this thesis, effects of MA compatibilization were also explored.

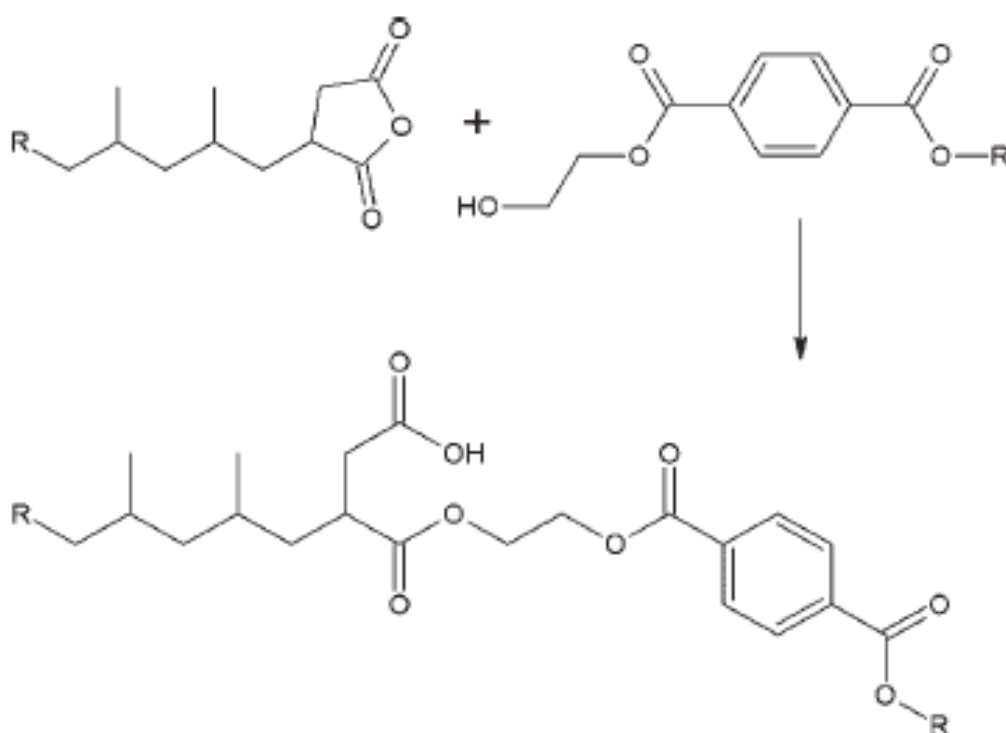


Figure 1.12 Schemes for a Proposed Structure of the Copolymer between PP-g-MA and PET [11]

1.5 Literature Survey

Poly(lactic acid) also known as polylactide (PLA) is a type of aliphatic polyester biopolymer having thermoplastic character. It can be obtained from renewable resources such as corn starch. PLA has biocompatibility and biodegradability making it an important alternative for food packaging and biomedical applications. Due to the scarcity of the oil resources, today in the other sectors of industry, PLA is being considered as an alternative biopolymer to replace petroleum based traditional polymers. However, although PLA has certain level of mechanical strength and elastic modulus properties required for industrial applications, the most critical deficiency is its very high level of brittleness. Therefore, studies on toughening of PLA attract many researches from academia and industry.

1.5.1 Studies on the Blending of PLA with Ethylene Copolymers

In order to decrease inherent brittleness of PLA, it has been thought that “rubber toughening” approach could be used. Therefore, in the literature there are numerous studies investigating the ductility and toughness improvement of PLA when blended with elastomeric materials. These studies include blending of PLA with natural rubber (NR) [12], poly(cis-1,4-isoprene) (IR) [12], poly(acrylonitrile-co-butadiene) (NBR) [12], poly(styrene-ethylene/butylene-styrene) triblock elastomer (SEBS) [13], poly(ϵ -caprolactone-co- δ -valerolactone) [14], poly(butylene succinate) [15], poly(3-hydroxybutyrate) [16], poly(butylene succinate-co-butylene adipate) (PBSA) [16], acrylonitrile-butadiene-styrene copolymer (ABS) [17], poly(butylenes adipate-co-terephthalate) (PBAT) [18], polyhydroxyalkanoate [19], polyamide elastomer (PAE) [20], thermoplastic polyolefin elastomer (TPO) [21].

On the other hand, there is limited number of studies investigating the effects of blending with ethylene copolymers. Such as blending with ethylene vinyl acetate (EVA) [22-25], ethylene methyl acrylate (EMA) [26], ethylene-*n*-butyl acrylate-glycidyl methacrylate (EBA-GMA) [27], ethylene-glycidyl-methacrylate (EGMA) [28, 29], ethylene-methyl-acrylate-glycidyl-methacrylate (EMA-GMA) [30, 31].

Morphological studies of these investigations [22-31] revealed that ethylene copolymers EVA, EMA, EBA-GMA, EGMA, EMA-GMA were thermodynamically immiscible with PLA. Depending on their amounts, generally, they formed round or other irregular shaped domains in the PLA matrix. Due to the rubber toughening mechanisms, their mechanical tests indicated that although there were certain reductions in strength and elastic modulus values, in return, ductility and impact toughness values of PLA increased significantly by blending with 5-20 wt% of these ethylene copolymers.

1.5.2 Studies on the Blending of PLA with Thermoplastic Elastomers

In order not to sacrifice strength and modulus values of PLA too much, it is believed that blending PLA with “thermoplastic elastomers” could be a solution. “Soft segments” of thermoplastic elastomers would again give ductility and flexibility improving toughness; on the other hand, “hard segments” of thermoplastic elastomers would keep the strength and modulus of PLA as much as possible. In the literature, there seems to be around four studies investigating the effects of blending with thermoplastic elastomers. Three of them are about using “thermoplastic polyurethane” (TPU), while the fourth one is about using “thermoplastic polyester” (TPE), as summarized below.

Feng and Ye [32], using 20 wt% TPU let to 70 times increase in % elongation at break, 6 times increase in impact toughness, but around 30% decrease in tensile strength values.

Han and Huang [33] studied blends of PLA with 10, 20, 25, 30 wt% TPU. Using 30 wt% TPU resulted in 46 times increase in the % elongation at break, and 8 times increase in the Izod impact toughness, but, yield strength decreased by almost 50%.

A similar study was conducted by Hong and his co-workers [34], this time blending was with 10, 20, 30, 40, 50 wt% TPU. In their study, PLA with only 10 wt% TPU resulted in 3 times increase in notched Izod impact toughness, 23% increase in %

elongation at break values, no decrease in tensile strength, but 37% decrease in elastic modulus values.

Zaman *et al.* [35] used various amounts (5, 10, 15, 20, 30 wt%) of TPE (thermoplastic polyester elastomer) to compare their effects on the tensile mechanical properties of PLA blends. They revealed that increasing the TPE content increases the % elongation at break ductility values starting from 2% up to 245%, while the reductions in tensile strength and elastic modulus could be almost 45% and 17%, respectively.

Morphological studies of these investigations [32-34, 35] generally indicated that TPU and TPE were immiscible with the formation of spherical phases in the PLA matrix. They stated that the reason of very high increases in the % elongation at break and impact toughness values was basically rubber toughening mechanisms, such as crazing, shear deformation and particle cavitation, while the reason of the decreases in the strength and elastic modulus was insufficient interfacial interactions between the PLA matrix and TPU or TPE spherical phases.

1.5.3 Studies on the Compatibilization of PLA Blends

Blending studies discussed above generally indicated that elastomeric materials used were immiscible with PLA leading to phase separation; and forming round or irregularly shaped domains in the continuous matrix of PLA.

Investigators reported that due to the rubber toughening mechanisms elastomeric domains in the PLA matrix increased ductility (% elongation at break) and toughness (Charpy or Izod impact) of PLA significantly. However, they also reported that, in return to the toughening, there were certain level of reductions in the stiffness and strength of PLA. Morphological studies of these investigations generally indicated that interfacial adhesion between the PLA matrix and elastomeric domains were very weak; which should be responsible for the reductions in strength.

It is known that, in the blend compatibilization studies one of the most widely used technique to improve interfacial interactions between the polymer matrix and the second phases is maleic anhydride (MA) compatibilization. This technique can be used in two ways; MA graft copolymerization of the matrix polymer, or maleation of the second phase.

In this respect, in order to not sacrifice strength and modulus values of PLA blends, there are limited number of studies using interfacial compatibilization via MA grafted PLA structure, i.e. PLA-g-MA. In these studies, PLA-g-MA compatibilization was used between PLA and soy protein [36], starch [37, 38, 39], poly (hydroxybutyrate) (PHB) [40, 41], poly(butylene adipate-co-terephthalate) (PBAT) [42-45]. They generally reported that using PLA-g-MA resulted in smaller domains, i.e. higher surface area, and improved interfacial adhesion between the PLA matrix and the second phase leading to higher mechanical performance.

1.6 Aim of the Study

In terms of engineering applications the most significant problem to replace petroleum based traditional polymers with biopolymer PLA is its inherent brittleness. In the literature, limited number of studies [22-31] used “rubber toughening” approach to increase the toughness of PLA by blending with ethylene copolymers. These studies in the literature generally used one type of ethylene copolymer, specimens were shaped in the form of sheets by compression molding, and toughness values were measured as Charpy or Izod impact and/or % elongation at break values.

Therefore, the aim of the first part of the thesis was to compare influences of three different elastomeric ethylene copolymers (EVA, EMA, EBA-GMA) on the toughness of PLA not only by impact tests but also “fracture toughness (K_{IC} and G_{IC}) tests” of bulk specimens shaped by injection molding. Moreover, influences of EVA, EMA and EBA-GMA on the engineering performance of PLA were also investigated by other mechanical tests (tensile, bending, hardness), thermal analyses (differential

scanning calorimetry (DSC), thermogravimetric analysis (TGA), dynamic mechanical analysis (DMA)) and melt flow index, while scanning electron microscopy (SEM) was used for morphological investigation.

In order not to sacrifice strength and modulus of PLA after blending with ethylene copolymers, there are only around four studies [32-34, 35] investigating the effects of blending PLA with thermoplastic elastomers.

Therefore, the aim of the second part of this thesis was to contribute to the limited number of PLA/thermoplastic elastomer blending studies by comparing the effects of two different thermoplastic elastomers (TPU and TPE) on the toughness and other properties of PLA. Moreover, thermoplastic polyester elastomer used in this study contains between 20% and 60% renewably sourced biomass. Therefore, it was designated as “BioTPE”, and its toughening effects in PLA will be the first one in the literature.

Investigators indicated that elastomeric materials used were generally immiscible with PLA leading to domain formation. It is known that compatibility between polymer matrices and domains could be improved by maleic anhydride compatibilization. However, to the best of our knowledge, there is no study reported yet using PLA-g-MA compatibilization for the blends of PLA with any thermoplastic elastomers.

Therefore, the purpose of the third part of this thesis is, for the first time, to investigate the effects of using PLA-g-MA on the toughness and other mechanical and thermal properties of PLA blended with two different thermoplastic elastomers TPU and BioTPE.

CHAPTER 2

EXPERIMENTAL WORK

2.1 Materials Used

(i) Matrix Polymer (PLA)

Poly lactide (PLA) used in this study was a commercial injection molding grade polymer (NaturePlast, PLI 003). Technical data sheet of this PLA indicates that its melting temperature range is 145°-155°C, degradation temperature range is 240°-250°C, melt flow index range at 190°C is 35 g/10 min, and its density is 1.25 g/cm³. In this study, in order to determine molecular weight of this PLA, gel permeation chromatography (GPC) (Polymer Laboratories PL-GPC 220) was conducted giving the results of $M_w=978949$ and $M_n=156654$ with a polydispersity index of 6.25.

(ii) Ethylene Copolymers (EVA, EMA, EBA-GMA)

The first elastomeric ethylene copolymer used was ethylene vinyl acetate (EVA) with 28 wt% vinyl acetate content (Dupont, Elvax 220W) having density of 0.951 g/cm³, melting and maximum process temperatures of 70° and 230°C, respectively.

The second ethylene copolymer was ethylene methyl acrylate (EMA) with 24 wt% methyl acrylate content (Dupont, BiomaxStrong 120) having density of 0.94 g/cm³, melting and maximum process temperatures of 72° and 280°C, respectively.

The third one was ethylene-*n*-butyl acrylate-glycidyl methacrylate (EBA-GMA) with 28 wt% butyl acrylate and 5.25 wt% glycidyl methacrylate content (Dupont, Elvaloy PTW) having density of 0.94 g/cm³, melting and maximum process temperatures of 72° and 310°C, respectively.

(iii) Thermoplastic Elastomers (TPU, BioTPE)

Thermoplastic Polyurethane Elastomer (TPU) used was also a commercial product (Interplast, Epaflex EL 392 A 25) with the given properties; density=1.19 kg/dm³, hardness=93 Shore A, tensile strength=40 MPa, and elongation at break=550%. TPU's are block copolymers formed by the reaction of diisocyanates, oligomeric diols and low molecular weight diols (also called chain extenders). Their soft segments usually consist of high molecular weight (600-4000) polyether or polyester glycols, while hard segments are composed of diisocyanate and low molecular weight (60-400) diols.

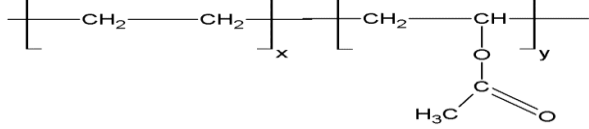
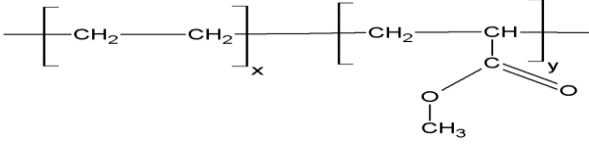
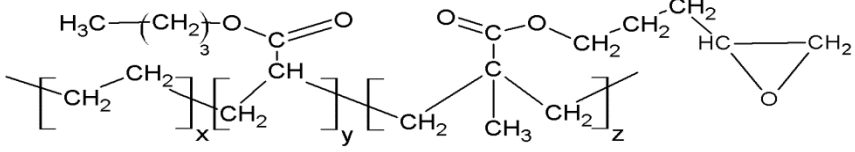
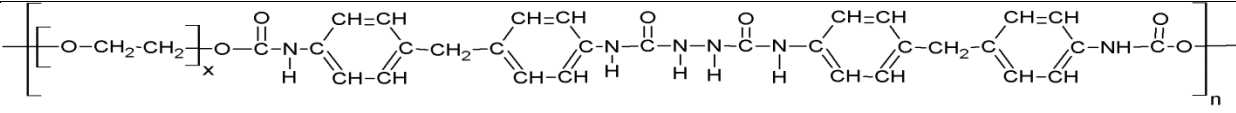
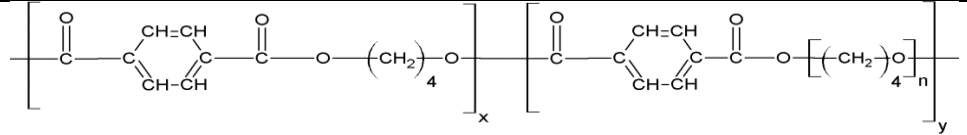
BioThermoplastic Polyester Elastomer (BioTPE) used was another commercial product (Dupont, Hytrel RS 40F3 NC010) with the given properties; density=1.11 g/cm³, hardness=37 Shore D, stress at break=26 MPa, strain at break=650%. It is another block copolymer with soft segments of poly(tetramethylene ether) glycol terephthalate blocks, and hard segments of poly(butylene terephthalate) blocks. The producer indicates that this BioTPE contains between 20% and 60% renewable sourced polyether glycol derived from non-food biomass.

Chemical structures of the ethylene copolymers and the thermoplastic elastomers used are shown in Table 2.1.

(iv) Compatibilizing Agent (MA)

Maleic anhydride (MA) (Sigma-Aldrich, purity 99%) used for grafting of PLA has molecular weight of 98.06 g/mol, melting temperature range of 51-56°C and boiling temperature of 200°C. Initiator used for MA grafting reaction was dicumyl peroxide (DCP) (Sigma-Aldrich, purity 99%) with melting temperature of 39°C.

Table 2.1 Chemical Structure of the Elastomeric Materials Used

Elastomeric Materials	Chemical Structures
Ethylene vinyl acetate (EVA)	
Ethylene methyl acrylate (EMA)	
Ethylene- <i>n</i> -butyl acrylate-glycidyl methacrylate (EBA-GMA)	
Thermoplastic polyurethane elastomer (TPU)	
Thermoplastic polyester elastomer (BioTPE)	

2.2 Compounding and Shaping of the Specimens

Before blending, raw materials were first dried in a 60°C vacuum oven. Pre-drying period for PLA granules and PLA-g-MA pellets was 12 hours while it was 4 hours for TPU and BioTPE granules. Pre-drying period for EVA, EMA, EBA-GMA granules was 3-4 hours at 50°C. Then, these dried materials were pre-mixed manually. Finally, these mixtures were melt blended via a lab-size twin-screw extruder (Rondol Microlab 400) having a screw diameter of 10 mm and L/D ratio of 20. The temperature profile used for this process was 117°-185°-195°-190°-165°C from feeder to die, and the screw speed was kept at 75 rpm. Then, the blended compounds were pelletized by using a four-blade cutter into pellets of 2-3 mm.

Before shaping, pellets were re-dried in a vacuum oven for 12 hours at 60°C. Specimens for testing and analyses were shaped by using a laboratory scale injection molder (DSM Xplore Micro). Barrel temperature was selected as 180°C whereas the mold temperature was kept at 35°C. Melting time for the blends in the barrel was about 7 minutes, while three-step pressure-time profile during molding was; 12 bar for 2 s, 10 bar for 5 s, and 10 bar for 5 s, respectively.

2.3 Morphological Analysis by Scanning Electron Microscopy

Scanning electron microscopy (SEM) (FEI Nova Nano 430) was conducted in order to observe morphology of fracture surfaces and distribution of EVA, EMA, EBA-GMA, TPU, and BioTPE domains in the PLA matrix. Sample surfaces were coated with a thin layer of gold to avoid electrostatic charging and provide conductive surfaces.

In order to determine average sizes of the round-shaped EVA, EMA, EBA-GMA, TPU and BioTPE domains, SEM images were evaluated using an image analyses software (ImageJ 1.48v, National Institutes of Health, USA). Size determinations were made by evaluating at least 150 domain images.

2.4 Mechanical Tests Performed

Mechanical tests were carried out to determine significant mechanical properties of all specimens. Tensile and flexural tests were conducted using a 5 kN universal testing machine (Instron 5565A) at a crosshead speed of 1 mm/min according to ISO 527-2 and ISO 178 standards, respectively.

K_{IC} and G_{IC} fracture toughness tests were performed on the same machine at a crosshead speed of 10 mm/min according to ISO 13586 standard by using single-edge-notched-bending specimens. On these specimens, required notches and initial pre-cracks were formed by a notching-precracking system (Ceast Notchvis). Charpy impact tests were performed for the unnotched specimens using a Ceast Resil Impactor 25 J according to ISO 179-1 standard.

All these mechanical tests were conducted at least for five specimens of each formulation, and the data were evaluated as the average values with standard deviations. Shore D type hardness tests were also conducted to the specimen surfaces with at least 10 measurements using a Zwick/Roell HPE II digital durometer.

2.5 Thermal Analyses Conducted

Three different thermal analyses were carried out to determine the thermal behavior of the specimens. First of all, differential scanning calorimetry analyses (DSC) (SII X-DSC 700 Exstar) were used to determine the important transition temperatures and enthalpies of melting and crystallization of the samples during a heating profile from -80° to 220°C at a rate of $10^{\circ}\text{C}/\text{min}$ under nitrogen flow.

Then, thermogravimetric analyses (TGA) (SII TG/DTA 7300 Exstar) were conducted to determine the thermal degradation temperatures of the selected specimens under a heating rate of $10^{\circ}\text{C}/\text{min}$ from 30° to 550°C under nitrogen flow.

Dynamic mechanical analyses (DMA) (Perkin Elmer DMA 8000) were also done in order to investigate thermomechanical properties of selected specimens having a size of 40x10x4 mm³. Analyses were performed in three-point bending mode at a frequency of 1 Hz. The temperature program was run from 20° to 100°C at a heating rate of 2°C/min.

2.6 Melt Flow Index Determination

Melt flow index measurements were performed for the constituent materials PLA, EVA, EMA, EBA-GMA, TPU, BioTPE separately, and for their blends of each combination according to ISO 1133 standard using an Instron/Ceast MF20 under a load of 2.16 kg. The temperature level for the blends with ethylene copolymers was 190°C, while for the blends with thermoplastic elastomers with and without compatibilization was 220°C.

2.7 Infrared Spectroscopy

In the third part of this thesis, Fourier transform-infrared (FTIR) spectroscopy was used first to characterize formation of PLA-g-MA structure, and then to characterize possible interfacial interactions between TPU, BioTPE domains and MA grafts. Analyses were conducted via attenuated total reflectance (ATR) unit of FTIR spectrometer (Bruker ALPHA). A minimum of 32 scans were signal-averaged with a resolution of 4 cm⁻¹ in the wavenumber range of 400 to 4000 cm⁻¹.

CHAPTER 3

RESULTS AND DISCUSSION

As stated before, since this dissertation has three different parts, their results are presented and discussed successively in the following three subsections.

3.1 Effects of Ethylene Copolymers

In this first part of the thesis, PLA was melt blended by using each ethylene copolymer with the loadings of 5, 10, 15 and 20 phr (parts per hundred resin). These blends were designated by using the format of “PLA/EVA x ”, “PLA/EMA x ” and “PLA/EBA-GMA x ”, where x denotes phr of EVA, EMA and EBA-GMA used.

3.1.1 Morphology and Distribution of the Ethylene Copolymer Domains

SEM images in Figure 3.1 were taken from the fracture surfaces of fracture toughness specimens. It was seen that neat PLA has very smooth fracture surface indicating its inherent brittleness. Contrarily, fracture surfaces of all PLA/ethylene copolymer blends were very rough due to the large amount of shear yielding, i.e. plastic deformation, occurred during fracture.

SEM fractographs in Figures 3.1 and 3.2 also revealed that all the ethylene copolymers were thermodynamically immiscible with PLA matrix resulting in “two-phase structure”, where PLA was the continuous phase while EVA, EMA and EBA-GMA were separated phases forming round-shaped domains.

It is known that mechanical properties of polymer blends are always influenced by the distribution and size of the domains. SEM images in Figures 3.1 and 3.2 show that EVA, EMA and EBA-GMA domains were distributed rather uniformly in the PLA matrix. It was also seen that these domains were finely sized between 1 and 5 microns. Average sizes of these domains tabulated in Table 3.1, determined by using an image analysis software, indicated that sizes of these domains increased from 1-2 microns at 5 phr content to 4-6 microns at 20 phr content. Increases in the domain size at higher contents were due to the “coalescence” of these domains with each other.

Table 3.1 Average Domain Sizes Determined by an Image Analysis Software

Specimens	Average Domain Size (μm)
PLA/EVA 5	1.10 \pm 0.99
PLA/EVA 10	3.45 \pm 3.06
PLA/EVA 20	5.65 \pm 4.25
PLA/EMA 5	2.01 \pm 1.50
PLA/EMA 10	2.54 \pm 1.68
PLA/EMA 20	4.17 \pm 2.65
PLA/EBA-GMA 5	1.24 \pm 1.01
PLA/EBA-GMA 10	2.11 \pm 1.83
PLA/EBA-GMA 20	5.02 \pm 4.09

Of course, mechanical properties of blends are influenced not only by the size and distribution of domains, but also by the compatibility between the polymer matrix and phase separated domains. It was expected that some level of compatibility would be obtained due to the possible chemical interactions between the carboxyl, hydroxyl end groups and carbonyl groups of PLA and polar groups of ethylene copolymers, such as; vinyl acetate group of EVA, methyl acrylate group of EMA, glycidyl methacrylate group (especially its epoxide group) of EBA-GMA.

However, SEM images in Figures 3.1 and 3.2 indicated that, there were certain level of debonding between the PLA matrix and domains of EVA, EMA and EBA-GMA. Many domains were pulled-out from the PLA matrix, either. Thus, it can be concluded that compatibility between PLA matrix and domains of EVA, EMA and EBA-GMA was very weak. On the other hand, as will be discussed in the following sections, even these slightly compatible elastomeric domains resulted in very significant improvements in ductility and toughness values of PLA.

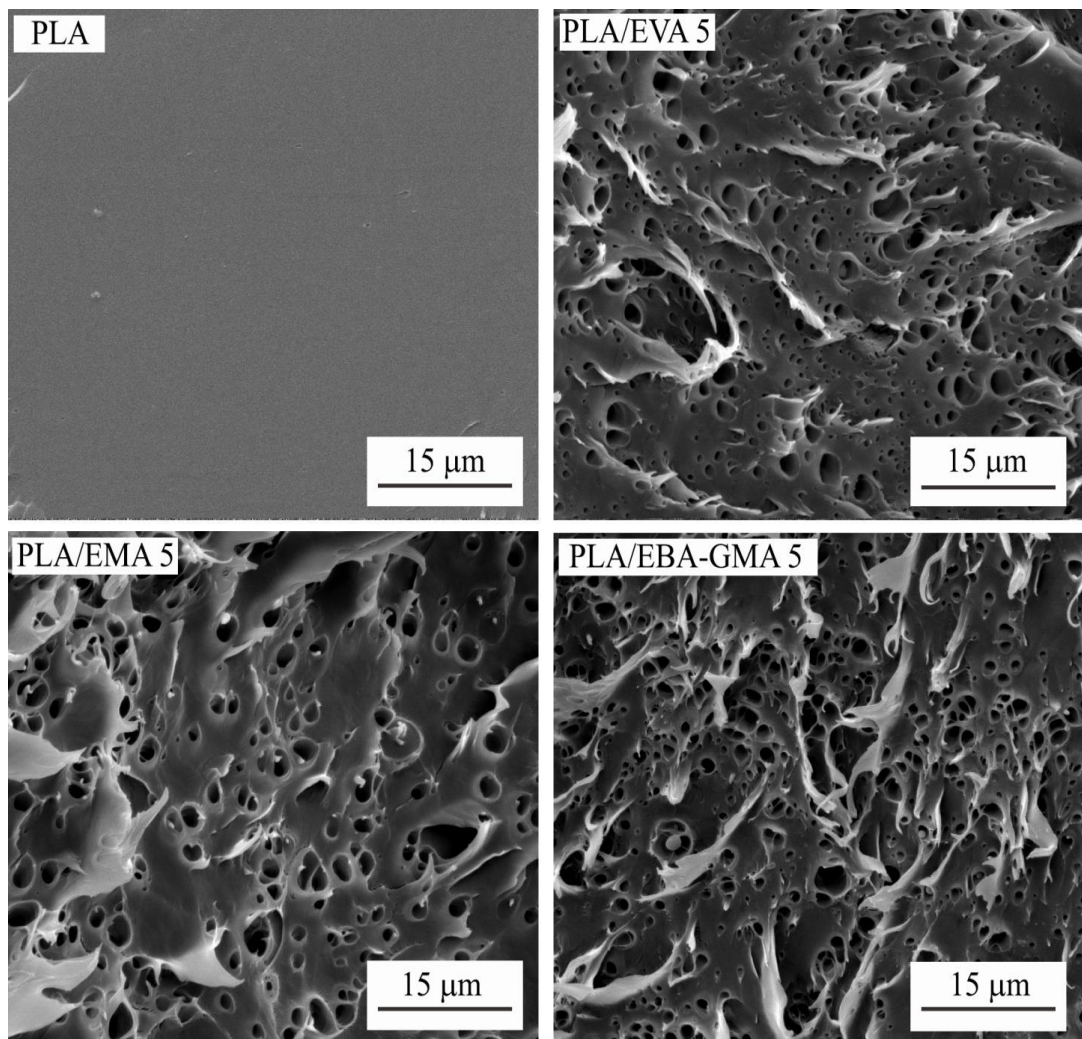


Figure 3.1 Smooth SEM Fractograph of Neat PLA and Rough Fractographs of PLA Blends Showing Finely and Uniformly Distributed EVA, EMA and EBA-GMA Domains

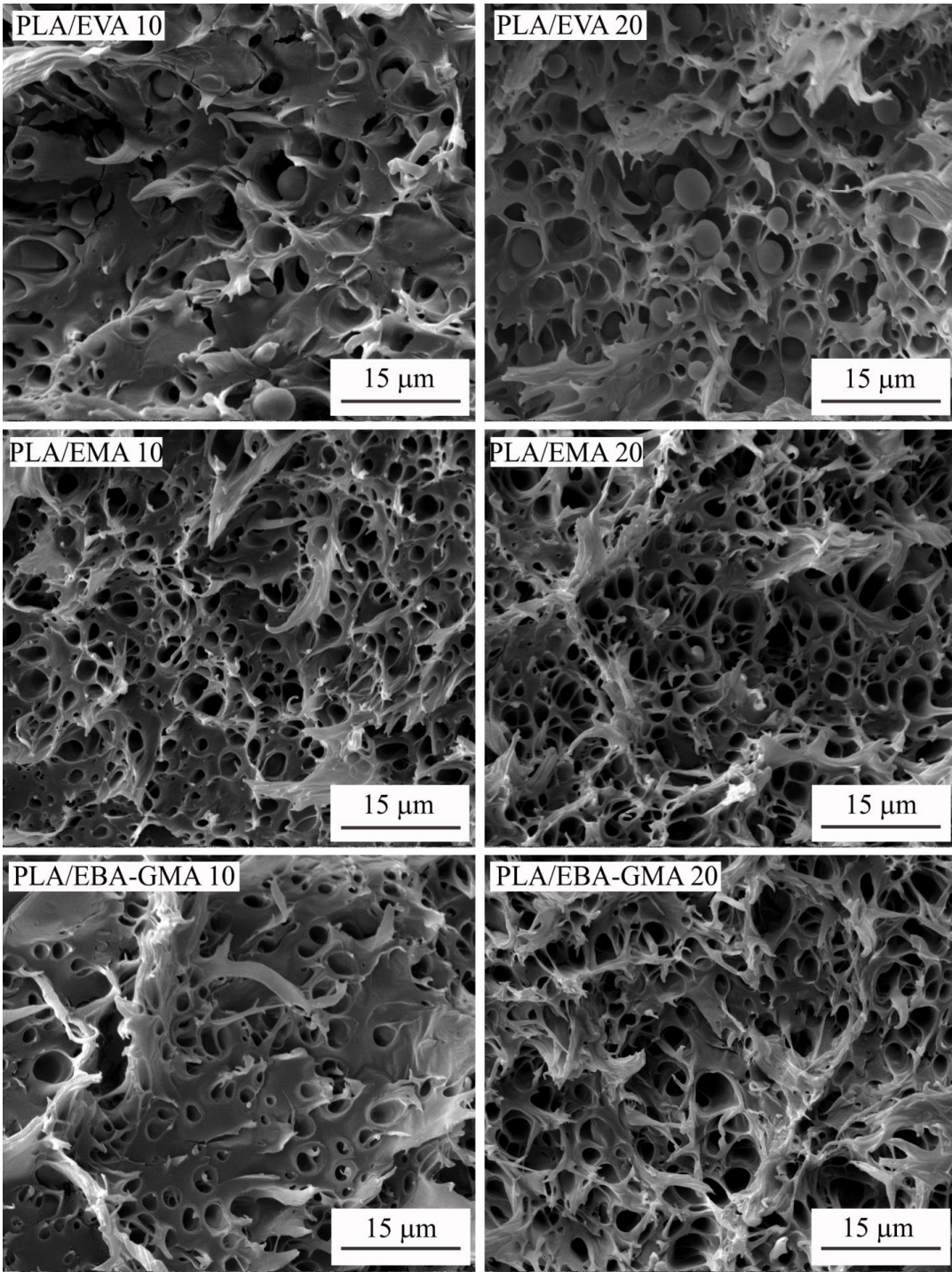


Figure 3.2 SEM Fractographs Showing Interfacial Interactions between PLA Matrix and Domains of EVA, EMA and EBA-GMA with Debonded and Pulled-Out Morphology

3.1.2 Melt Flow Behavior of the Blends with Ethylene Copolymers

Many industrial melt processing methods such as extrusion and injection molding of the blends are influenced by their melt flow index (MFI) values. Thus, in this study, MFI values were measured for the neat constituent materials (i.e. PLA, EVA, EMA, EBA-GMA) and for their blend combinations, as given in Table 3.2.

Table 3.2 Melt Flow Index (MFI) Values of the Constituent Materials and Blends with Ethylene Copolymers at 190°C under 2.16 kg

Blends	MFI (g/10 min)
PLA	55±1
EVA	150±1
EMA	9±1
EBA-GMA	16±1
PLA/EVA 5	63±1
PLA/EVA 10	65±1
PLA/EVA 15	72±1
PLA/EVA 20	101±1
PLA/EMA 5	64±1
PLA/EMA 10	56±1
PLA/EMA 15	58±1
PLA/EMA 20	56±1
PLA/EBA-GMA 5	79±1
PLA/EBA-GMA 10	65±1
PLA/EBA-GMA 15	58±1
PLA/EBA-GMA 20	57±1

Table 3.2 indicated that MFI value of PLA increased slight when ethylene copolymers were incorporated. It is known that elastomeric nature of these ethylene copolymers might act as plasticizer which increases mobility of the PLA macromolecular chains. In this case, since viscosities of PLA blends were lowered, then in return, their MFI values were increased.

Table 3.2 also showed that increases in MFI values were only important at 15 phr and 20 phr EVA incorporation, while there were slight increases with EMA and EBA-GMA incorporation. Therefore, it can be said that, blending PLA with these ethylene copolymers up to 20 phr content has no significant influence on the melt processability of PLA.

3.1.3 Stiffness, Strength and Hardness of the Blends with Ethylene Copolymers

Stiffness (elastic modulus) and strength of the specimens were examined under two different types of loading; tensile and flexural. That is, both tension and three-point bending tests were applied. Stress-strain curves obtained during these tests are given in Figure 3.3, while values of elastic modulus and strength of the specimens determined are tabulated in Table 3.3 together with hardness values measured by Shore D type digital durometer. Effects of three different ethylene copolymer content on modulus, strength and hardness are also evaluated in Figures 3.4 and 3.5.

Elastic modulus i.e. stiffness of polymers depends on resistance to flexibility and mobility of their chain structure. Ethylene copolymers used have very low sub-zero T_g values. Therefore, at room temperature they give mobility to the molecular structure of PLA. Thus, Figures 3.3 and 3.4, and Table 3.3 indicate that both elastic modulus values, i.e. “Young’s Modulus” (E) determined by tension tests and “Flexural Modulus” (E_{Flex}) determined by bending tests decreased gradually with the addition of each ethylene copolymers. For instance, when 5 phr EVA, EMA and EBA-GMA were added, decreases in E value of PLA were 18%, 17% and 13%, respectively, while in terms of E_{Flex} these decreases were 15%, 7% and 11%,

respectively. Increasing the ethylene copolymer content decreased these elastic modulus values even further. Highest decreases in elastic modulus values were of course with 20 phr contents. For example, using 20 phr EBA-GMA resulted in 33% and 30% decreases in E and E_{Flex} values, respectively.

Hardness is the resistance of the material surface against indentation which again decreases with the flexibility and mobility of the polymer chain structure. Therefore, Table 3.3 also indicated that using ethylene copolymers decreased hardness of PLA at a certain level. For example, blending with 5 phr EVA, EMA and EBA-GMA decreased Shore D hardness value by 7%, 9% and 6%, respectively. Increasing the ethylene copolymer content resulted in further slight decreases.

In terms of strength, Figures 3.3 and 3.5, and Table 3.3 indicated that when ethylene copolymer contents were 5 phr, then there were almost no detrimental effects of ethylene copolymers on both “Tensile Strength” (σ_{TS}) and “Flexural Strength” (σ_{Flex}) values of PLA. However, these strength values decreased at higher contents of EVA, EMA and EBA-GMA due to their elastomeric nature. Highest decreases were naturally obtained at 20 phr contents. For example, the decreases in σ_{TS} and σ_{Flex} values were as much as 27% and 18%, respectively when 20 phr EVA was incorporated.

Table 3.3 Young's Modulus (E), Flexural Modulus (E_{Flex}), Tensile Strength (σ_{TS}), Flexural Strength (σ_{Flex}) and Hardness (H) Values of the Specimens with Ethylene Copolymers

Blends	E (GPa)	E_{Flex} (GPa)	σ_{TS} (MPa)	σ_{Flex} (MPa)	H (Shore D)
PLA	3.05±0.03	3.72±0.08	51.4±0.7	64.2±1.1	82.3±0.6
PLA/EVA 5	2.51±0.07	3.14±0.06	49.1±1.8	64.8±0.7	76.8±0.7
PLA/EVA 10	2.35±0.04	2.83±0.02	49.0±1.3	59.6±0.9	75.4±0.9
PLA/EVA 15	2.24±0.11	2.72±0.03	38.9±0.7	58.0±0.2	73.3±1.3
PLA/EVA 20	2.17±0.07	2.69±0.05	37.6±1.0	52.4±1.5	73.0±1.3
PLA/EMA 5	2.53±0.06	3.45±0.08	51.4±1.9	62.3±0.9	74.9±0.9
PLA/EMA 10	2.36±0.07	2.91±0.08	48.2±0.8	60.6±1.8	74.3±1.8
PLA/EMA 15	2.22±0.01	2.73±0.05	44.2±2.3	53.9±1.3	74.2±0.6
PLA/EMA 20	2.09±0.02	2.56±0.07	38.8±3.3	51.5±1.6	65.6±0.8
PLA/EBA-GMA 5	2.64±0.13	3.30±0.14	46.9±1.3	59.9±1.9	77.3±0.8
PLA/EBA-GMA 10	2.48±0.05	3.00±0.03	46.5±1.7	58.0±1.1	74.2±1.1
PLA/EBA-GMA 15	2.05±0.08	2.63±0.03	42.0±1.0	57.8±1.2	71.8±0.6
PLA/EBA-GMA 20	2.04±0.02	2.59±0.04	41.0±0.6	54.6±0.7	65.8±0.9

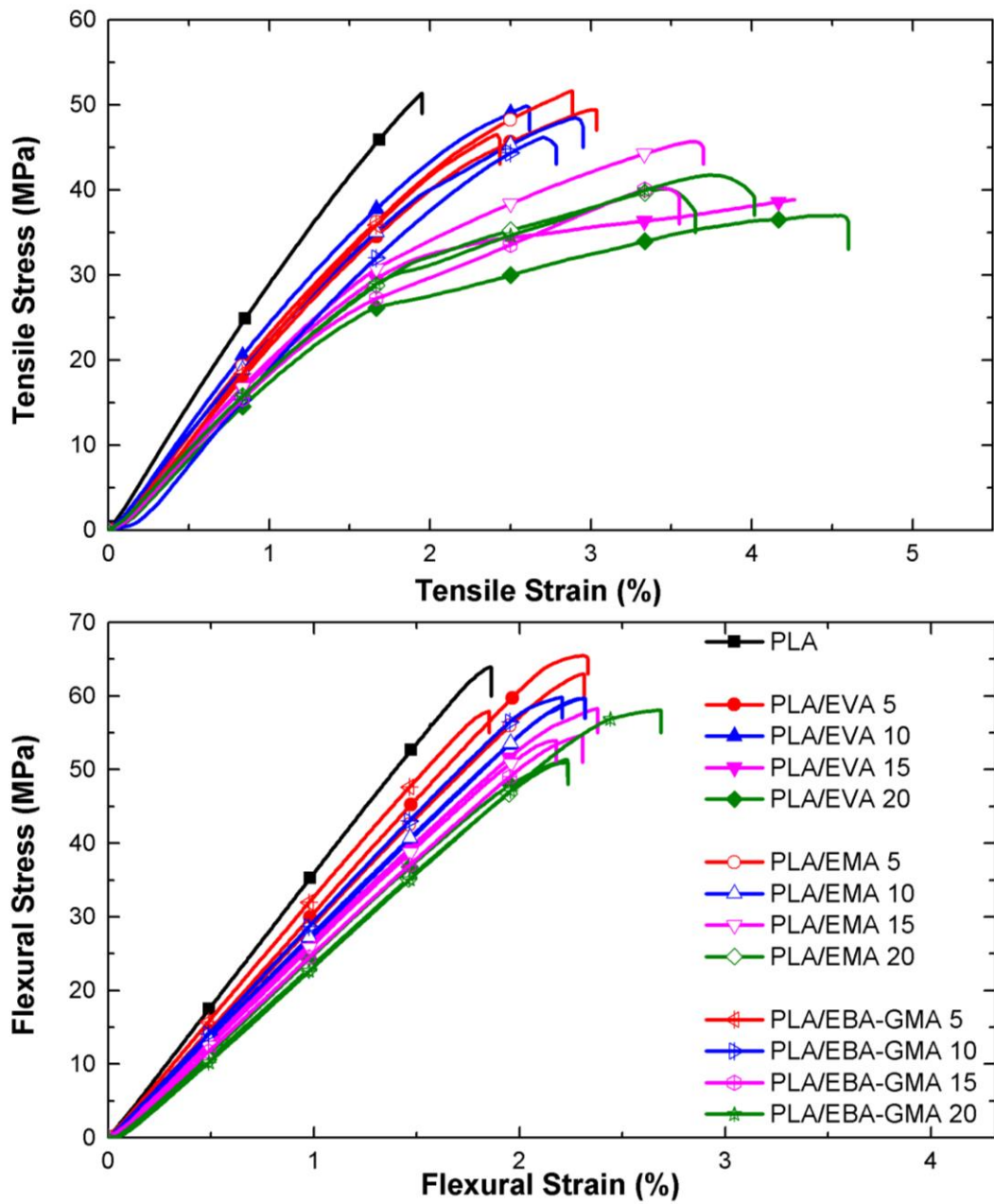


Figure 3.3 Stress-Strain Curves of the Specimens with Ethylene Copolymers Obtained During Tensile and 3-Point Bending (Flexural) Test

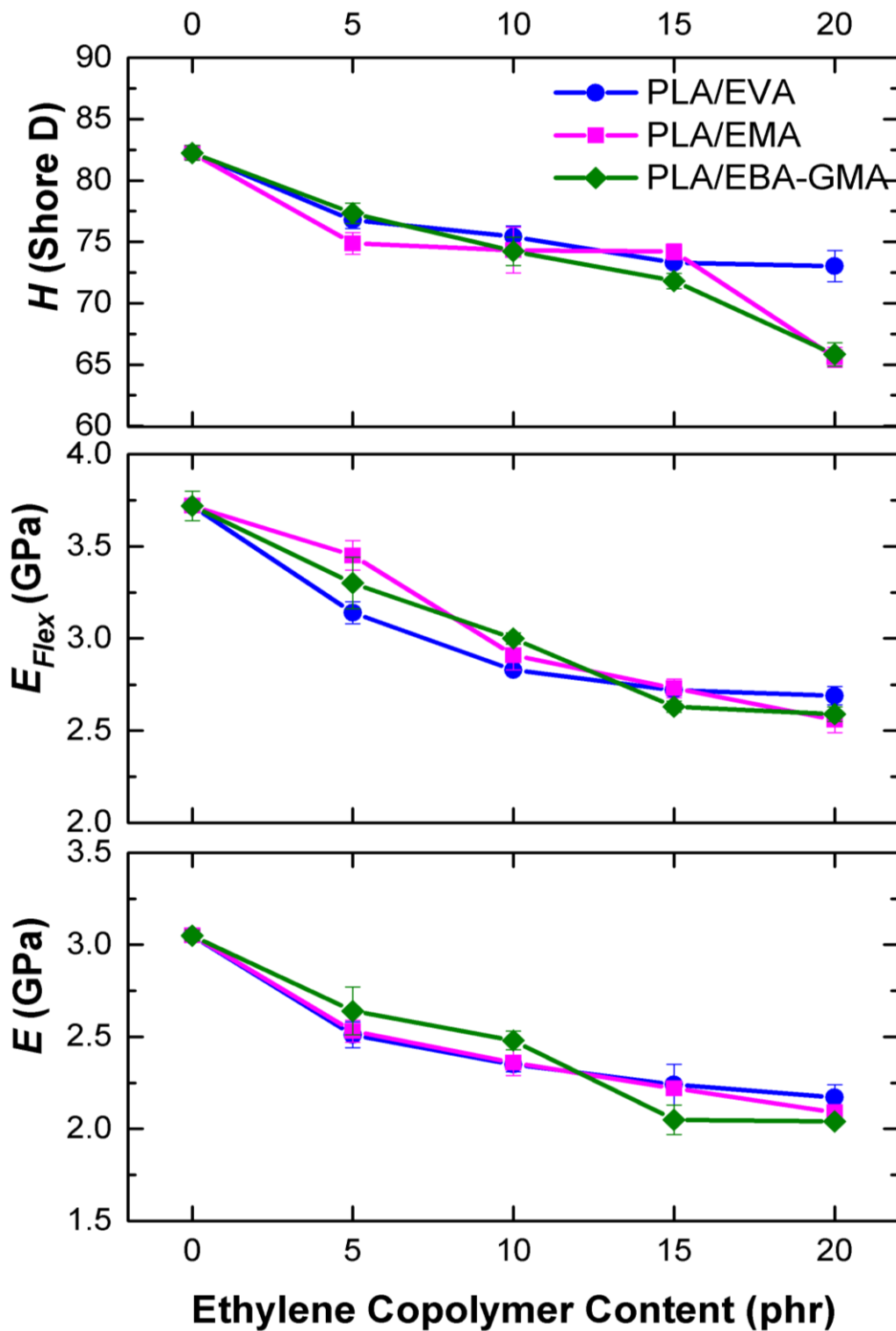


Figure 3.4 Effects of EVA, EMA and EBA-GMA Content on the Tensile Modulus (E), Flexural Modulus (E_{Flex}) and Hardness (H) of the Specimens

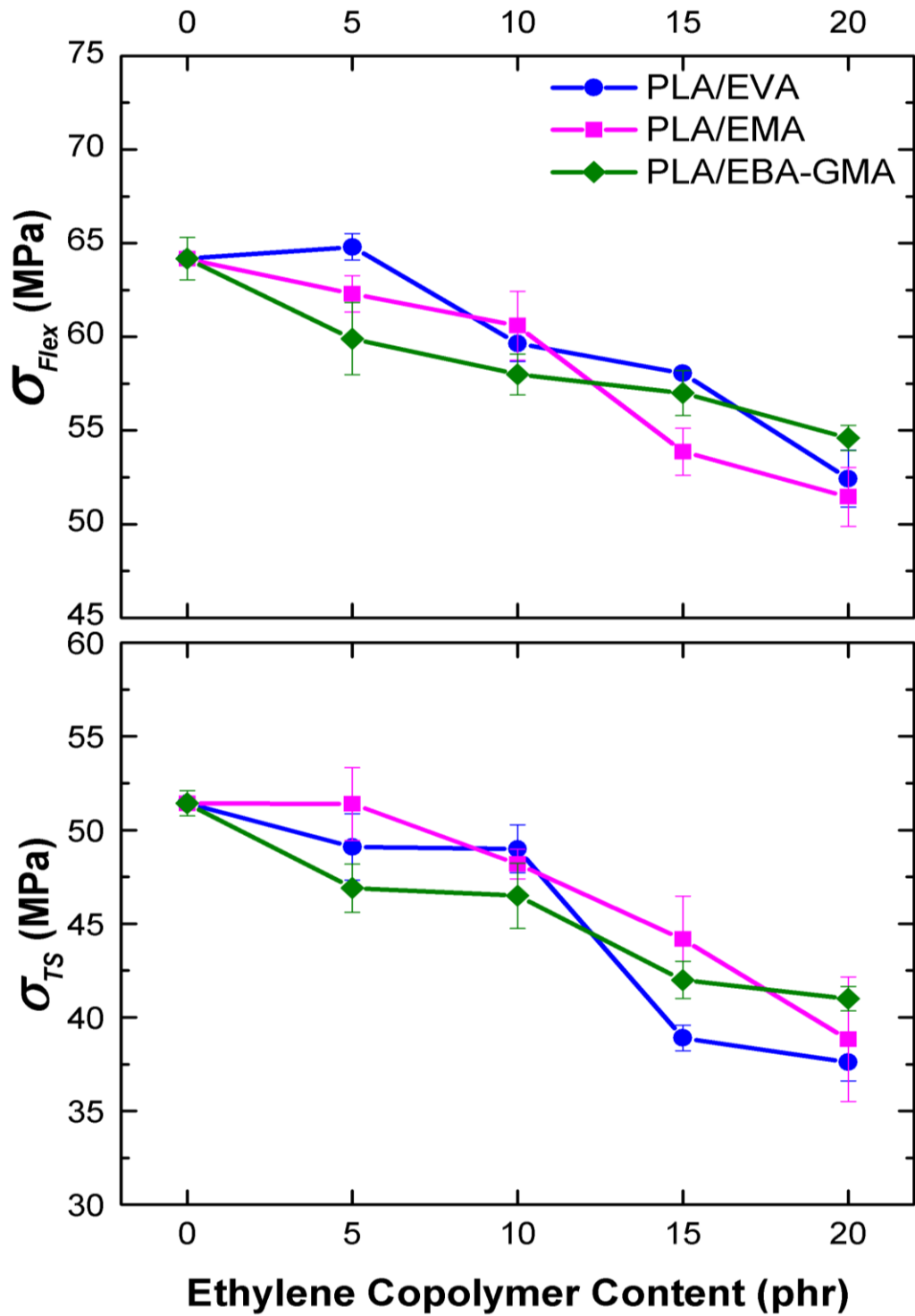


Figure 3.5 Effects of EVA, EMA and EBA-GMA Content on the Tensile Strength (σ_{TS}) and Flexural Strength (σ_{Flex}) of the Specimens

3.1.4 Ductility and Toughness of the Blends with Ethylene Copolymers

Ductility is the ability of materials to have permanent plastic deformation up to fracture; it can be measured by the amount of final strain at break in the tension test. Tensile stress-strain curves in Figure 3.3 revealed that linear curve of neat PLA with very little plastic strain transforms into non-linear curves with larger amounts of plastic deformation when ethylene copolymers were incorporated.

This transition from brittle to ductile behavior could be due to the plasticizing effects of ethylene copolymers added. Ductility values in terms of % final strain at break (ϵ_f) in Table 3.4 and Figure 3.6 showed that increasing the amount of ethylene copolymers increased the ϵ_f values. For instance, ductility of PLA increased from 1.95% up to 5.01%, 3.67% and 4.25% by introducing 20 phr EVA, EMA and EBA-GMA, respectively, i.e. an increase of more than twice.

The most significant problem of PLA to be used in many applications is its inherent brittleness, i.e. low toughness. Therefore, in this study, effects of blending with three different ethylene copolymers on the toughness of PLA were investigated by Charpy impact toughness and also by fracture toughness tests according to ISO 179-1 and ISO 13586 standards, respectively. “Unnotched Charpy Impact Toughness (C_U)” values and “Fracture Toughness” in terms of both “ K_{IC} ” (Critical Stress Intensity Factor) and “ G_{IC} ” (Critical Strain Energy Release Rate) values are tabulated in Table 3.4, and the effects of EVA, EMA and EBA-GMA contents are evaluated in Figure 3.6.

Impact toughness is the ability of materials to absorb energy of the dynamic impact loads. Just like ductility (ϵ_f) values, Table 3.4 and Figure 3.6 indicated that unnotched Charpy impact toughness (C_U) of neat PLA increased significantly by blending with all ethylene copolymers. Increases in the C_U value of neat PLA (15.6 kJ/m²) was more than twice with 20 phr EVA content, while it was more than 4 times with 20 phr EMA and EBA-GMA contents.

Table 3.4 Tensile Strain at Break (ϵ_f), Unnotched Charpy Impact Toughness (C_U), and Fracture Toughness (K_{IC} and G_{IC}) Values of the Specimens with Ethylene Copolymers

Blends	ϵ_f (%)	C_U (kJ/m ²)	K_{IC} (MPa√m)	G_{IC} (kJ/m ²)
PLA	1.95±0.05	15.6±0.5	2.93±0.14	3.75±0.02
PLA/EVA 5	2.62±0.19	18.4±1.5	3.35±0.17	6.55±0.04
PLA/EVA 10	3.07±0.37	29.7±8.2	3.53±0.13	8.60±0.11
PLA/EVA 15	5.01±0.58	36.7±5.2	3.54±0.09	8.72±0.02
PLA/EVA 20	5.01±0.36	38.2±8.9	3.59±0.04	9.68±0.29
PLA/EMA 5	2.89±0.11	38.9±9.5	3.37±0.12	7.77±0.16
PLA/EMA 10	2.92±0.12	52.7±0.8	3.47±0.06	8.29±0.15
PLA/EMA 15	3.36±0.22	63.1±4.5	3.61±0.05	8.56±0.19
PLA/EMA 20	3.67±0.53	65.2±9.5	3.69±0.08	8.83±0.03
PLA/EBA-GMA 5	2.51±0.08	17.0±0.7	3.32±0.19	7.53±0.86
PLA/EBA-GMA 10	2.89±0.14	60.6±9.0	3.39±0.13	7.84±0.49
PLA/EBA-GMA 15	3.65±0.39	62.2±8.2	3.41±0.06	7.90±0.01
PLA/EBA-GMA 20	4.25±0.17	66.4±4.9	4.10±0.04	8.74±0.59

Fracture toughness is the most significant toughness value in engineering applications. Because, in these applications components have usually complicated geometries having notches, surface irregularities, etc., making them very prone to crack initiation and growth leading to failure of the components. Thus, fracture toughness values in terms of K_{IC} or G_{IC} represent resistance of the components against crack initiation and crack growth rate.

Table 3.4 and Figure 3.6 revealed that blending of PLA with even 5 phr of each ethylene copolymer resulted in very significant increases in the values of K_{IC} and G_{IC} . Of course, increasing the content of ethylene copolymers increased the K_{IC} and G_{IC} values even further. For example, use of 20 phr EVA, EMA and EBA-GMA

resulted in 23%, 26% and 40% increases in K_{IC} values, while these increases were as much as 158%, 136% and 133% in G_{IC} values.

3.1.5 Toughening Mechanisms of the Blends with Ethylene Copolymers

In this study, one of the “rubber toughening” mechanism was “crazing” or “whitening” observed in the necked region of the specimens during tensile tests. These microvoided regions could form due to the microcavitation around the elastomeric domains in the matrix.

Another important rubber toughening mechanism observed was “shear banding” also named “shear yielding” or “shear deformation”, i.e. formation of large extent of plastic deformation before fracture. As discussed above, SEM fractographs (Figures 3.1 and 3.2) revealed that very smooth fracture surface of neat PLA without any sign of plastic deformation transformed into very rough fracture surfaces after blending with EVA, EMA and EBA-GMA. These rough surfaces especially around the elastomeric domains represent large amount of plastic deformation that could absorb the energy required for the crack propagation. In this mechanism, size and distribution of the elastomeric domains are also important. Because, decreasing the size will increase the surface area of domains leading to formation of more plastic deformation. In this study, EVA, EMA and EBA-GMA domains were uniformly distributed with very fine sizes of less than 5 microns.

Other toughening mechanisms especially responsible for the improved K_{IC} and G_{IC} fracture toughness values observed were “debonding” at the interface between the PLA matrix and EVA, EMA and EBA-GMA domains, and “pull-out” of these domains from the matrix, as shown in SEM fractographs of Figures 3.1 and 3.2. Because, these two mechanisms together with the well known “crack deflection” mechanism would absorb the energy of the main cracks started to propagate. Thus, mechanisms of debonding, pull-out and crack deflection would delay the fracture of the component.

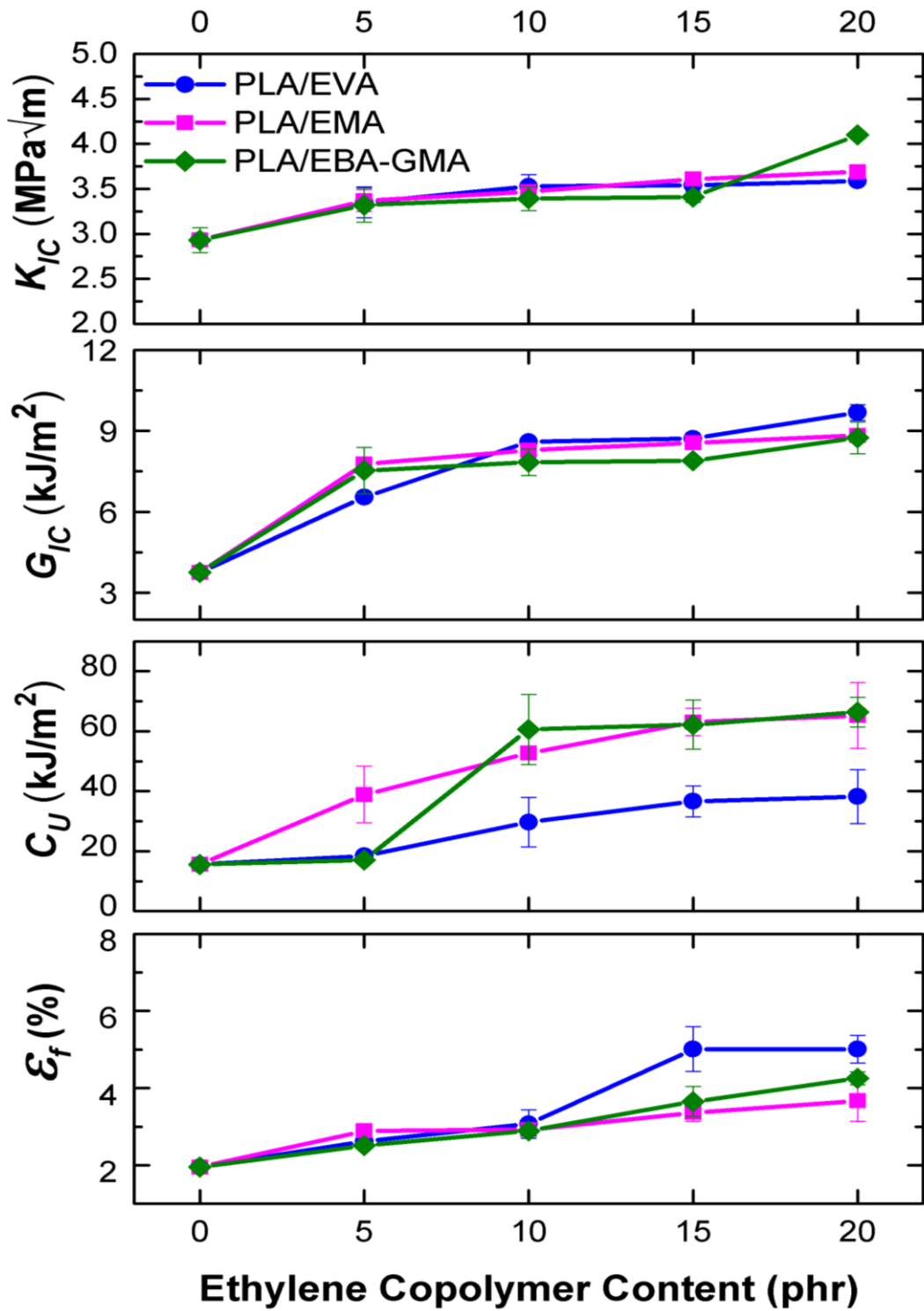


Figure 3.6 Effects of EVA, EMA and EBA-GMA Content on the Ductility (% Strain at Break- ϵ_f), Impact Toughness (Unnotched Charpy- C_U) and Fracture Toughness (K_{IC} and G_{IC}) of the Specimens

3.1.6 Thermal Transition Temperatures and Crystallinity of the Blends with Ethylene Copolymers

Thermal behaviors of the specimens were first investigated by conducting differential scanning calorimetry (DSC) analyses. Figure 3.7 shows heating thermograms of the specimens obtained after erasing their thermal history. Then, important transition temperatures, i.e. “glass transition, crystallization, melting” (T_g , T_c , T_m), together with “enthalpies of melting and crystallization” (ΔH_m and ΔH_c) were determined and tabulated in Table 3.5. This table also includes “percent crystallinity” (X_c) of the specimens obtained using the following relation:

$$X_c = \frac{\Delta H_m - \Delta H_c}{w_{PLA} \Delta H_m^o} \times 100 \quad (3.1)$$

where w_{PLA} is the weight fraction of the PLA matrix, while ΔH_m^o is the melting enthalpy of 100 % crystalline PLA given as 93 J/g in the literature [46].

It was seen in Table 3.5 that incorporation of ethylene copolymers has almost no influence on the T_g , T_c and T_m values of the PLA matrix. As discussed before in SEM analysis, phase separation occurred via formation of round ethylene copolymer domains indicated the immiscibility of PLA with these three copolymeric materials. Therefore, DSC analysis showing no change in the T_g of PLA and its blends could be another confirmation of the immiscibility of PLA with EVA, EMA and EBA-GMA.

Table 3.5 also showed that there were certain variations in the crystallinity percent (X_c) of neat PLA and its blends. Especially at higher ethylene copolymer contents, X_c increased significantly. For instance, X_c of neat PLA (14.7%) increased up to 27%, 22.8% and 18.3% with the incorporation of 20 phr EVA, EMA and EBA-GMA, respectively. Because, at higher ethylene copolymer contents their plasticizing effect would be sufficient for the required level of mobility of PLA molecular chains to crystallize more.

Table 3.5 Transition Temperatures (T_g , T_c , T_m), Enthalpies (ΔH_m , ΔH_c) and Crystallinity Percent (X_C) of the Specimens with Ethylene Copolymers During Heating Profile

Specimens	T_g (°C)	T_c (°C)	T_m (°C)	ΔH_m (J/g)	ΔH_c (J/g)	X_C (%)
PLA	60.1	106.2	169.8	41.0	27.3	14.7
PLA/EVA 5	60.9	107.3	170.9	39.9	31.8	9.2
PLA/EVA 10	61.7	105.4	170.6	33.3	19.0	17.1
PLA/EVA 15	61.9	105.1	170.7	34.0	20.0	17.7
PLA/EVA 20	61.2	102.4	170.0	36.5	16.4	27.0
PLA/EMA 5	61.4	110.5	171.0	40.1	32.0	9.2
PLA/EMA 10	61.1	104.5	170.3	36.5	22.2	17.1
PLA/EMA 15	61.2	107.4	170.5	34.4	23.9	13.3
PLA/EMA 20	61.4	102.6	170.2	35.5	18.5	22.8
PLA/EBA-GMA 5	61.3	107.7	170.8	37.7	28.8	10.1
PLA/EBA-GMA 10	61.6	107.5	171.5	35.8	23.5	14.7
PLA/EBA-GMA 15	60.8	109.3	170.5	35.3	25.6	12.3
PLA/EBA-GMA 20	61.4	108.8	170.5	35.7	22.1	18.3

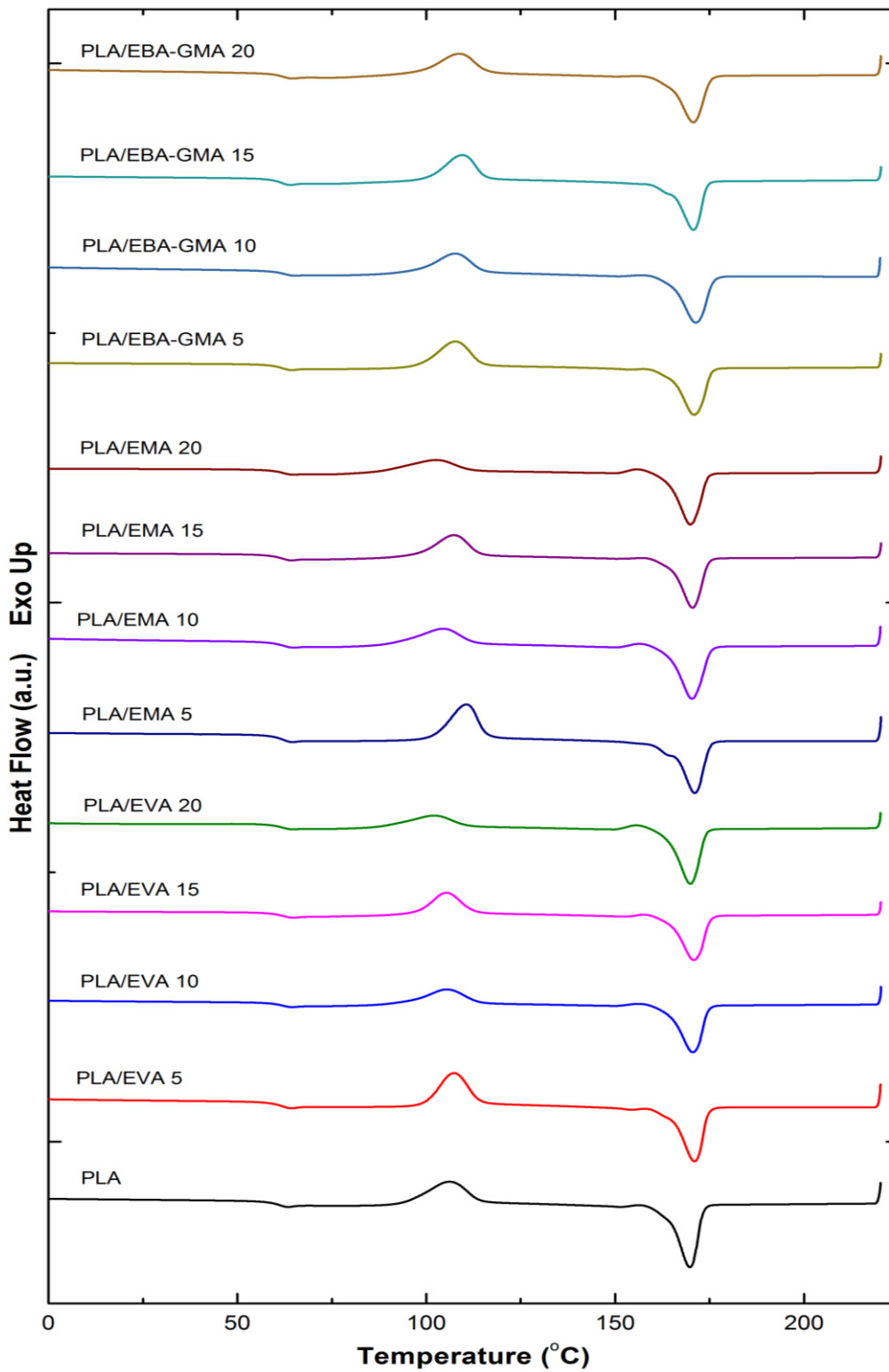


Figure 3.7 DSC Heating Thermograms of the Specimens with Ethylene Copolymers Obtained After Erasing their Thermal History

3.1.7 Thermal Degradation and Thermomechanical Behavior of the Blends with Ethylene Copolymers

Thermal degradation behavior of the constituent materials and their 5 phr blends was investigated by thermogravimetric analysis (TGA), where data were evaluated in the form of thermogravimetric (TG) and differential thermogravimetric (DTG) curves. In Figure 3.8, only PLA and its 5 phr blends are shown. Certain levels of thermal degradation temperatures determined from these curves are tabulated in Table 3.6. In this table, $T_{5\%}$, $T_{10\%}$, $T_{25\%}$ represent thermal degradation temperatures of the specimens at 5, 10, 25 wt% mass loss in TG curves, while T_{max} represents maximum mass loss rate peak temperature of the specimens in DTG curves.

Since all thermal degradation temperatures of ethylene copolymers were higher than that of neat PLA, Table 3.6 indicated that there were no decreases; instead there were a few degrees of improvement, in the thermal degradation temperatures of PLA blends. Thus, it can be said that there were no detrimental effects on the thermal degradation of PLA when blended with EVA, EMA and EBA-GMA.

Thermomechanical behavior of the neat PLA and its blends with 5 phr ethylene copolymers were investigated by conducting dynamic mechanical analysis (DMA). Storage modulus versus temperature curves obtained are given in Figure 3.9. Then, two levels of “Storage Modulus” (E') at 25° and 50°C were determined and tabulated in Table 3.7.

Table 3.6 Thermal Degradation Temperatures ($T_{5\%}$, $T_{10\%}$, $T_{25\%}$) of the Constituent Materials and 5 phr Blends with Ethylene Copolymers at 5, 10, 25 wt% Mass Losses and their Maximum Mass Loss Rate Peak (T_{max})

Specimens	$T_{5\%}$ (°C)	$T_{10\%}$ (°C)	$T_{25\%}$ (°C)	T_{max} (°C)
PLA	327	337	350	366
EVA	337	350	428	473
EMA	405	418	435	448
EBA-GMA	406	420	439	450
PLA/EVA 5	332	341	352	367
PLA/EMA 5	332	341	353	368
PLA/EBA-GMA 5	330	340	352	366

Table 3.7 Storage Modulus (E') Values of PLA and its Blends with 5 phr Ethylene Copolymers at 25° and 50°C

Specimens	E' at 25°C (GPa)	E' at 50°C (GPa)
PLA	2.78	2.72
PLA/EVA 5	2.95	2.85
PLA/EMA 5	2.63	2.58
PLA/EBA-GMA 5	3.12	2.93

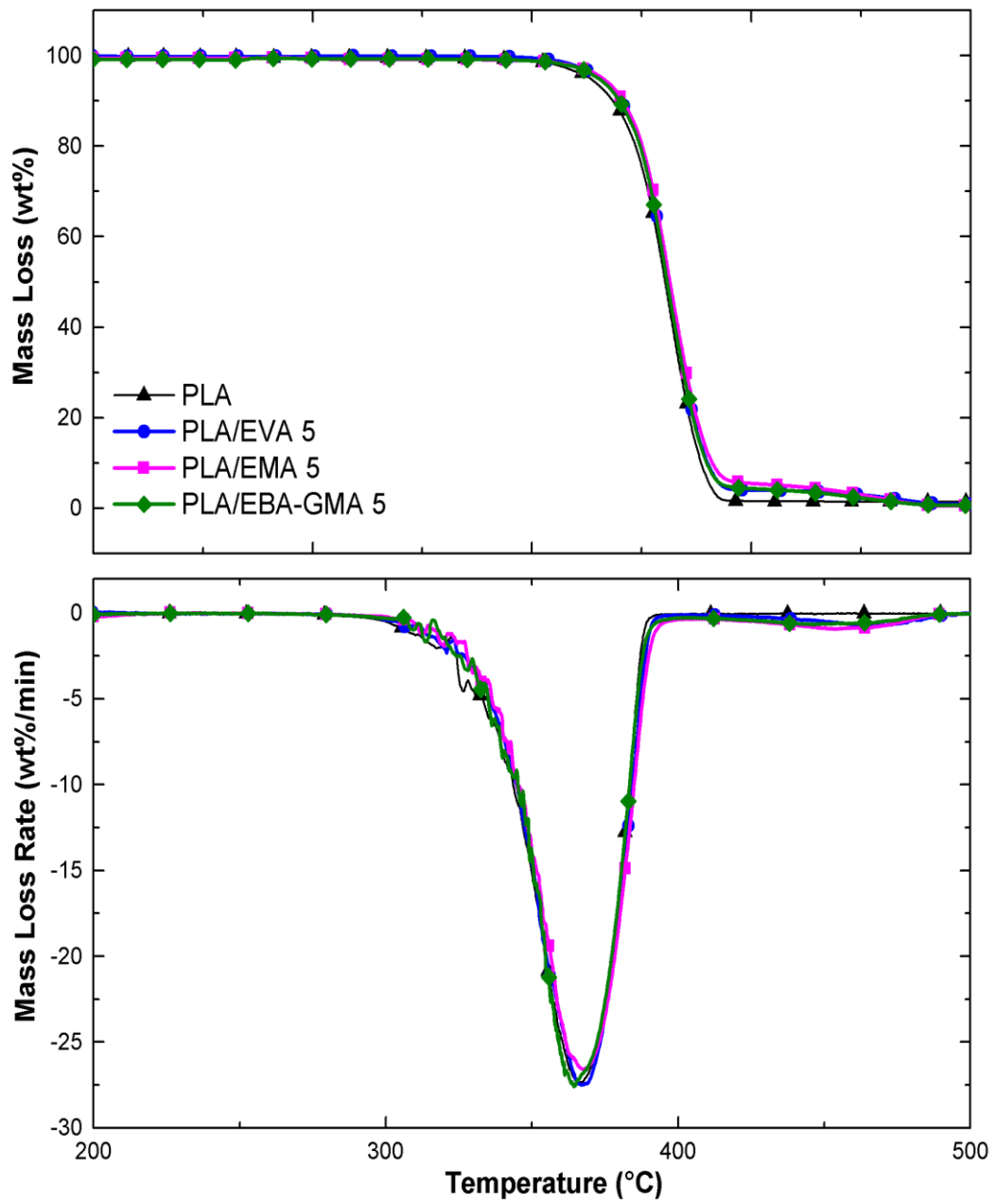


Figure 3.8 Thermogravimetric (TG) and Differential Thermogravimetric (DTG) Curves of PLA and its Blends with 5 phr Ethylene Copolymers

Figure 3.9 showed that storage modulus of PLA and its blends vanished at 60°C which was the T_g of PLA where blocks of polymer chain segments move over each other easily and quickly. Although addition of EMA decreased E' values of PLA slightly, addition of EVA and EBA-GMA increased. For example, increases in the value of E' at 50°C were 5% and 8% when PLA was blended with 5 phr EVA and EBA-GMA, respectively. Therefore, it can be said that incorporation of EVA, EMA and EBA-GMA had no detrimental effects on the thermomechanical behavior of PLA.

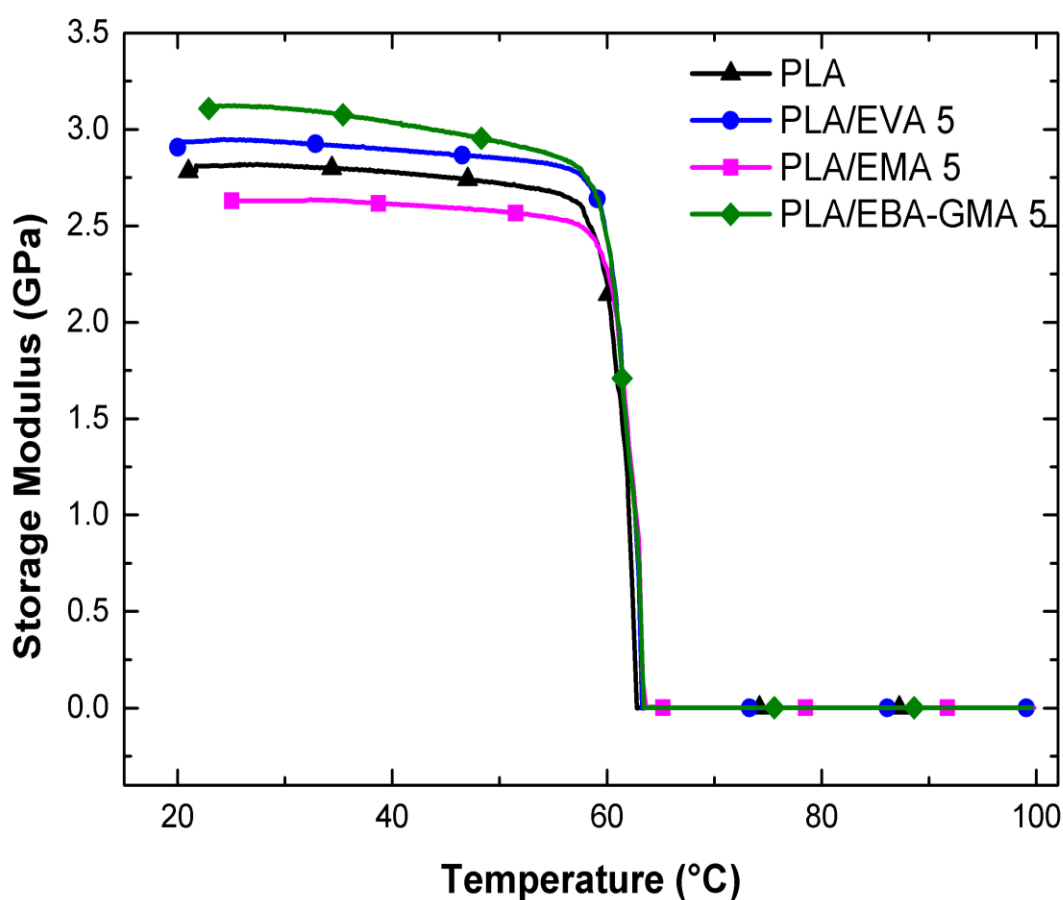


Figure 3.9 Storage Modulus Curves of PLA and its Blends with 5 phr Ethylene Copolymers Obtained by DMA

3.2 Effects of Thermoplastic Elastomers

In this second part of the thesis, PLA was melt blended using each thermoplastic elastomer with the loadings of 5, 10, 15, and 20 phr (parts per hundred resin). These blends were designated using the format of “PLA/TPU x ” and “PLA/BioTPE x ”, where x denotes phr of TPU and BioTPE used.

3.2.1 Morphology and Distribution of the Thermoplastic Elastomer Domains

SEM examination conducted on the fracture surfaces of fracture toughness specimens in Figure 3.10 simply show that neat PLA has very smooth fracture surface indicating its inherent brittleness. On the other hand, fracture surfaces of all PLA blends were again very rough due to the large amount of plastic deformation, i.e. shear yielding, occurred during fracture.

SEM images in Figures 3.10 and 3.11 also clearly show that both of the thermoplastic elastomers were immiscible with PLA leading to two-phase structure, where PLA is the continuous phase while TPU and BioTPE were separated phases forming round-shaped domains.

Distribution and size of the domains are very important influencing the mechanical properties of polymer blends. SEM fractographs taken rather at a lower magnification of 3000X given in Figure 3.10 show that both TPU and BioTPE domains were distributed very homogeneously in the PLA matrix. SEM images also show that domains were finely sized between 1 and 8 microns. Average sizes of the domains given in the Table 3.8 were determined using an image analysis software. Table 3.8 shows that average sizes of the domains increased from 1-2 microns at 5 phr content to 7-8 microns at 20 phr content. The increase in the domain size at higher contents is due to the coalescence of the domains with each other.

Table 3.8 Average Domain Sizes Determined by an Image Analysis Software

Specimens	Average Domain Size (μm)
PLA/TPU 5	1.29 \pm 0.67
PLA/TPU 10	5.13 \pm 2.71
PLA/TPU 20	7.83 \pm 3.44
PLA/BioTPE 5	2.22 \pm 2.17
PLA/BioTPE 10	4.38 \pm 2.13
PLA/BioTPE 20	7.01 \pm 3.22

Apart from size and distribution of domains, another significant aspect influencing all mechanical properties of blends is the compatibility between the polymer matrix and phase separated domains. It was expected that there could be certain chemical interactions between the carboxyl, hydroxyl end groups and carbonyl groups of PLA and polar groups of especially hard segments of thermoplastic elastomers, leading to some compatibility.

On the other hand, SEM fractographs taken at a higher magnification of 5000X given in Figure 3.11 reveal that, there were certain level of debonding between the PLA matrix and domains of TPU and BioTPE. Moreover, some of the domains were pulled-out from the PLA matrix. Therefore, it can be said that compatibility between PLA and domains of TPU and BioTPE was very weak. However, as will be discussed in the following sections, even these slightly compatible domains resulted in very significant improvements in ductility and toughness of PLA.

In the next part of this thesis, in order to have further improvements in toughness together with strength, effects of graft-copolymer compatibilization studies are discussed.

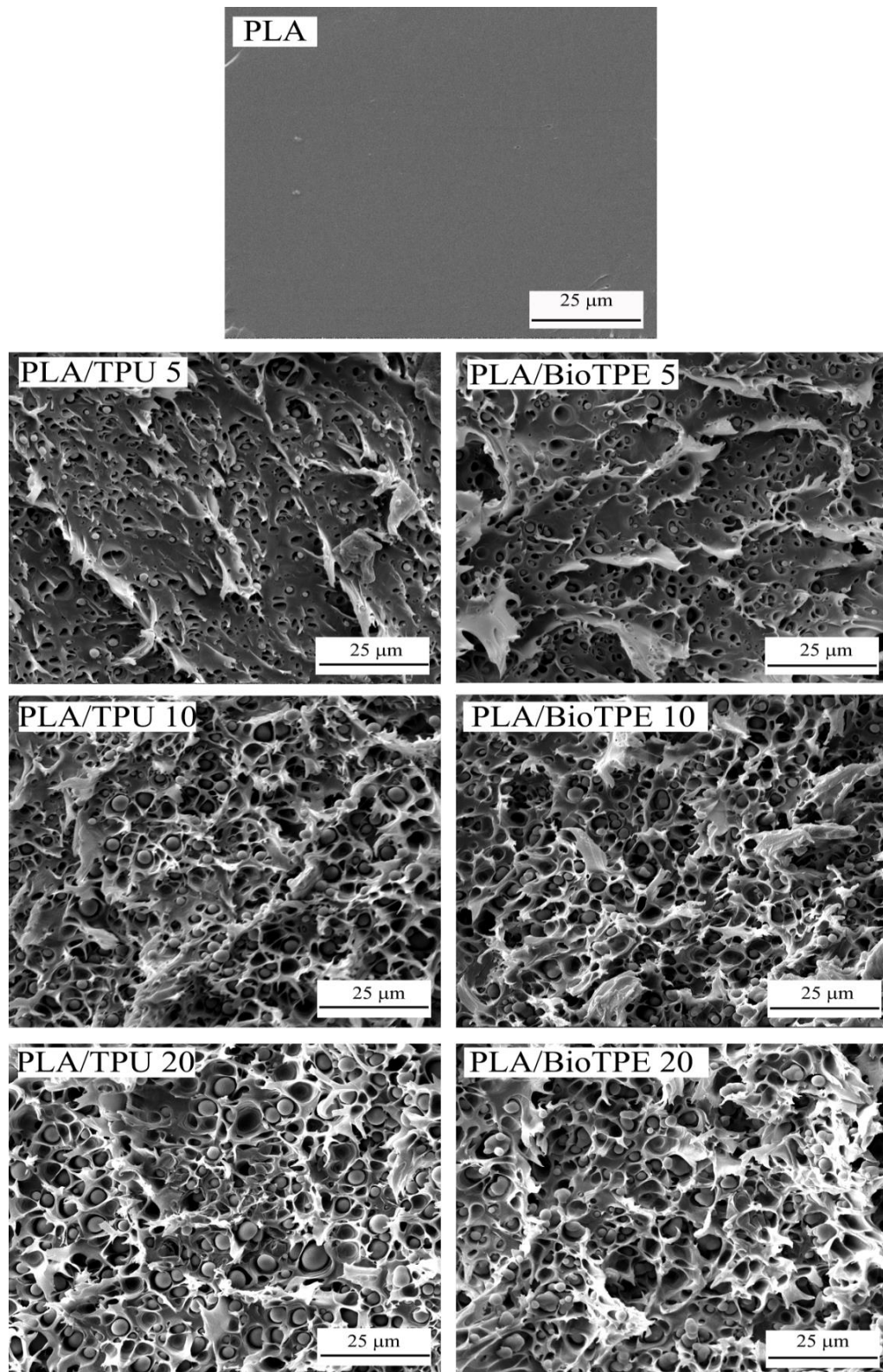


Figure 3.10 Smooth SEM Fractograph of Neat PLA and Rough Fractographs of PLA Blends Showing Finely and Uniformly Distributed TPU and BioTPE Domains

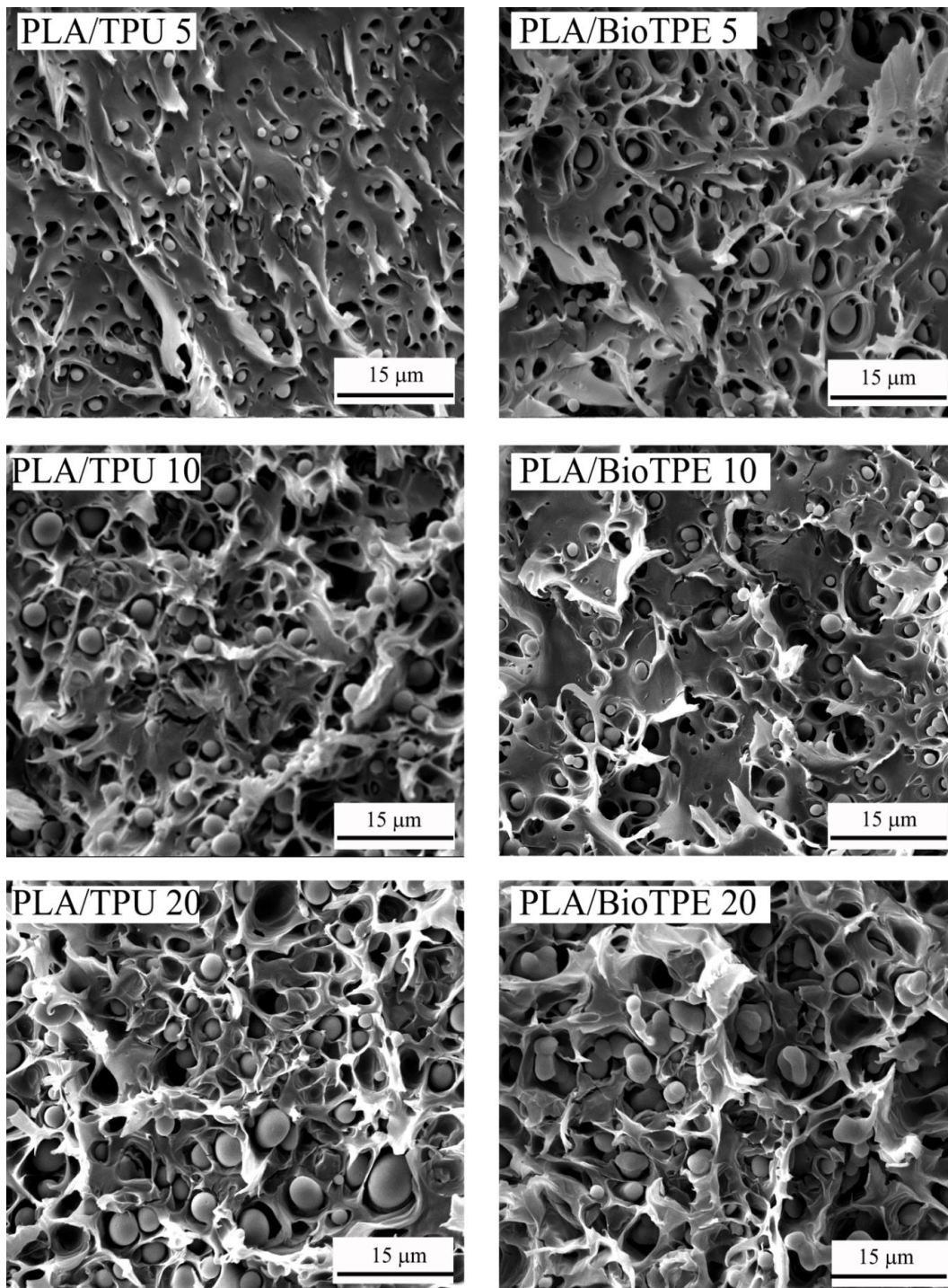


Figure 3.11 SEM Fractographs Showing Interfacial Interactions between PLA Matrix and Domains of TPU and BioTPE with Debonded and Pulled-Out Morphology

3.2.2 Melt Flow Behavior of the Blends with Thermoplastic Elastomers

In the polymer industry to determine the melt processability (such as extrusion and injection molding) of the blends, especially their melt flow index (MFI) values are evaluated. These values measured for the neat constituent materials (i.e. PLA, TPU, BioTPE) and for their blend combinations are tabulated in Table 3.9.

It is seen that neat PLA has much higher MFI value compared to each thermoplastic elastomer. Table 3.9 also shows that when thermoplastic elastomers were incorporated, MFI value of PLA increased even more. For instance, using 10 phr TPU increased MFI value of PLA from 162 to 218 g/10 min; while using 10 phr BioTPE increased to 198 g/10 min. Because, soft segments of these thermoplastic elastomers could act as plasticizers increasing the mobility of the macromolecular chains of PLA. Thus, increased MFI values would be obtained due to the lowered viscosities.

Table 3.9 Melt Flow Index (MFI) Values of the Constituent Materials and Blends with Thermoplastic Elastomers at 220°C under 2.16 kg

Specimens	MFI (g/10 min)
PLA	162±3
TPU	73±4
BioTPE	25±1
PLA/TPU 5	189±3
PLA/TPU 10	218±4
PLA/TPU 15	241±4
PLA/TPU 20	244±5
PLA/BioTPE 5	221±2
PLA/BioTPE 10	198±4
PLA/BioTPE 15	173±2
PLA/BioTPE 20	167±1

3.2.3 Stiffness, Strength and Hardness of the Blends with Thermoplastic Elastomers

Stress-strain curves obtained during tension and three-point bending tests are given in Figure 3.12, while values of elastic modulus and strength of the specimens determined are tabulated in Table 3.10 together with hardness values measured by Shore D type durometer. Effects of thermoplastic elastomer content on modulus, strength and hardness are also evaluated in Figures 3.13 and 3.14.

Soft segments of thermoplastic elastomers have usually amorphous conformation with low T_g values. Therefore, at room temperature they impart mobility to the PLA structure. Thus, Figures 3.12 and 3.13, and Table 3.10 indicate that both elastic modulus values, i.e. Young's modulus (E) and flexural modulus (E_{Flex}) decreased gradually with the addition of each thermoplastic elastomer. For instance, E value of PLA decreased by 12% and 20% with 10 phr TPU and BioTPE, while E_{Flex} value decreased by 8% and 18%, respectively.

Table 3.10 also indicates that soft segments of the thermoplastic elastomers decreased hardness of PLA slightly. Blending with 10 phr TPU and BioTPE decreased Shore D hardness only by 6% and 9%, respectively.

Figures 3.12 and 3.14, and Table 3.10 indicate that there were almost no detrimental effects of thermoplastic elastomers on both tensile strength (σ_{TS}) and flexural strength (σ_{Flex}) values of PLA. Although there were very slight decreases at higher contents (15 and 20 phr) of TPU and BioTPE, there were even slight increases at lower contents (5 and 10 phr).

PLA blends in this study keep the strength values basically due to the hard segments of the thermoplastic elastomers having high T_m values with quite polar intermolecular bonding. Thus, these hard segments could act as fillers or physical crosslinks in the PLA structure compensating the loss of strength due to the plasticizing effects of the soft segments of TPU and BioTPE.

Normally, elastomeric materials increase the ductility and toughness of brittle polymeric materials significantly but with drastic decrease in strength. Therefore, improving toughness of PLA without sacrificing strength by blending with TPU and BioTPE would be an advantage in engineering applications.

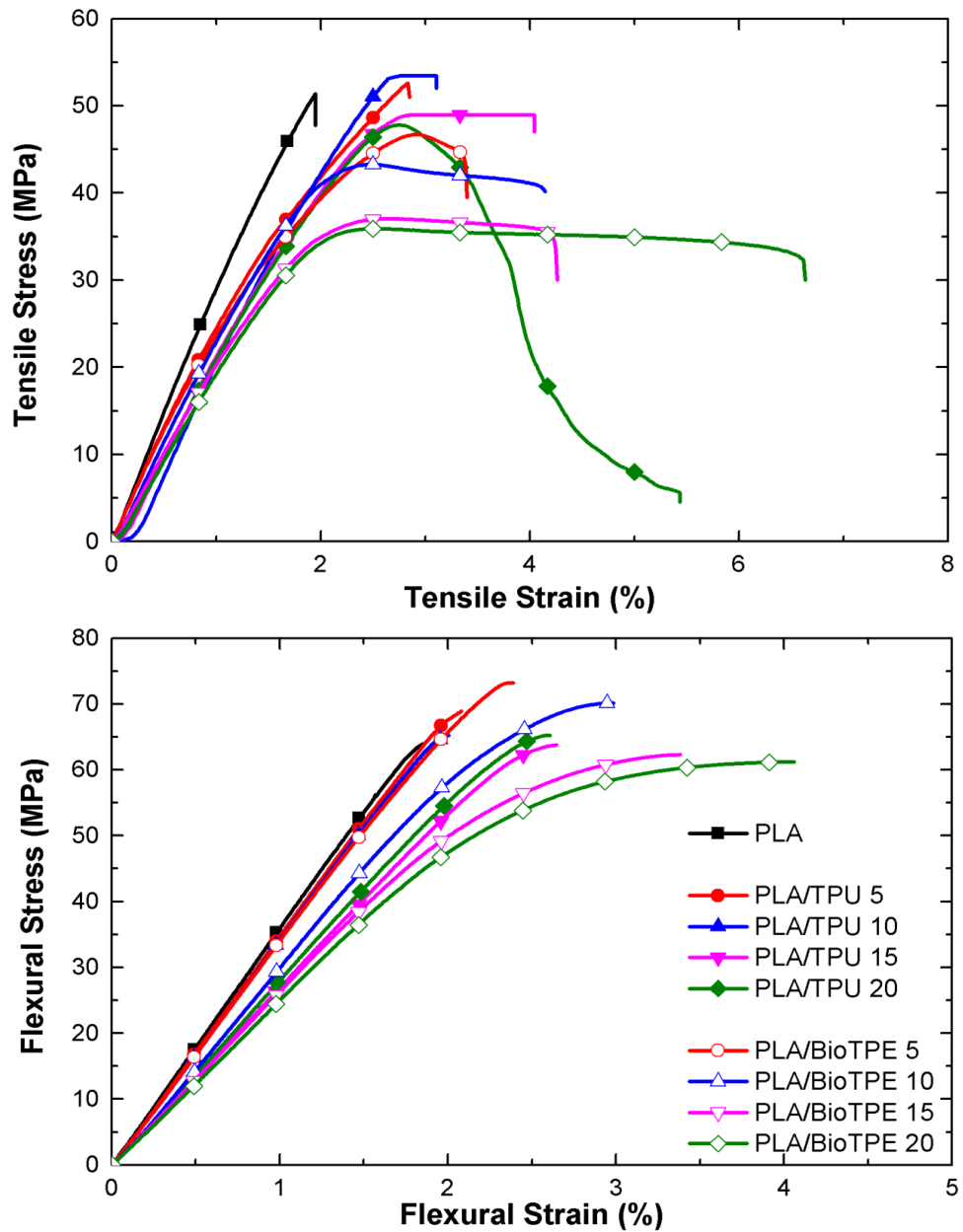


Figure 3.12 Stress-Strain Curves of the Specimens with Thermoplastic Elastomers Obtained During Tensile and 3-Point Bending (Flexural) Test

Table 3.10 Young's Modulus (E), Flexural Modulus (E_{Flex}), Tensile Strength (σ_{TS}), Flexural Strength (σ_{Flex}) and Hardness (H) Values of the Specimens with Thermoplastic Elastomers

Specimens	E (GPa)	E_{Flex} (GPa)	σ_{TS} (MPa)	σ_{Flex} (MPa)	H (Shore D)
PLA	3.05±0.03	3.72±0.08	51.4±0.7	64.2±1.1	82.3±0.6
PLA/TPU 5	2.67±0.06	3.50±0.05	54.7±1.6	68.6±2.5	79.2±1.4
PLA/TPU 10	2.62±0.04	3.40±0.11	53.7±0.6	67.5±1.2	77.4±0.7
PLA/TPU 15	2.43±0.03	2.94±0.05	49.4±0.8	64.1±1.3	76.4±1.0
PLA/TPU 20	2.28±0.07	2.77±0.03	48.0±0.3	63.3±3.0	74.0±1.0
PLA/BioTPE 5	2.65±0.05	3.51±0.03	47.1±0.5	73.6±1.0	76.6±0.9
PLA/BioTPE 10	2.48±0.05	3.00±0.14	42.8±0.6	69.5±2.1	74.9±0.7
PLA/BioTPE 15	2.21±0.03	2.63±0.05	36.5±0.9	61.3±1.0	74.7±0.7
PLA/BioTPE 20	2.10±0.03	2.52±0.05	36.0±0.5	61.2±1.3	74.0±0.8

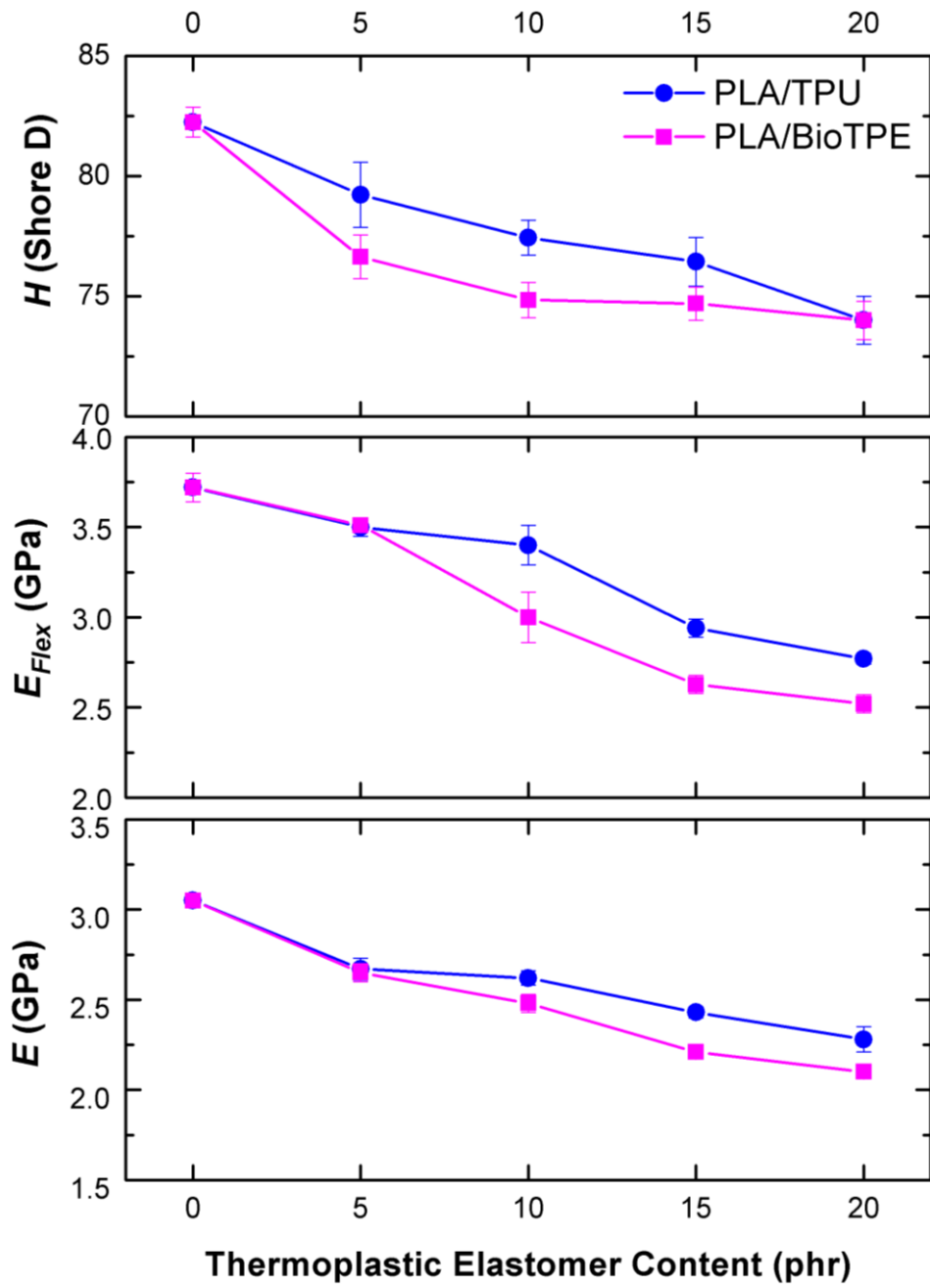


Figure 3.13 Effects of TPU and BioTPE Content on the Tensile Modulus (E), Flexural Modulus (E_{Flex}) and Hardness (H) of the Specimens

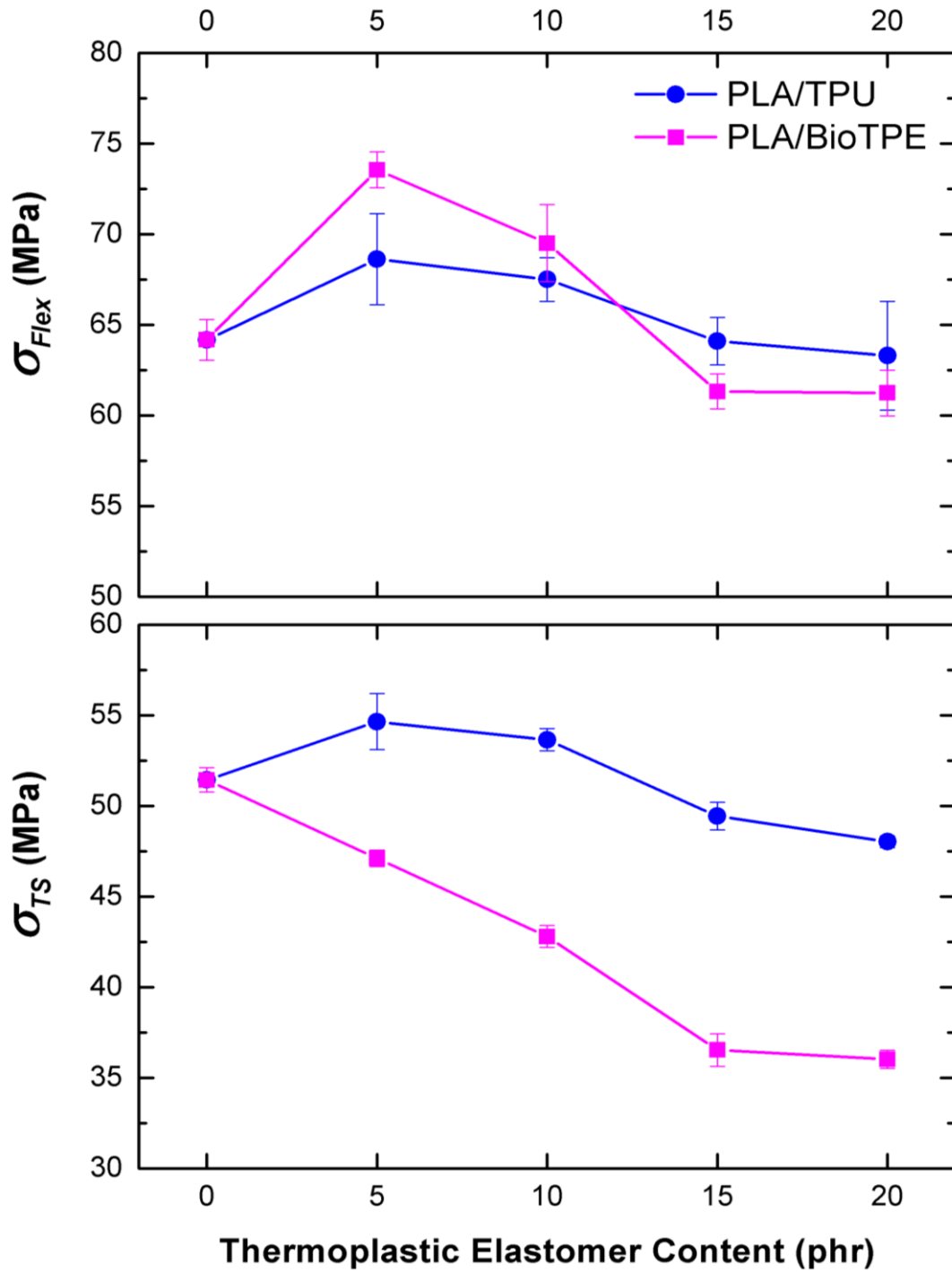


Figure 3.14 Effects of TPU and BioTPE Content on the Tensile Strength (σ_{Ts}) and Flexural Strength (σ_{Flex}) of the Specimens

3.2.4 Ductility and Toughness of the Blends with Thermoplastic Elastomers

Tensile stress-strain curves in Figure 3.12 reveal that linear curve of neat PLA with very little plastic strain transformed into non-linear curves with large amounts of plastic deformation when thermoplastic elastomers were incorporated.

This transition from brittle to ductile behavior should be again due to the plasticizing effects of the soft segments of thermoplastic elastomers added. Ductility values in terms of % final strain at break (ϵ_f) in Table 3.11 and Figure 3.15 show that increasing the amount of thermoplastic elastomers increases the ϵ_f values. For instance, ductility of PLA increased from 1.95% up to 5.43% and 6.32% by using 20 phr TPU and BioTPE, respectively, i.e. an increase of around 3 times.

Unnotched Charpy impact toughness (C_U) values and fracture toughness in terms of both K_{IC} and G_{IC} values are tabulated in Table 3.11, and effects of TPU and BioTPE contents are evaluated in Figure 3.15.

Table 3.11 Tensile Strain at Break (ϵ_f), Unnotched Charpy Impact Toughness (C_U), and Fracture Toughness (K_{IC} and G_{IC}) Values of the Specimens with Thermoplastic Elastomers

Specimens	ϵ_f (%)	C_U (kJ/m ²)	K_{IC} (MPa√m)	G_{IC} (kJ/m ²)
PLA	1.95±0.05	15.6±0.5	2.93±0.14	3.75±0.02
PLA/TPU 5	2.79±0.09	37.7±1.5	3.31±0.19	6.18±0.02
PLA/TPU 10	3.11±0.08	55.9±3.4	3.64±0.47	6.73±0.32
PLA/TPU 15	4.05±0.32	77.7±9.5	3.61±0.05	7.25±0.04
PLA/TPU 20	5.43±0.19	88.6±1.3	3.32±0.05	6.96±0.03
PLA/BioTPE 5	3.41±0.29	64.2±1.7	3.61±0.01	7.29±0.05
PLA/BioTPE 10	3.97±0.46	74.1±5.5	3.94±0.19	8.53±0.08
PLA/BioTPE 15	4.37±0.29	81.1±4.9	3.56±0.19	8.69±0.41
PLA/BioTPE 20	6.32±0.37	95.2±3.4	3.09±0.03	7.26±0.25

Just like ductility (ϵ_f) values, Table 3.11 and Figure 3.15 indicate that unnotched Charpy impact toughness (C_U) of neat PLA increased significantly by blending with both thermoplastic elastomers. Increases in the C_U value of neat PLA (15.6 kJ/m^2) is more than 3 times with 10 phr thermoplastic elastomer content, while it is more than 5 times with 20 phr content.

Table 3.11 and Figure 3.15 reveal that blending PLA with both thermoplastic elastomers results in very significant increases in the values of K_{IC} and G_{IC} . For example, use of 10 phr TPU or BioTPE led to increases in the K_{IC} of neat PLA by 25% and 35%, respectively. Similarly, use of 15 phr TPU or BioTPE resulted in G_{IC} increases as much as 90% and 130%, respectively.

3.2.5 Toughening Mechanisms of the Blends with Thermoplastic Elastomers

The most significant rubber toughening mechanism observed in this part was shear banding also named shear yielding or shear deformation, i.e. formation of large extent of plastic deformation before fracture. SEM fractographs (Figures 3.10 and 3.11) revealed that very smooth fracture surface of neat PLA without any sign of plastic deformation transformed into very rough fracture surfaces after blending with TPU and BioTPE. These rough surfaces especially around the elastomeric domains represent large amount of plastic deformation which could absorb the energy required for crack initiation and crack growth leading to fracture.

In this mechanism, size and distribution of the elastomeric domains are also important. Because, decreasing the size would increase the surface area of domains leading to formation of more plastic deformation. In this part, TPU and BioTPE domains were uniformly distributed with rather fine sizes. However, at high thermoplastic elastomer contents, e.g. at 20 phr, there was a tendency of coalescence of domains resulting in larger domain sizes as shown in Table 3.8 and Figures 3.10 and 3.11. Therefore, there were slight decreases in the values of K_{IC} and G_{IC} of the blends with 20 phr TPU and BioTPE content.

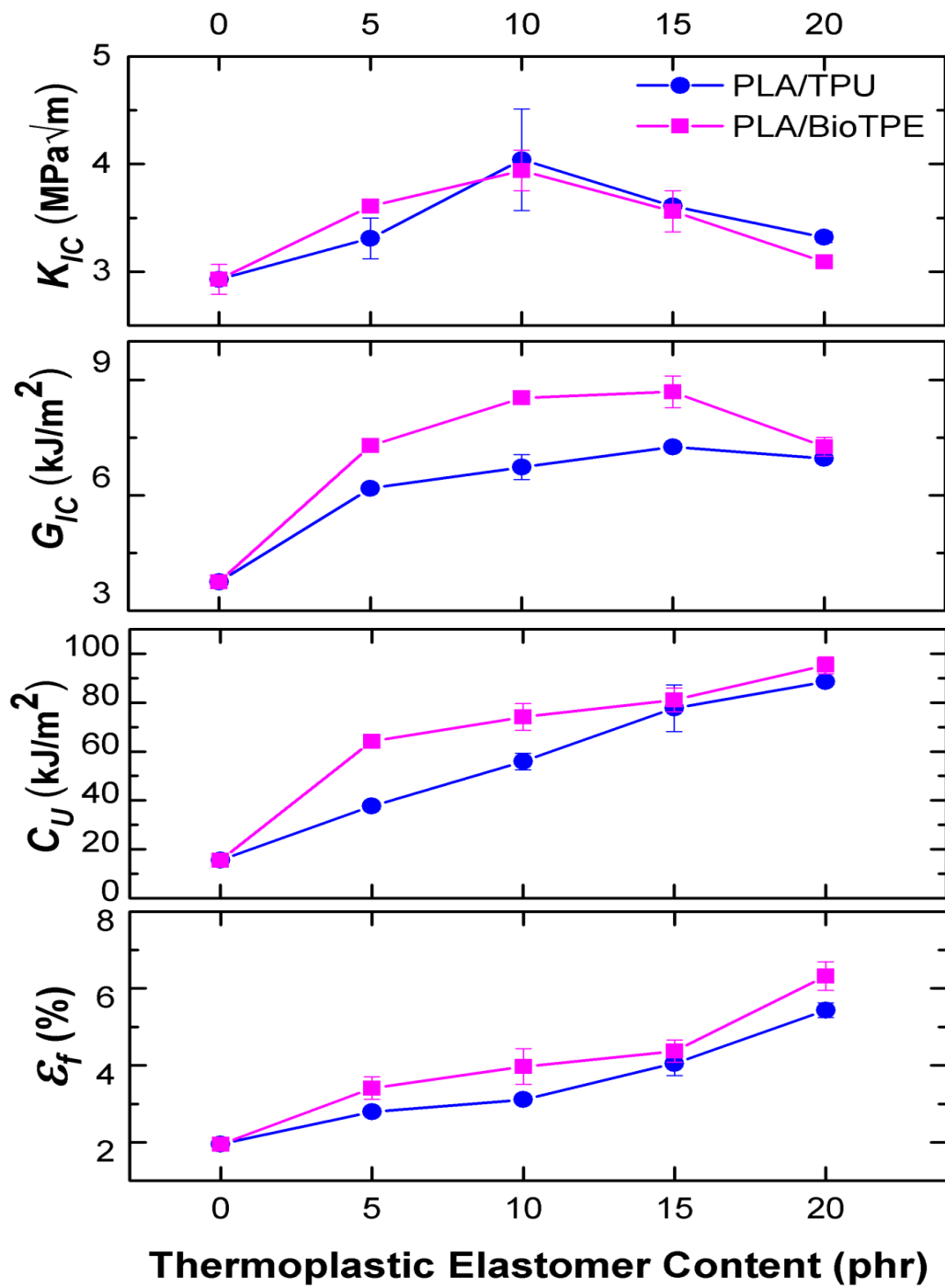


Figure 3.15 Effects of TPU and BioTPE Content on the Ductility (% strain at break- ϵ_f), Impact Toughness (Unnotched Charpy- C_U) and Fracture Toughness (K_{IC} and G_{IC}) of the Specimens

Debonding at the interface between the PLA matrix and the domains of TPU or BioTPE, and pull-out of these domains from the matrix observed in SEM fractographs (Figure 3.11) could be also considered as secondary toughening mechanism especially responsible for the improved fracture toughness values. Because, these two mechanisms together with “crack deflection” mechanism would retard the growth rate of the main cracks by absorbing their energy required for propagation. Thus, mechanisms of debonding, pull-out, and crack deflection would delay the fracture of the component.

3.2.6 Thermal Transition Temperatures and Crystallinity of the Blends with Thermoplastic Elastomers

Figure 3.16 shows heating thermograms of the specimens obtained after erasing their thermal history. Then, important transition temperatures, i.e. glass transition, crystallization, melting (T_g , T_c , T_m), together with enthalpies of melting and crystallization (ΔH_m and ΔH_c) were determined and tabulated in Table 3.12. This table also includes percent crystallinity (X_C) of the specimens obtained using the equation given in Section 3.1.6.

Table 3.12 indicates that incorporation of thermoplastic elastomers has almost no influence on the T_g and T_m values of the PLA matrix. As discussed above in SEM analysis, phase separation by formation of round thermoplastic elastomer domains revealed again the immiscibility of PLA with both materials. Therefore, DSC analysis showing no change in the T_g of PLA and its blends could be another confirmation of the immiscibility of PLA with TPU and BioTPE.

Table 3.12 also shows that there were 6°-7°C decreases in the T_c values of blends compared to neat PLA. This could be interpreted that cold crystallization of blends started at lower temperatures possibly due to the fine sized thermoplastic elastomer domains acting as heterogeneous nucleation sites.

Table 3.12 Transition Temperatures (T_g , T_c , T_m), Enthalpies (ΔH_m , ΔH_c) and Crystallinity Percent (X_c) of the Specimens with Thermoplastic Elastomers During Heating Profile

Specimens	T_g (°C)	T_c (°C)	T_m (°C)	ΔH_m (J/g)	ΔH_c (J/g)	X_c (%)
PLA	60.1	106.2	169.8	41.0	27.3	14.7
PLA/TPU 5	59.5	99.7	169.6	38.4	27.6	12.2
PLA/TPU 10	60.5	99.4	169.3	34.6	25.5	11.5
PLA/TPU 20	60.5	98.6	169.0	30.4	21.2	11.6
PLA/BioTPE 5	61.0	98.8	169.5	39.5	28.9	12.6
PLA/BioTPE 10	60.7	100.3	169.3	34.7	25.7	11.4
PLA/BioTPE 20	60.7	100.9	169.3	32.3	24.3	10.8

However, it is seen in Table 3.12 that melting enthalpies (ΔH_m) of the blends were lower than the ΔH_m of neat PLA leading to slightly lower amounts of crystallinity (X_c). For instance, X_c of neat PLA (14.7%) decreases down to 11.6% and 10.8% with the incorporation of 20 phr TPU and BioTPE, respectively. This means that, although cold crystallization of the blends started at a lower temperature, the growth of spherulitic crystals was hindered by the thermoplastic elastomer domains. That is, conformational mobility of the PLA chains required for the spherulitic growth could be constrained due to the chemical interactions between the polar end groups of PLA and hard segments of TPU and BioTPE.

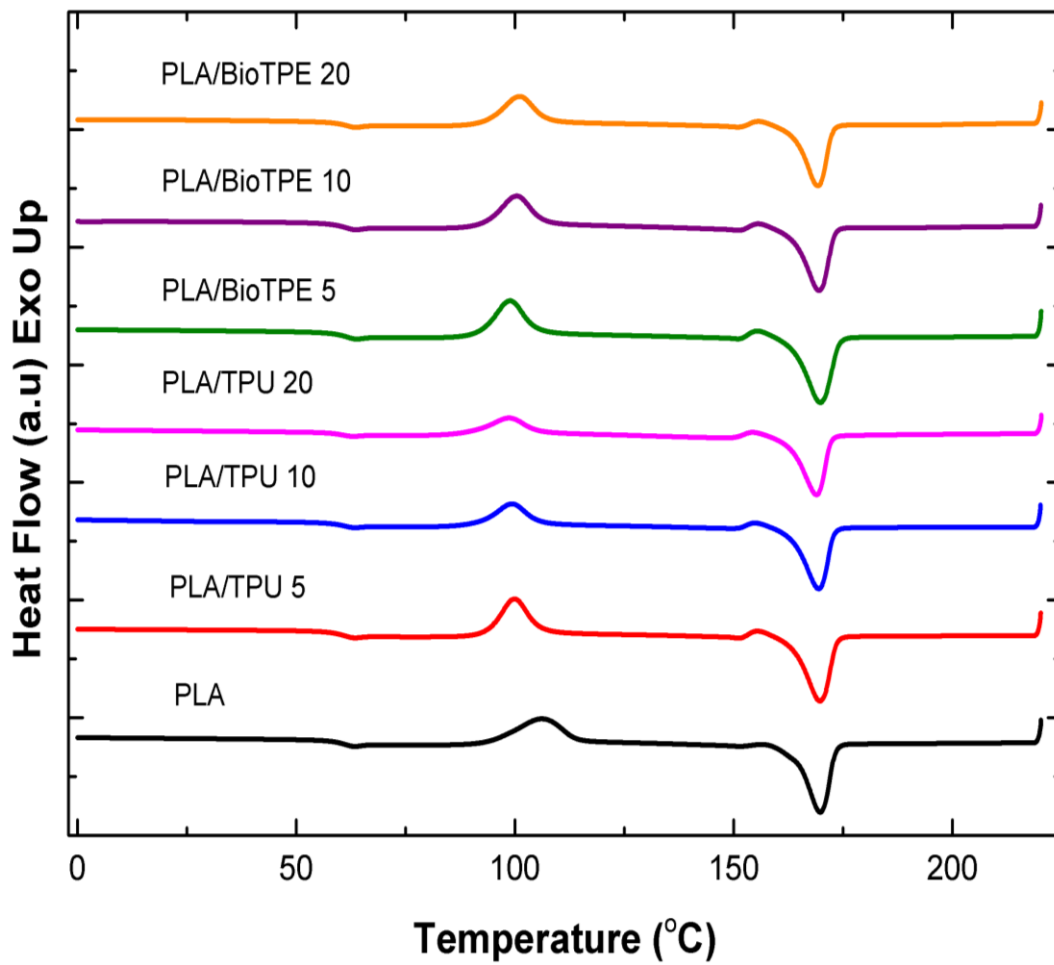


Figure 3.16 DSC Heating Thermograms of the Specimens with Thermoplastic Elastomers Obtained After Erasing their Thermal History

3.2.7 Thermal Degradation and Thermomechanical Behavior of the Blends with Thermoplastic Elastomers

Since thermal degradation temperatures of PLA, TPU and BioTPE are all close to each other, TG and DTG curves in Figure 3.17 simply show that PLA and its blends mainly degrade at only one step. Certain levels of thermal degradation temperatures determined from these curves are tabulated in Table 3.13. In this table, $T_{5\%}$, $T_{10\%}$, $T_{25\%}$ represent thermal degradation temperatures of the specimens at 5, 10, 25 wt% mass loss in TG curves, while T_{max} represents maximum mass loss rate peak temperature of the specimens in DTG curves.

Table 3.13 Thermal Degradation Temperatures ($T_{5\%}$, $T_{10\%}$, $T_{25\%}$) of the Specimens with Thermoplastic Elastomers at 5, 10, 25 wt% Mass Losses and Maximum Mass Loss Rate Peak (T_{max}) of the Specimens

Specimens	$T_{5\%}$ (°C)	$T_{10\%}$ (°C)	$T_{25\%}$ (°C)	T_{max} (°C)
TPU	301	319	352	402
BioTPE	378	386	397	412
PLA	327	337	350	366
PLA/TPU 5	324	334	349	368
PLA/TPU 10	322	333	349	368
PLA/TPU 15	320	328	343	365
PLA/TPU 20	316	325	340	363
PLA/BioTPE 5	330	338	350	365
PLA/BioTPE 10	328	337	349	363
PLA/BioTPE 15	327	336	347	360
PLA/BioTPE 20	325	334	345	358

It is seen in Table 3.13 that there is almost no decrease in the thermal degradation temperatures of blends with lower thermoplastic elastomer contents (5 and 10 phr), while there were slight decreases, only a few degrees, for the blends with higher thermoplastic elastomer contents (15 and 20 phr). Thus, it can be said that there were no detrimental effects on the thermal degradation of PLA when it was blended with TPU or BioTPE.

Storage modulus versus temperature curves obtained by DMA are given in Figure 3.18. Then, two levels of storage modulus (E') at 25° and 50°C were determined and tabulated in Table 3.14.

Table 3.14 Storage Modulus (E') Values of PLA and Blends with 10 phr Thermoplastic Elastomers at 25° and 50°C

Specimens	E' at 25°C (GPa)	E' at 50°C (GPa)
PLA	2.78	2.72
PLA/TPU 10	2.66	2.62
PLA/BioTPE 10	2.29	2.26

Figure 3.18 shows that storage modulus of PLA and its blends vanished at 60°C which is the T_g of PLA. Addition of thermoplastic elastomers decreased E' values of PLA due to the increased mobility of PLA chains and soft segments of TPU or BioTPE. Compared to neat PLA, decreases in the value of E' at 50°C are 3% and 16% with the addition of 10 phr TPU or BioTPE, respectively.

However, compared to the decreases in the values of Young's modulus (E) and flexural modulus (E_{Flex}) values at 10 phr contents discussed above, it was seen that decreases in storage modulus (E') values were not higher. Therefore, it can be said that incorporation of TPU or BioTPE had no significant detrimental effects on the thermomechanical behaviour of PLA.

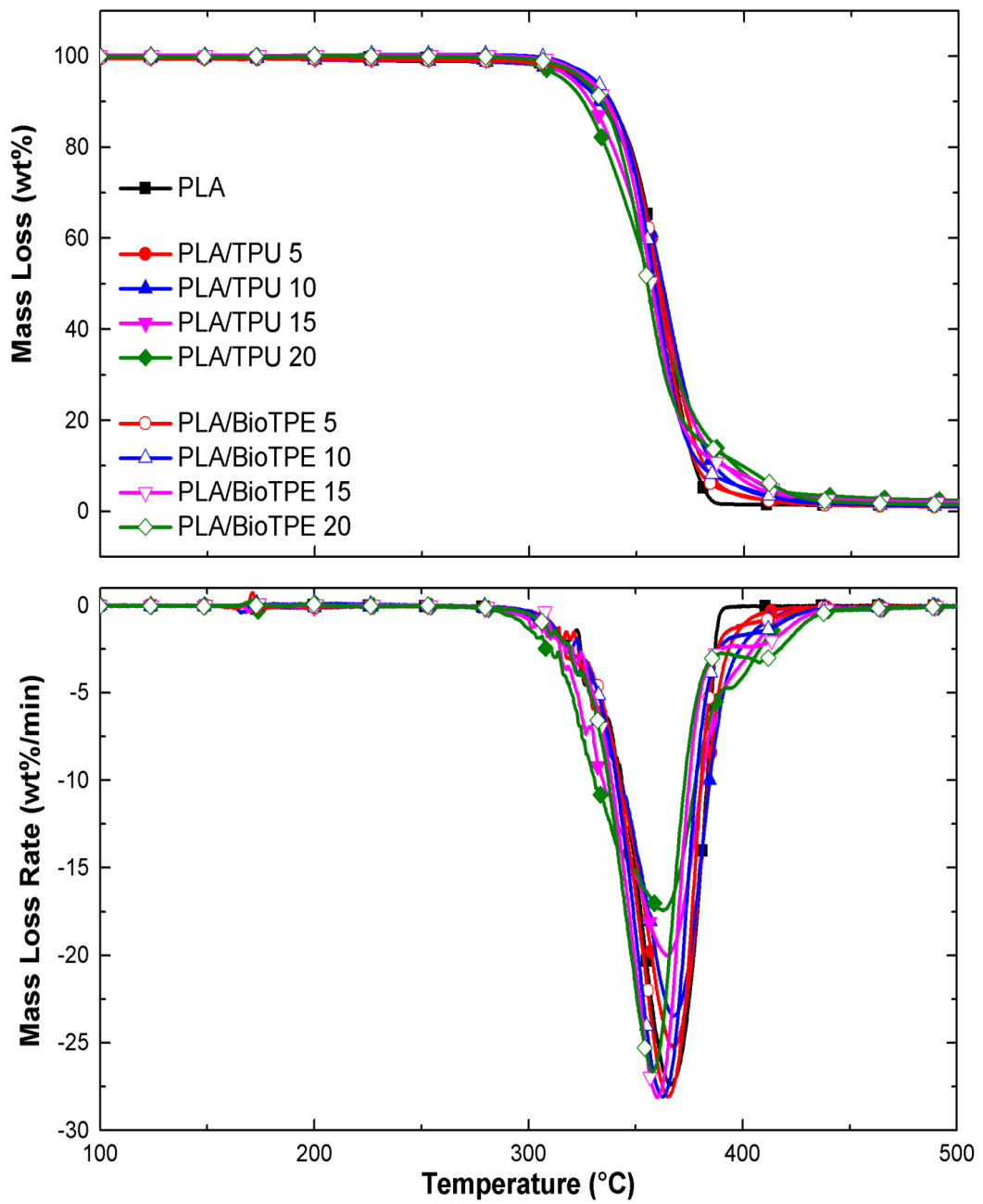


Figure 3.17 Thermogravimetric (TG) and Differential Thermogravimetric (DTG) Curves of the Specimens with Thermoplastic Elastomers

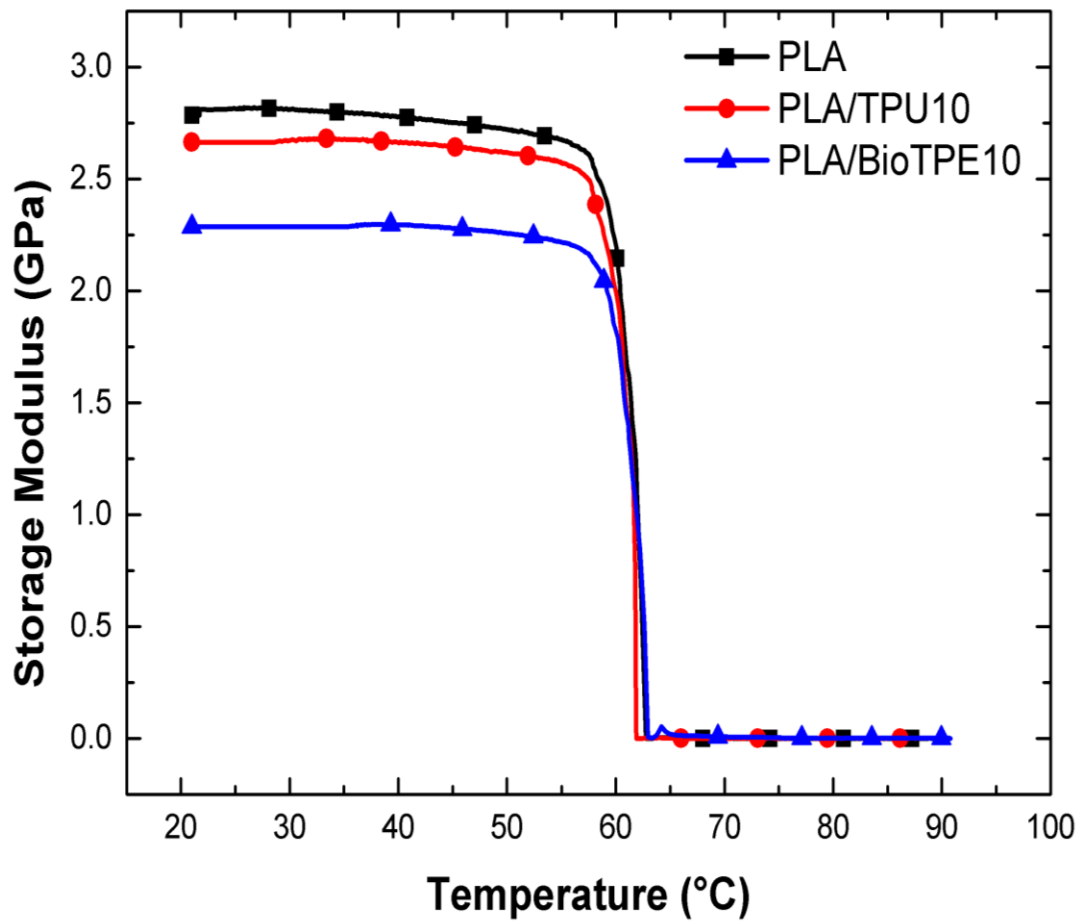


Figure 3.18 Storage Modulus Curves of PLA and Blends with 10 phr Thermoplastic Elastomers Obtained by DMA

3.3 Effects of Maleic Anhydride Compatibilization

In the previous parts it was determined that the optimum loading of elastomeric materials to have optimum combination of toughness and strength was 10 phr (parts per hundred resin).

Therefore, in this third part of thesis, in order to determine the optimum amount of PLA-g-MA, PLA/TPU and PLA/BioTPE blends were compatibilized by various loadings of PLA-g-MA. It was revealed that compatibilization beyond 5 phr resulted in no significant improvements. Therefore, effects of compatibilization were investigated by comparing the mechanical and thermal properties of PLA blends with and without 5 phr PLA-g-MA.

3.3.1 Compatibilization of PLA/Thermoplastic Elastomer Blends with PLA-g-MA

PLA matrix and elastomeric domains can be compatibilized by following two routes. In the first route; PLA-g-MA can be prepared “*in situ*”, i.e. it can be formed during melt blending of PLA and elastomers at the same time in the same extruder, this route is called “one-step compatibilization”. In the second route; PLA-g-MA can be prepared separately before blending, and then it can be added at certain amounts during the melt blending of PLA and elastomers, thus this route is called as “two-step compatibilization”.

In this part, since it was more practical and easier to control, “two-step” procedure was used. As the first step, PLA-g-MA was prepared separately by reactive extrusion mixing of pre-dried PLA and 2 wt% MA and 0.5 wt% dicumyl peroxide (DCP) free radical initiator using the same lab-scale twin-screw extruder blending parameters explained in the experimental Section 2.2 above. The amounts of MA and DCP used were in accordance with the literature [36, 47]. After characterization of PLA-g-MA by titration method and infrared spectroscopy, the second step was applied, i.e. PLA-g-MA was added as 5 phr during melt blending of PLA with TPU and BioTPE.

In the literature [48, 49], the proposed mechanism for the formation of PLA-g-MA is the free radical reaction as shown in Figure 3.19. In this reaction, first peroxide free radical initiator leads to hydrogen abstraction from the backbone of PLA making it a macro-radical, then MA easily react with PLA forming as grafts to the backbone structure.

In order to determine amount of MA grafted on PLA, the titration method was used as follows: after dissolution of 1 g of PLA-g-MA in 200 mL of chloroform at boiling temperature ($\sim 60^{\circ}\text{C}$), 5 μL water was added to hydrolyze anhydride functions into carboxylic acid functions. The boiling temperature was maintained 4-5 hours to dissolve PLA-g-MA completely. Then, the solution was titrated with another solution having 0.2 g potassium hydroxide (KOH) (85% purity, $MW=56.11$ g/mol) in 100 mL methanol and two drops of phenolphthalein as an indicator to observe the color change. The functionalized PLA, i.e. PLA-g-MA was completely soluble at the boiling temperature of chloroform and no precipitation was observed during the titration. Then, the carboxylic acid concentration was easily converted to the MA content as follows:

$$\text{MA}(\text{wt}\%) = \left[\frac{MW_{MA} N V}{2 W} \right] 100 \quad (3.2)$$

where MW_{MA} is the molecular weight of maleic anhydride (98 g/mol), N and V are the concentration (mol/L) and volume (L) of potassium hydroxide-methanol standard solution, respectively, and W (g) is the weight of the PLA-g-MA used. In this method, amount of grafted MA on PLA was found as 1.18%. Similar levels were determined in the other investigations [36, 47, 49].

After titration technique, grafting of MA on PLA structure was also characterized by infrared spectroscopy. Distinctive IR bands related to chemical structures of PLA and MA were compiled from the literature [39, 50] and tabulated in Table 3.15. Then, as shown in Figure 3.20, ATR-FTIR spectrum of PLA and PLA-g-MA were taken.

Table 3.15 Positions and Assignments of Distinctive IR Bands Related to PLA, MA, TPU and TPE [39, 50-53, 57, 58]

Materials	Position (cm⁻¹)	Assignments
PLA	1190-1090	C-C(O)-O stretching
	1300	CH ₃ bending
	1385	C-H deformation
	1760	Symmetric C=O stretching
	3000-2940	CH ₃ stretching
MA	1590	Cyclic C=C stretching
	1780	Cyclic Anhydride
	1850	Symmetric and asymmetric C=O stretching
TPU	1220, 1530	-C-N- (amide in urethane)
	1528-1504	-NH (amine in urethane)
	1475-1600	-C=C aromatic rings
	2340	-N=C=O isocyanate group
TPE	900	C=O bending
	1220	C-O vibration
	1455	CH ₂ bending
	1720	C=O vibration

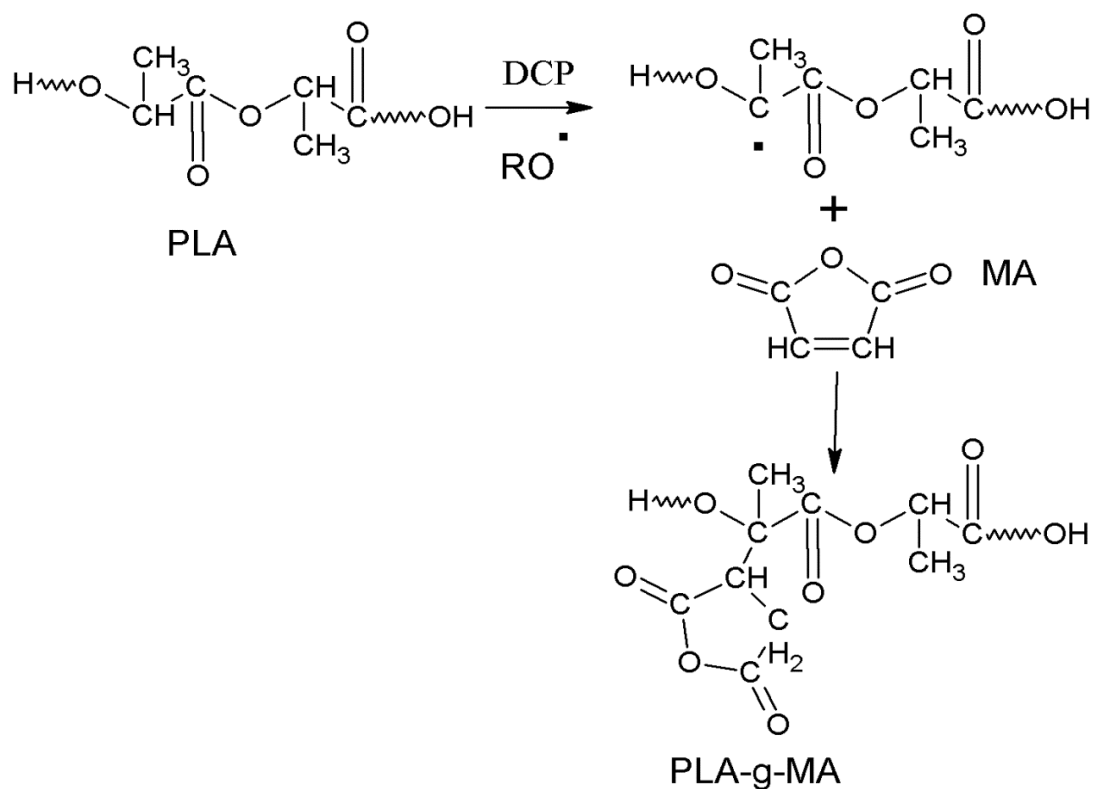


Figure 3.19 Grafting of MA onto PLA Backbone by Free Radical Reaction

Distinctive IR bands observed in the literature [39] for PLA were: C-C(O)-O stretching of ester bonds at $1190\text{-}1090\text{ cm}^{-1}$, CH_3 bending at 1300 cm^{-1} , symmetric C=O stretching at 1760 cm^{-1} , CH_3 stretching at $3000\text{-}2940\text{ cm}^{-1}$. Figure 3.20 shows these important bands of PLA observed in this study: C-C(O)-O stretching at 1090 cm^{-1} , CH_3 bending at 1274 cm^{-1} , C=O stretching at 1756 cm^{-1} , and CH_3 stretching at 2925 cm^{-1} . For the MA structure distinctive IR bands in the literature [50, 51] were: cyclic C=C stretching band at 1590 cm^{-1} , cyclic anhydride structure at 1780 cm^{-1} , symmetric and asymmetric C=O stretching at around 1850 cm^{-1} . It is also stated that [50], the absence of the cyclic C=C stretching at 1590 cm^{-1} might be a confirmation of the chemical interaction between PLA and MA, which was not observed in the IR spectrum of PLA-g-MA as shown in Figure 3.20. On the other hand, cyclic anhydride band at 1780 cm^{-1} of MA was overlapped by the very large carbonyl C=O stretching of PLA at around 1756 cm^{-1} .

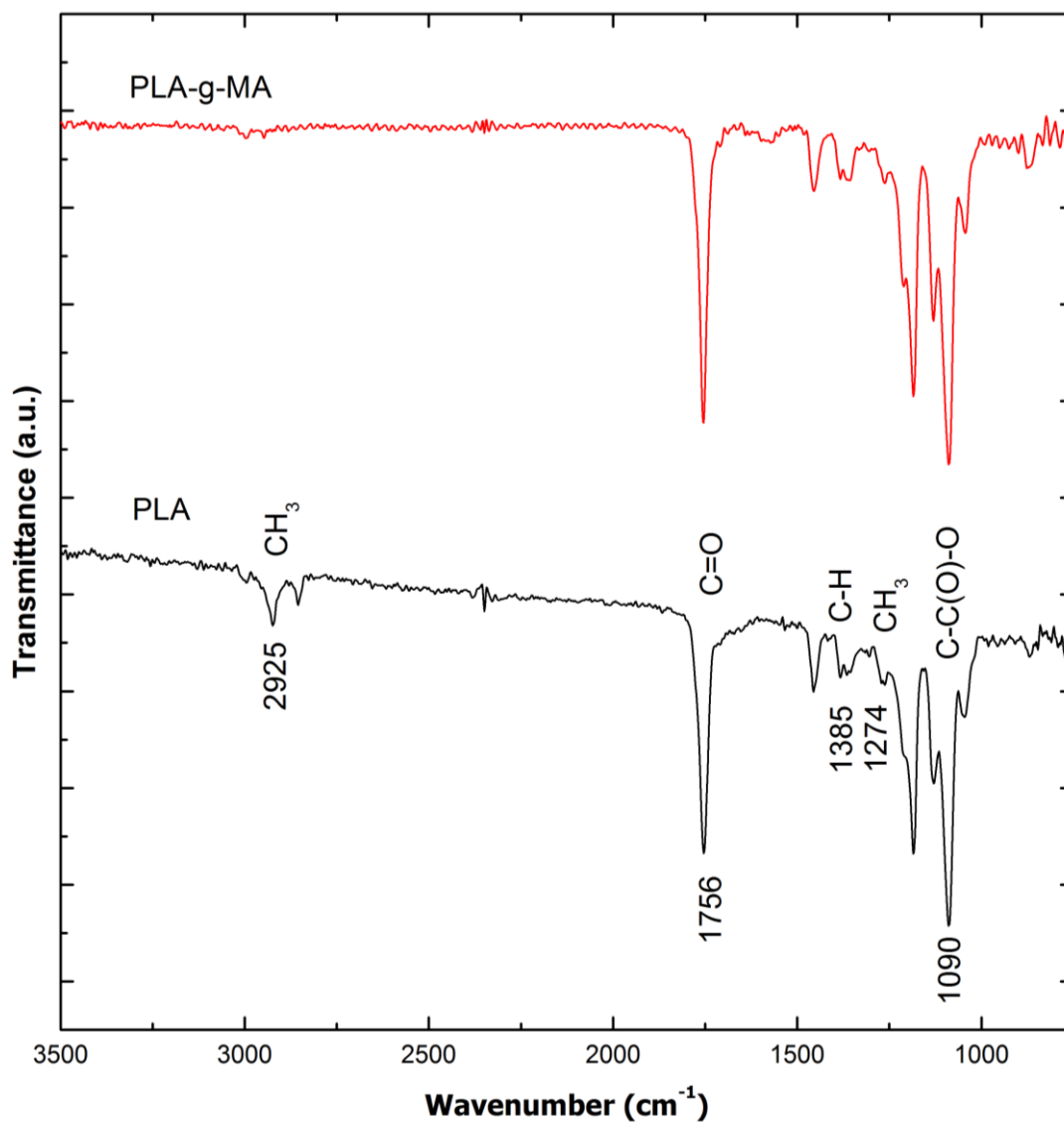


Figure 3.20 ATR-FTIR Spectra of PLA and PLA-g-MA

For the interactions between PLA, MA and the thermoplastic elastomers used, it was important to analyze structure of TPU and BioTPE. Since, hard segments of these thermoplastic elastomers are more reactive, their distinctive IR bands were also compiled in Table 3.15. Then, as shown in Figure 3.21, ATR-FTIR spectra of PLA/TPU and PLA/BioTPE blends with and without PLA-g-MA compatibilization were compared.

Distinctive IR bands of TPU in the literature [52] were: -C-N amide band (in the urethane) at $1220, 1530\text{ cm}^{-1}$, -NH amine band (in the urethane) at $1528\text{-}1504\text{ cm}^{-1}$, -C=C in aromatic rings at $1475\text{-}1600\text{ cm}^{-1}$, and -N=C=O isocyanate group at around 2340 cm^{-1} . IR spectrum of PLA/TPU blend in Figure 3.21 shows not only typical bands of PLA mentioned above but also typical bands of TPU, i.e.: -C-N at 1233 cm^{-1} , -NH at 1499 cm^{-1} , and -C=C at 1591 cm^{-1} . However, no new peak was observed, this could mean that there was no direct primary chemical interaction between PLA and TPU, but, certain level of secondary chemical interactions were expected between the carboxyl, hydroxyl end groups and the carbonyl groups of PLA with the polar groups of especially hard segment (diisocyanate in urethane) of TPU.

It is discussed in the literature [53, 54] that there should be an imide linkage (R'(O=)CNC(=O)R) formation between the isocyanate group of TPU and anhydride group of MA with C=O stretching band at around 1700 cm^{-1} and C-N-C axial stretching at around 1350 cm^{-1} . In this study, in the spectrum of PLA/PLA-g-MA/TPU (Figure 3.21), C=O stretching was observed as a tiny peak at 1690 cm^{-1} , while C-N-C stretching was overlapped by the large C-H deformation of PLA at 1385 cm^{-1} . The reason of the very small intensity of these imide linkage bands was the very low amount of MA (only 2 wt% of PLA) used.

Distinctive IR bands of the butylene terephthalate group of TPE given in the literature [51] are: C=O bending, C-O vibration, CH_2 bending, and C=O vibration at around $900, 1220, 1455, \text{ and } 1720\text{ cm}^{-1}$, respectively. IR spectrum of PLA/BioTPE blend in Figure 3.21 again shows not only typical bands of PLA, but also these typical bands of the hard segment of BioTPE, i.e.: C=O bending, C-O vibration, CH_2 bending, and C=O vibration at around $871, 1210, 1455, \text{ and } 1721\text{ cm}^{-1}$, respectively. However, there was no new peak, either. Thus, it can be stated that there were no primary chemical interaction between PLA and BioTPE, but, there could be certain level of secondary chemical interactions between the carboxyl, hydroxyl end groups and the carbonyl groups of PLA with the polar groups of especially hard segment (butylene terephthalate) of BioTPE.

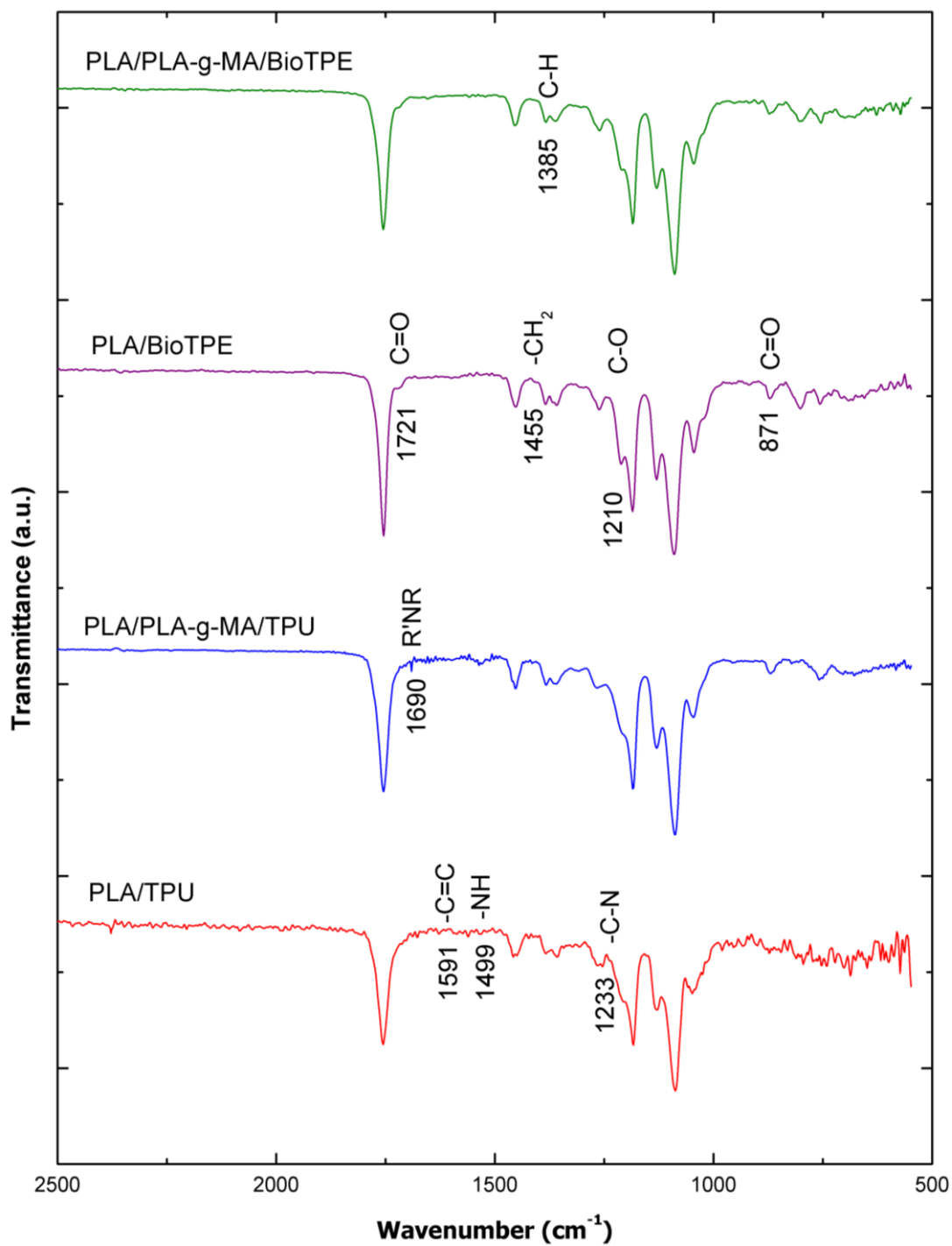


Figure 3.21 ATR-FTIR Spectra of PLA/Thermoplastic Elastomer Blends with and without PLA-g-MA Compatibilization

In the literature [55], it was stated that there could be two different interactions between the MA and the hydroxyl end group of butylene terephthalate in the hard segment of TPE. The first one is the intermolecular dipole-dipole interaction between the carbonyl oxygen in MA and the hydrogen in the hydroxyl end group of butylene terephthalate. The second one is the direct grafting reaction between each group leading to the formation of the C-H vibration seen at around 1385 cm^{-1} [58]. In this study, PLA/PLA-g-MA/BioTPE spectrum in Figure 3.21 shows that, this distinctive grafting band was overlapped by the C-H deformation band of the PLA at around 1385 cm^{-1} .

3.3.2 Effects of PLA-g-MA on the Morphology of Domains and Melt Flow Index of the Blends

SEM examination conducted on the fracture surfaces of fracture toughness specimens in Figure 3.22 shows that PLA blends with and without compatibilization have very high level of roughness due to the large amount of plastic deformation, i.e. shear yielding, occurred during fracture. It was also clearly seen that both of the thermoplastic elastomers were immiscible with PLA leading to two-phase structure, where PLA was the continuous phase while TPU and BioTPE were separated phases forming round-shaped domains.

Distribution and size of the domains are very important influencing the mechanical properties of polymer blends. For each case, Figure 3.22 indicates that both TPU and BioTPE domains were distributed finely and very homogeneously in the PLA matrix.

In order to have data on the domain sizes, an image analysis software was used, and the results are tabulated in Table 3.16. It was seen that, use of PLA-g-MA compatibilization reduced the average domain sizes. The decrease for TPU domains was more significant, from $5.13\text{ }\mu\text{m}$ down to $1.13\text{ }\mu\text{m}$; while for BioTPE domains only from $4.38\text{ }\mu\text{m}$ to $3.88\text{ }\mu\text{m}$. Decreased domain size means increased surface area leading to more interfacial interactions with the matrix, and consequently more influences on the properties of blends. Moreover, closer views of the SEM images in

Figure 3.23 show that existence of the certain level of coalescence of domains, especially for BioTPE, disappeared after compatibilization with PLA-g-MA.

Apart from size and distribution of domains, another significant aspect influencing all mechanical properties of blends is the compatibility between the polymer matrix and phase separated domains. As discussed above there could be secondary chemical interactions between the carboxyl, hydroxyl end groups and the carbonyl groups of PLA with the polar groups of especially hard segments of the thermoplastic elastomers, leading to some compatibility. On the other hand, closer SEM images in Figure 3.23 revealed that, there were certain level of debonding between the PLA matrix and the domains of TPU and BioTPE. Moreover, some of the domains were pulled-out from the PLA matrix. Therefore, it can be said that compatibility between PLA and the domains of TPU and BioTPE was weak.

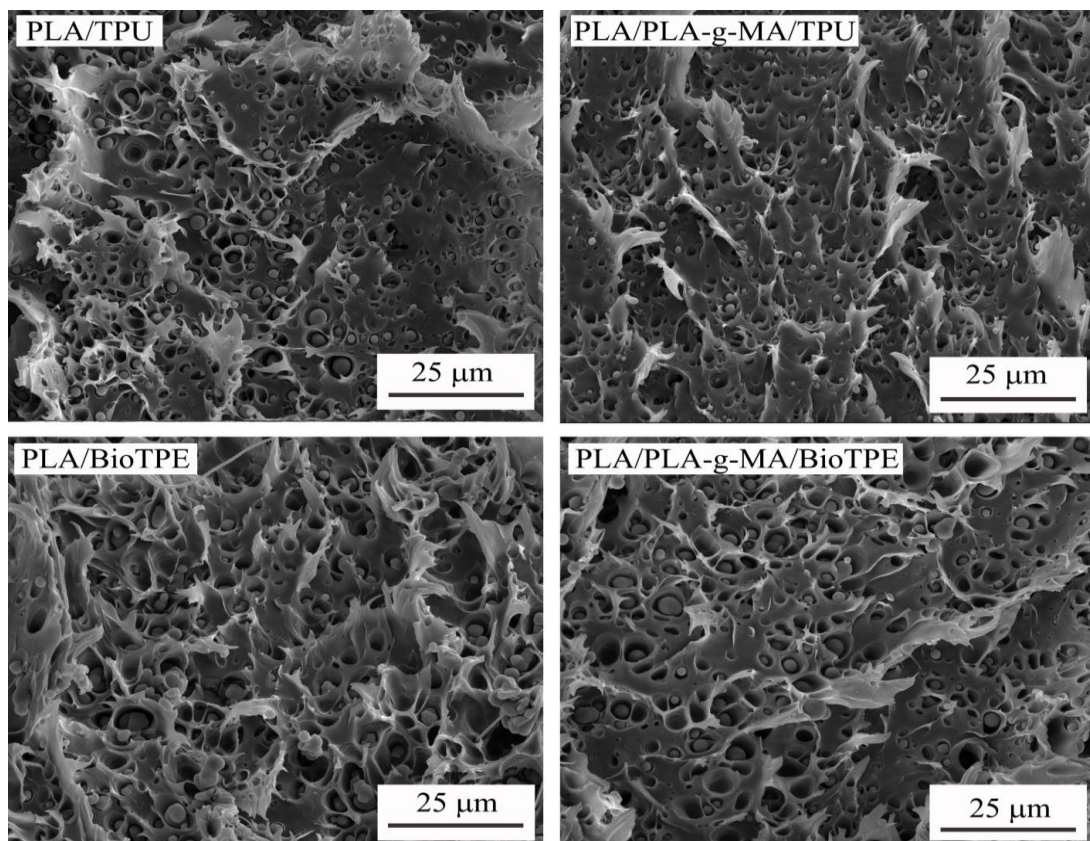


Figure 3.22 Very Rough SEM Fractographs of PLA Blends with and without Compatibilization Showing Finely and Uniformly Distributed TPU and BioTPE Domains

However, after compatibilization with PLA-g-MA, Figure 3.23 shows that the degree of debonding and the number of pull-out sites were decreased significantly. It is believed that these interfacial improvements were due to the primary chemical interactions discussed in the previous section.

Melt flow index (MFI) values measured for the neat PLA and blends are tabulated also in Table 3.16. It is seen that when thermoplastic elastomers were incorporated, MFI value of PLA increased. Because, soft segments of these thermoplastic elastomers could act as plasticizers increasing the mobility of the macromolecular chains of PLA. Thus, increased MFI values would be obtained due to the lowered viscosities.

On the other hand, compatibilization with PLA-g-MA decreased the MFI values of the blends. Table 3.16 indicates that the decrease for PLA/TPU was 10%, while it was 13% for PLA/BioTPE. Of course, these reductions were again due to the increased chemical interactions restricting the mobility of the chains leading to higher viscosities.

Table 3.16 Effects of PLA-g-MA on the Domain Sizes and Melt Flow Index of the Blends

Specimens	Average Domain Size (μm)	MFI (g/10 min) (at 220°C, 2.16 kg)
PLA	---	162 \pm 3
PLA/TPU	5.13 \pm 2.71	218 \pm 4
PLA/PLA-g-MA/TPU	1.13 \pm 0.46	197 \pm 3
PLA/BioTPE	4.38 \pm 2.13	198 \pm 4
PLA/PLA-g-MA/BioTPE	3.88 \pm 2.64	172 \pm 4

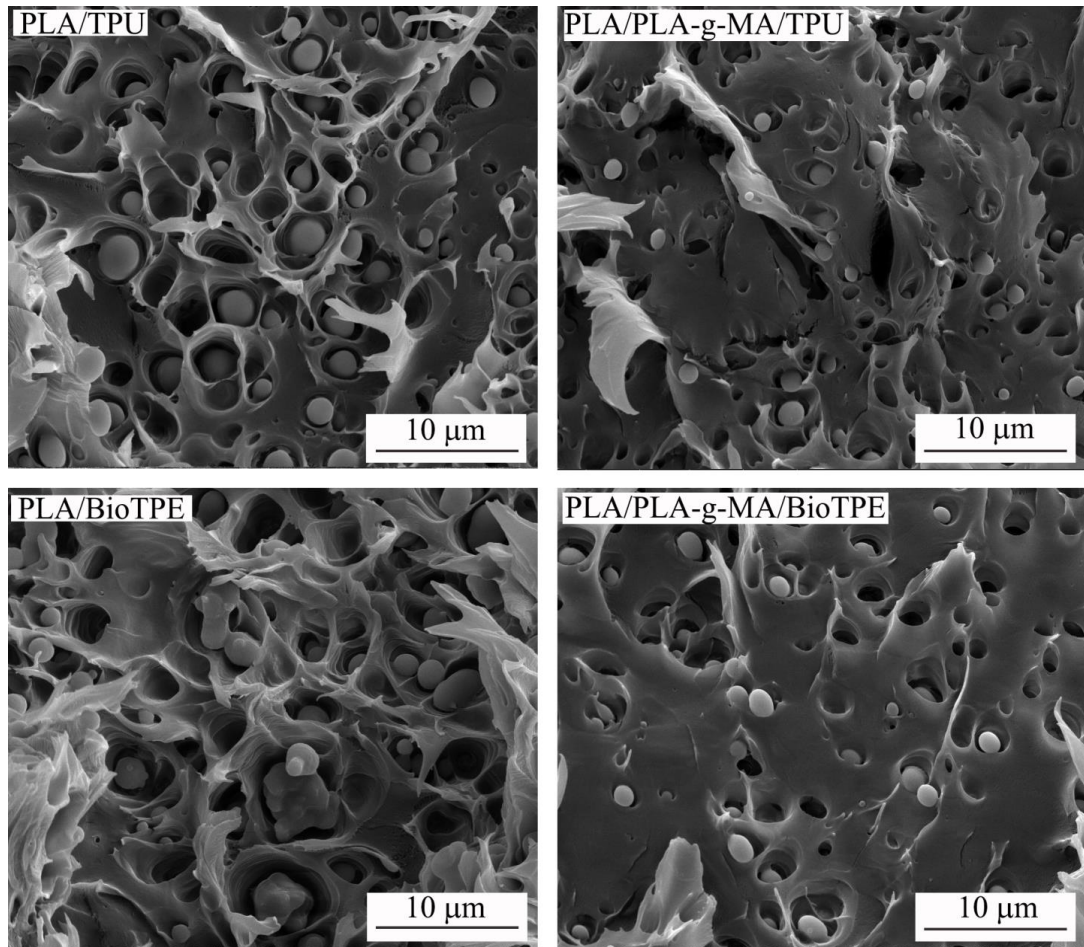


Figure 3.23 SEM Fractographs Showing Interfacial Interactions (Coalescence, Debonding, Pull-Out) between PLA Matrix and TPU, BioTPE Domains with and without Compatibilization

3.3.3 Effects of PLA-g-MA on the Mechanical Properties of the Blends

Effects of PLA-g-MA on the stiffness (elastic modulus) and strength of the blends were examined under both tension and three-point bending tests. Stress-strain curves obtained during these tests are given in Figure 3.24, while values of elastic modulus and strength of the blends determined are tabulated in Table 3.17 together with hardness values measured by Shore D type durometer. Effects on these properties are also evaluated in Figures 3.25 and 3.26, respectively.

Soft segments of thermoplastic elastomers have usually amorphous conformation with low T_g values. Therefore, at room temperature they impart mobility to the PLA structure. Thus, Figures 3.24 and 3.25, and Table 3.17 indicate that both Young's modulus (E) and flexural modulus (E_{Flex}) decreased gradually with the addition of each thermoplastic elastomer. Table 3.17 also indicates that soft segments of the thermoplastic elastomers decreased hardness of PLA slightly. However, when these blends were compatibilized with PLA-g-MA, it was seen that, there were no further reductions in the elastic modulus and hardness values.

In terms of strength, Figures 3.24 and 3.26, and Table 3.17 indicate that there were almost no detrimental effects of thermoplastic elastomers on both tensile strength (σ_{TS}) and flexural strength (σ_{Flex}) values of PLA. There was only a slight decrease of σ_{TS} for PLA/BioTPE. PLA blends without compatibilization keep or even increase the strength values slightly due to the hard segments of the thermoplastic elastomers having high T_m values with quite polar intermolecular bonding. Thus, these hard segments could act as fillers or physical crosslinks in the PLA structure compensating the loss of strength due to the plasticizing effects of the soft segments of TPU and BioTPE.

Moreover, Figure 3.26 and Table 3.17 also show that, when blends were compatibilized with PLA-g-MA, due to the increased interfacial adhesion and efficient load transfer, strength values were increased even more. For instance, without compatibilization, blending with TPU and BioTPE increased σ_{Flex} of PLA by 5% and 8%, respectively. After compatibilization, these increases reached to 11% and 20%, respectively. Normally, elastomeric materials increase the ductility and toughness of brittle polymeric materials significantly, but always with drastic decreases in strength. Therefore, improving toughness of PLA without sacrificing strength by blending with compatibilized TPU and BioTPE would be an advantage in many engineering applications.

Table 3.17 Effects of PLA-g-MA on the Young's Modulus (E), Flexural Modulus (E_{Flex}), Tensile Strength (σ_{TS}), Flexural Strength (σ_{Flex}) and Hardness (H) of the Blends

Specimens	E (GPa)	E_{Flex} (GPa)	σ_{TS} (MPa)	σ_{Flex} (MPa)	H (Shore D)
PLA	3.05±0.03	3.72±0.08	51.4±0.7	64.2±1.1	82.3±0.6
PLA/TPU	2.62±0.04	3.40±0.11	53.7±0.6	67.5±1.3	77.4±0.7
PLA/PLA-g-MA/TPU	2.63±0.04	3.48±0.03	54.2±1.4	71.1±0.1	77.8±0.7
PLA/BioTPE	2.48±0.05	3.00±0.14	42.8±0.6	69.5±2.1	74.9±0.7
PLA/PLA-g-MA/BioTPE	2.49±0.05	3.48±0.04	48.8±0.9	76.5±0.7	77.5±0.4

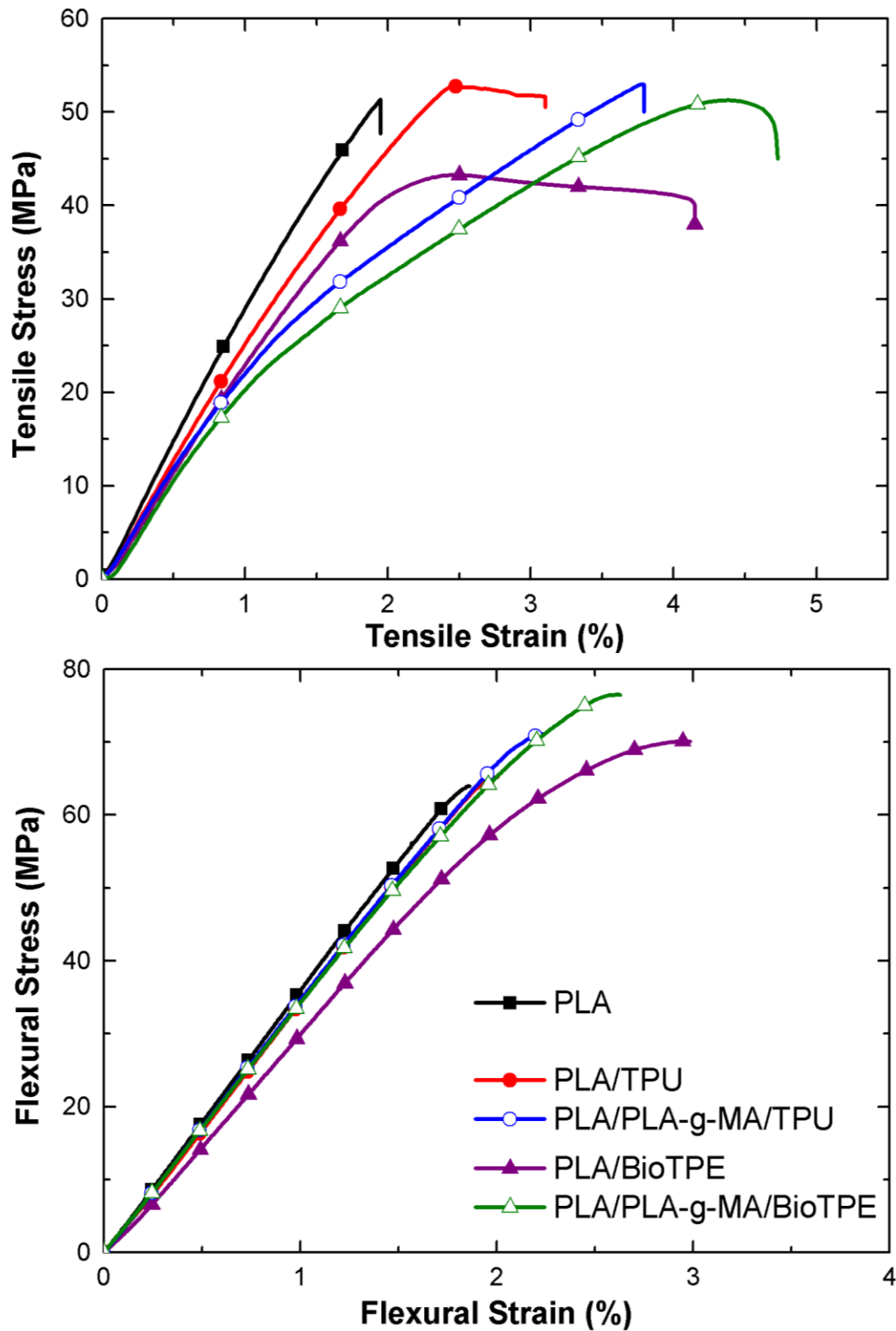


Figure 3.24 Stress-Strain Curves of the Blends with and without Compatibilization Obtained During Tensile and 3-Point Bending (Flexural) Tests

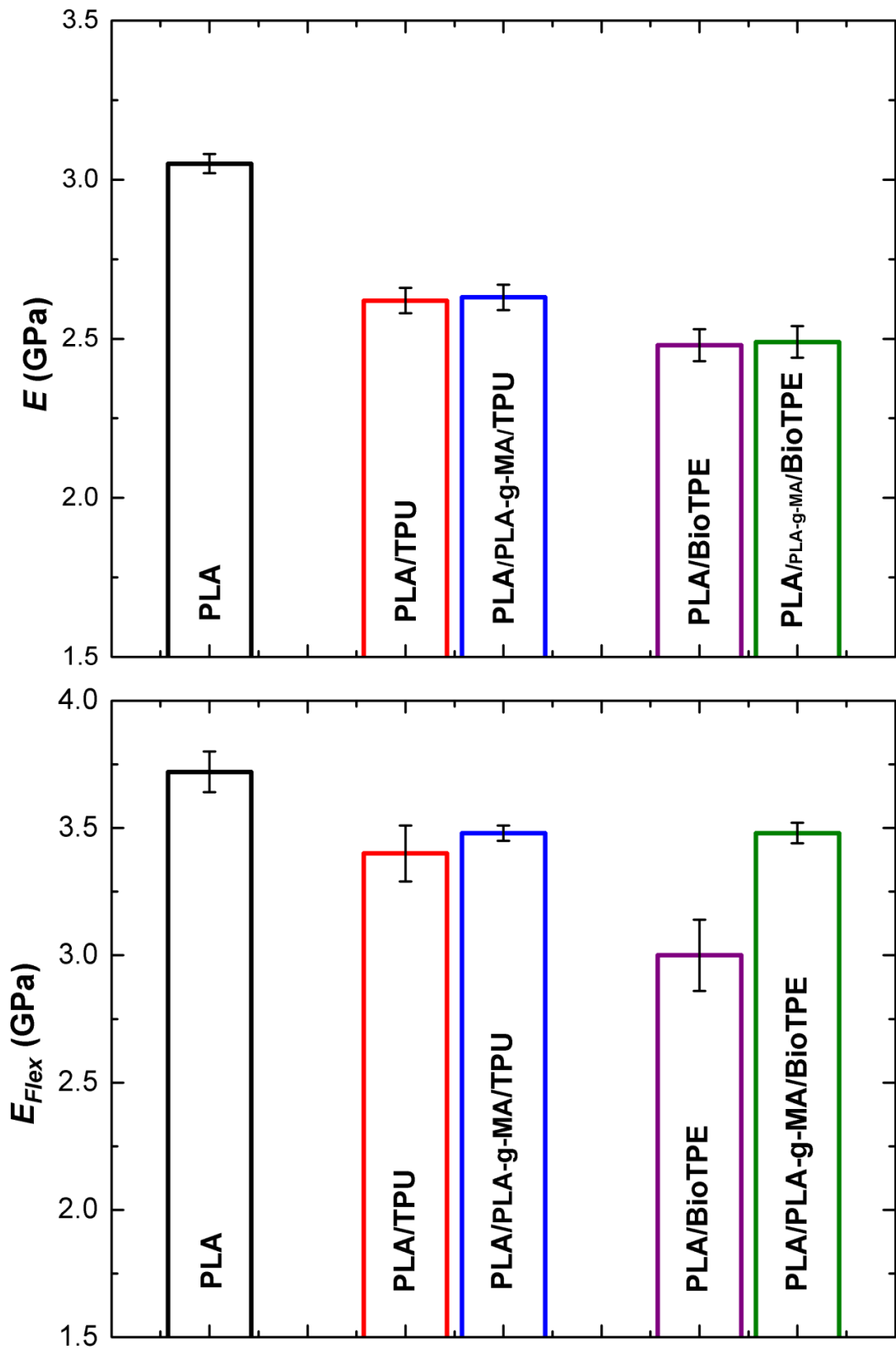


Figure 3.25 Effects of PLA-g-MA on the Elastic Modulus (E and E_{Flex}) of the Blends

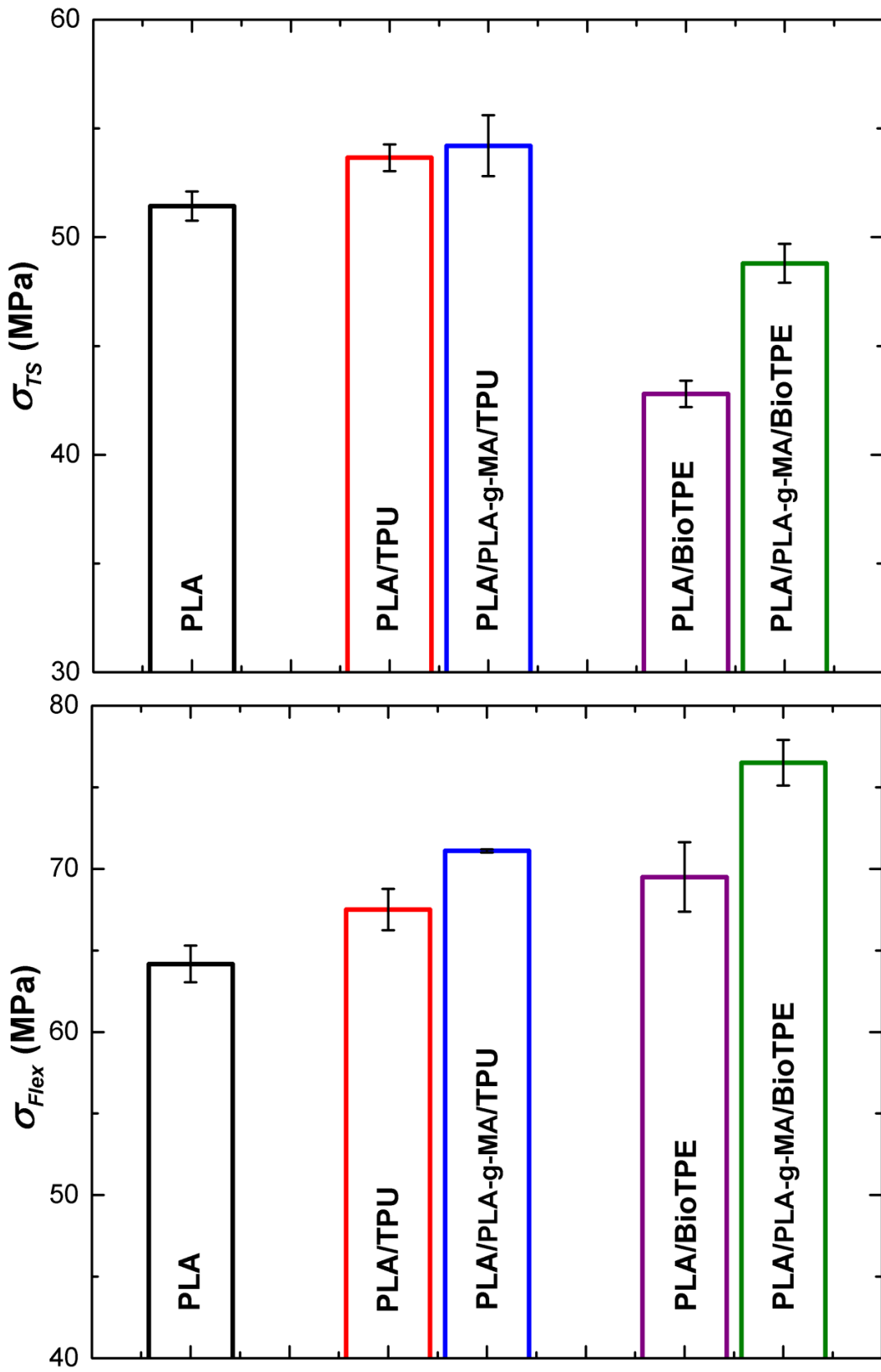


Figure 3.26 Effects of PLA-g-MA on the Strength (σ_{TS} and σ_{Flex}) of the Blends

Ductility values in terms of % final strain at break (ϵ_f) in Table 3.18 and Figure 3.27 show that ductility of PLA increased from 1.95% up to 3.11% and 3.97% by using 10 phr TPU and BioTPE, respectively. After compatibilization, they were 3.64% and 4.34%, i.e. compared to PLA, an increase of around 2 times.

Unnotched Charpy impact toughness (C_U) values and fracture toughness in terms of both K_{IC} and G_{IC} values are tabulated in Table 3.18, and the effects of TPU, BioTPE and compatibilization are evaluated in Figure 3.27.

Table 3.18 Effects of PLA-g-MA on the Tensile Strain at Break (ϵ_f), Unnotched Charpy Impact Toughness (C_U), and Fracture Toughness (K_{IC} and G_{IC}) of the Blends

Specimens	ϵ_f (%)	C_U (kJ/m ²)	K_{IC} (MPa√m)	G_{IC} (kJ/m ²)
PLA	1.95±0.05	15.6±0.5	2.93±0.14	3.75±0.02
PLA/TPU	3.11±0.08	55.9±3.4	3.64±0.47	6.73±0.32
PLA/PLA-g-MA/TPU	3.64±0.18	63.4±3.0	4.77±0.14	7.84±0.41
PLA/BioTPE	3.97±0.46	74.1±5.5	3.94±0.19	8.53±0.08
PLA/PLA-g-MA/BioTPE	4.34±0.33	86.1±4.2	4.90±0.24	9.98±0.68

Table 3.18 and Figure 3.27 indicate that unnotched Charpy impact toughness (C_U) of neat PLA increased significantly by blending with both thermoplastic elastomers. Increases in the C_U value of neat PLA (15.6 kJ/m²) was more than 3 and 4 times with 10 phr TPU and BioTPE, respectively; while their increases were more than 4 and 5 times after compatibilization with PLA-g-MA.

Table 3.18 and Figure 3.28 reveal that blending PLA with both thermoplastic elastomers results in very significant increases in the values of K_{IC} and G_{IC} . When these blends were compatibilized with PLA-g-MA, increases were much more significant. For instance, G_{IC} of PLA increased by 80% and 128% with 10 phr TPU and BioTPE, respectively; after compatibilizing these blends, G_{IC} increases reached up to 110% and 166%, respectively.

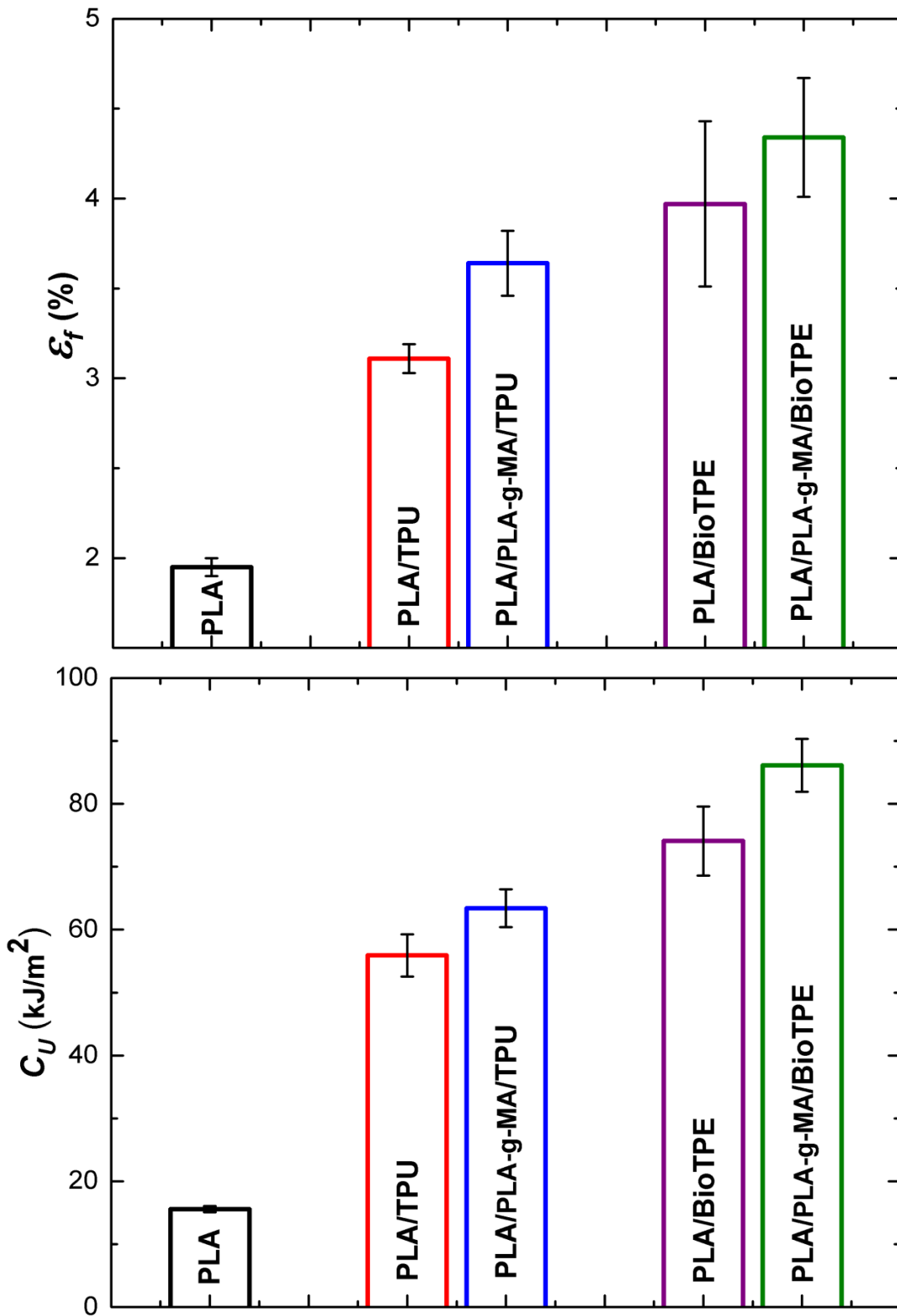


Figure 3.27 Effects of PLA-g-MA on the Ductility (% Strain at Break- ϵ_f) and Impact Toughness (Unnotched Charpy- C_U) of the Blends

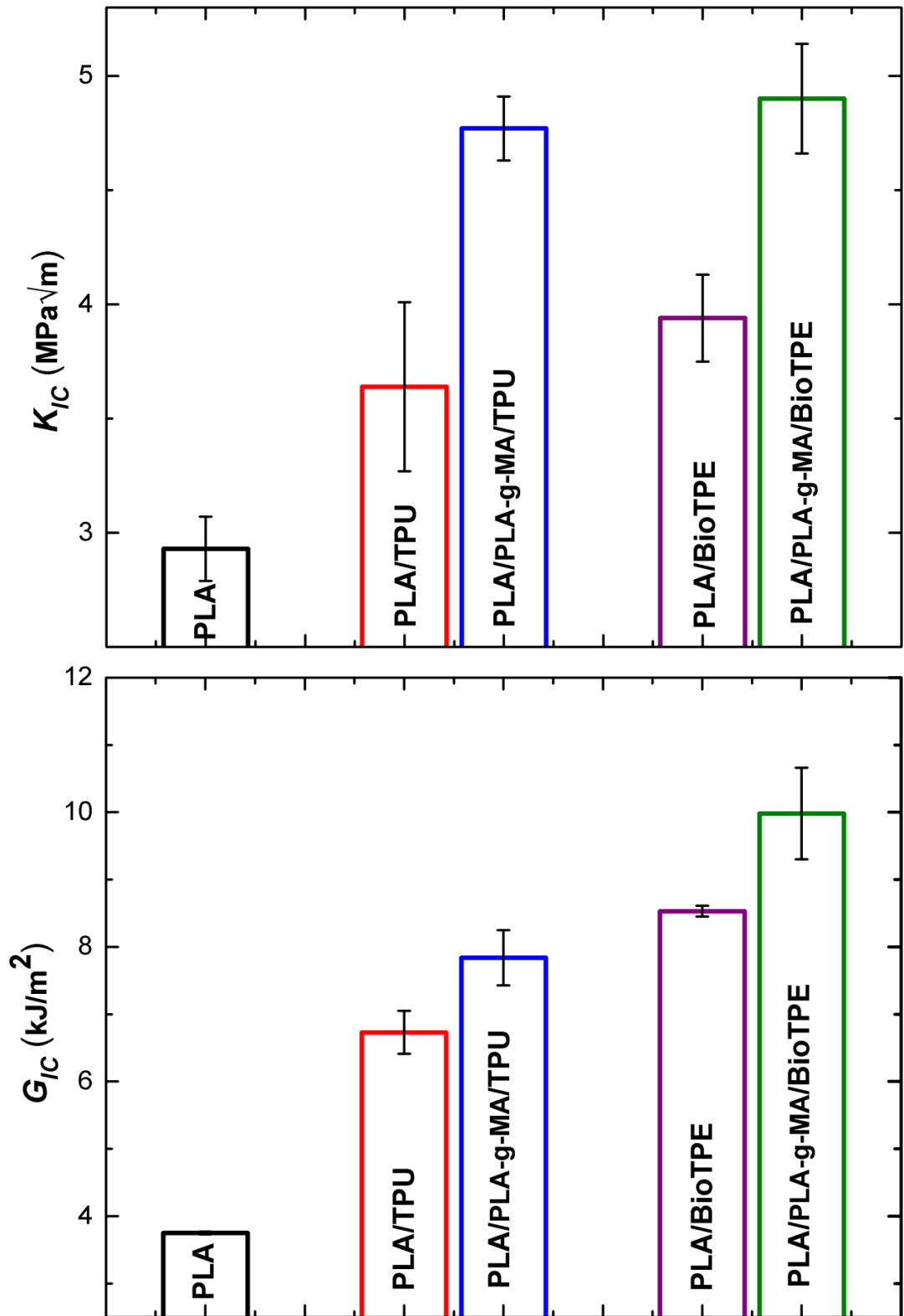


Figure 3.28 Effects of PLA-g-MA on the Fracture Toughness (K_{IC} and G_{IC}) of the Blends

Apart from crazing or whitening during tensile tests, the most significant rubber toughening mechanism observed was shear yielding, i.e. formation of large extent of plastic deformation before fracture. SEM fractographs (Figures 3.22 and 3.23) revealed that very smooth fracture surface of neat PLA without any sign of plastic deformation transformed into very rough fracture surfaces after blending with TPU or BioTPE. These rough surfaces represent large amount of plastic deformation which could absorb the energy required for crack initiation and crack growth leading to fracture.

Size and distribution of the elastomeric domains are also important. Because, decreasing the size would increase the surface area of domains leading to formation of more plastic deformation. As discussed before, TPU and BioTPE domains were uniformly and finely distributed in the PLA matrix. Moreover, PLA-g-MA compatibilization resulted in even finer domain sizes and no coalescences, which increased the efficiency of this toughening mechanism.

3.3.4 Effects of PLA-g-MA on the Thermal Behavior of the Blends

Figure 3.29 shows heating thermograms of the blends obtained after erasing their thermal history. Then, important transition temperatures, i.e. glass transition, crystallization, melting (T_g , T_c , T_m), together with enthalpies of melting and crystallization (ΔH_m and ΔH_c) and percent crystallinity (X_c) of the specimens determined are tabulated in Table 3.19.

Table 3.19 indicates that incorporation of thermoplastic elastomers with and without compatibilization has almost no influence on the T_g and T_m values of the PLA matrix. Table 3.19 also shows that compared to neat PLA there were 6°-7°C decreases in the T_c values of blends with and without compatibilization. This could be interpreted that cold crystallization of blends started at lower temperatures possibly due to the fine sized thermoplastic elastomer domains acting as heterogeneous nucleation sites. On the other hand, X_c values revealed that crystallinity amount was lower for the blends with and without compatibilization. This means that, although cold crystallization of the blends started at a lower temperature, the growth of spherulitic crystals was hindered by the thermoplastic elastomer domains. That is, mobility of the PLA

Table 3.19 Effects of PLA-g-MA on the Transition Temperatures (T_g , T_c , T_m), Enthalpies (ΔH_m , ΔH_c) and Crystallinity Percent (X_C) of the Blends During Heating

Specimens	T_g (°C)	T_c (°C)	T_m (°C)	ΔH_m (J/g)	ΔH_c (J/g)	X_C (%)
PLA	60.1	106.2	169.8	41.0	27.3	14.7
PLA/TPU	60.5	99.4	169.3	34.6	25.5	11.5
PLA/PLA-g-MA/TPU	60.7	100.3	170.2	32.2	22.7	12.0
PLA/BioTPE	60.7	100.3	169.3	34.7	25.7	10.8
PLA/ PLA-g-MA/BioTPE	60.5	100.1	170.1	35.2	28.2	8.9

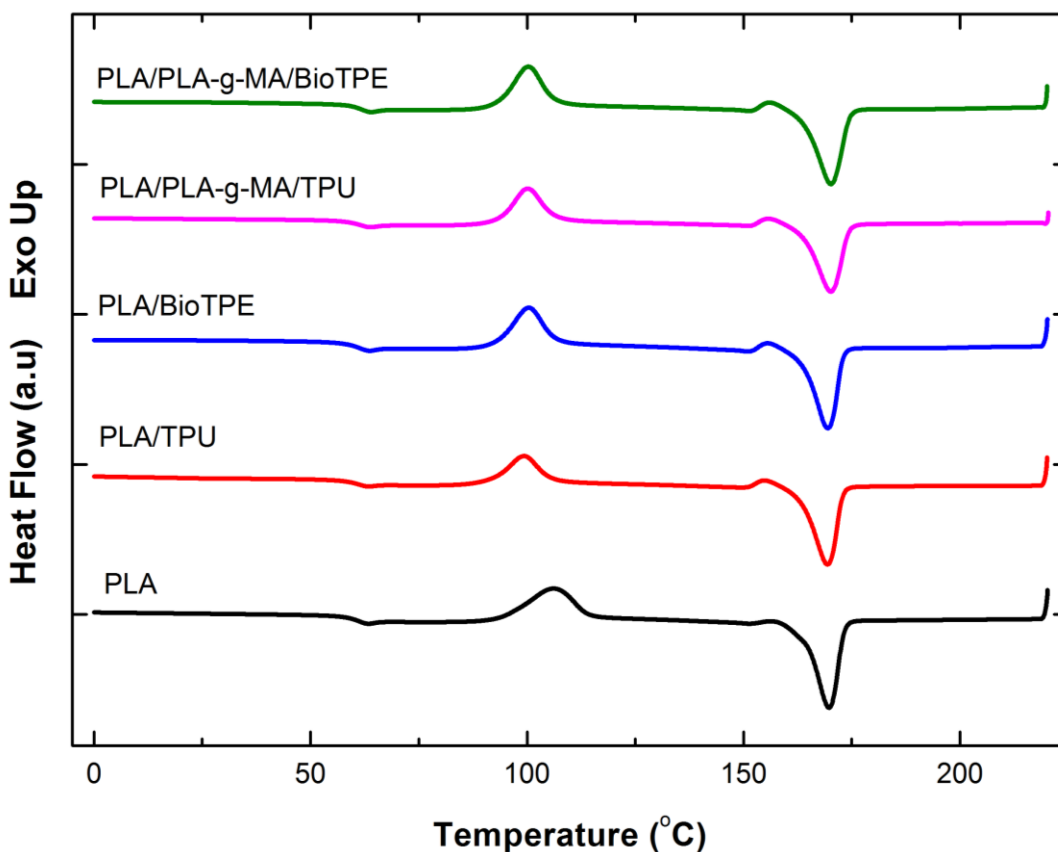


Figure 3.29 DSC Heating Thermograms of the Blends with and without Compatibilization Obtained after Erasing their Thermal History

chains required for the spherulitic growth could be constrained due to the chemical interactions discussed above.

Thermal degradation temperatures (T_d), i.e. maximum mass loss rate peak temperature, were determined from the TGA curves in Figure 3.30 and tabulated in Table 3.20. It is seen that there were slight decreases, only a few degrees, for the blends with and without PLA-g-MA compatibilization. Thus, it can be said that there were no detrimental effects on the thermal degradation of PLA when it was blended with TPU or BioTPE.

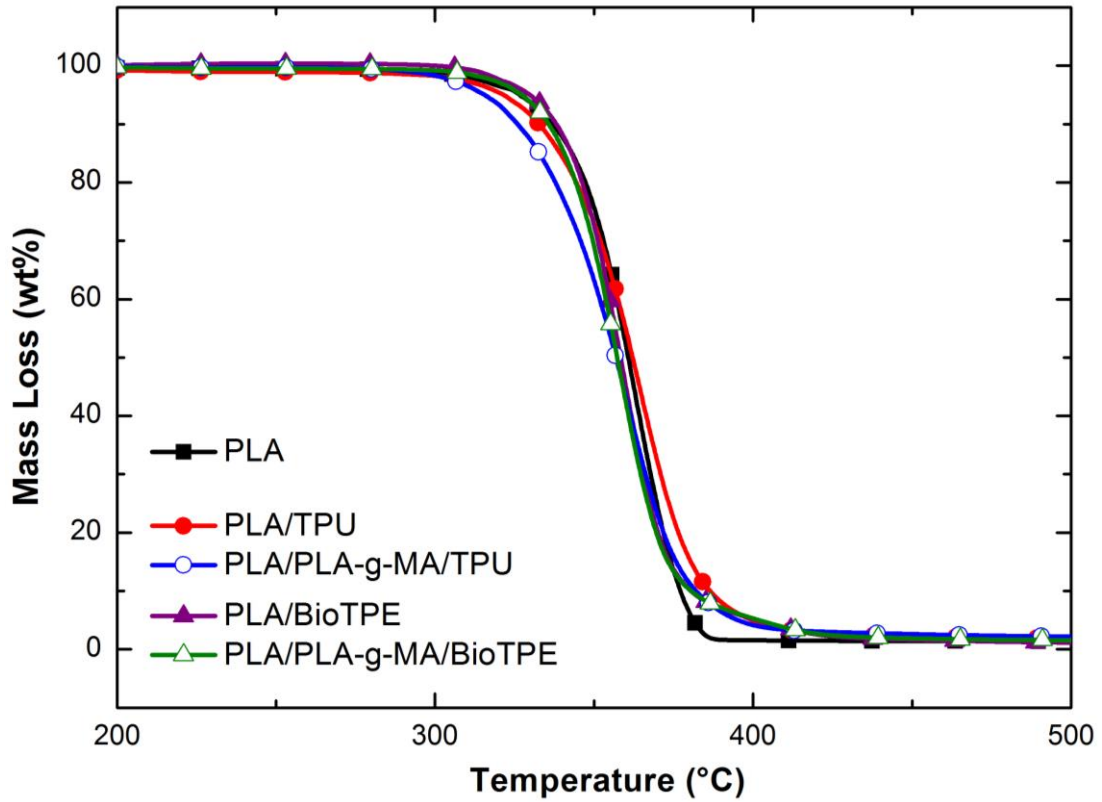


Figure 3.30 Thermogravimetric Curves of the Blends with and without Compatibilization

Table 3.20 Effects of PLA-g-MA on the Thermal Degradation Temperatures (T_d) and Storage Modulus (E') Values of the Blends at 25° and 50°C

Specimens	T_d (°C)	E' at 25°C (GPa)	E' at 50°C (GPa)
PLA	366	2.78	2.72
PLA/TPU	368	2.76	2.62
PLA/PLA-g-MA/TPU	364	3.04	2.88
PLA/BioTPE	363	2.29	2.26
PLA/ PLA-g-MA/BioTPE	362	2.87	2.73

Storage modulus versus temperature curves obtained by DMA are given in Figure 3.31. Then, two levels of storage modulus (E') at 25° and 50°C were determined and tabulated in Table 3.20. Figure 3.31 shows that addition of thermoplastic elastomers decreased E' values of PLA due to the increased mobility of PLA chains and soft segments of TPU or BioTPE. However, when these blends were compatibilized with PLA-g-MA, all reductions in E' values were not only recovered, but also increased to the levels slightly above the E' values of neat PLA. Therefore, it can be said that if compatibilization was used, incorporation of TPU or BioTPE had no detrimental effects on the thermomechanical behavior of PLA.

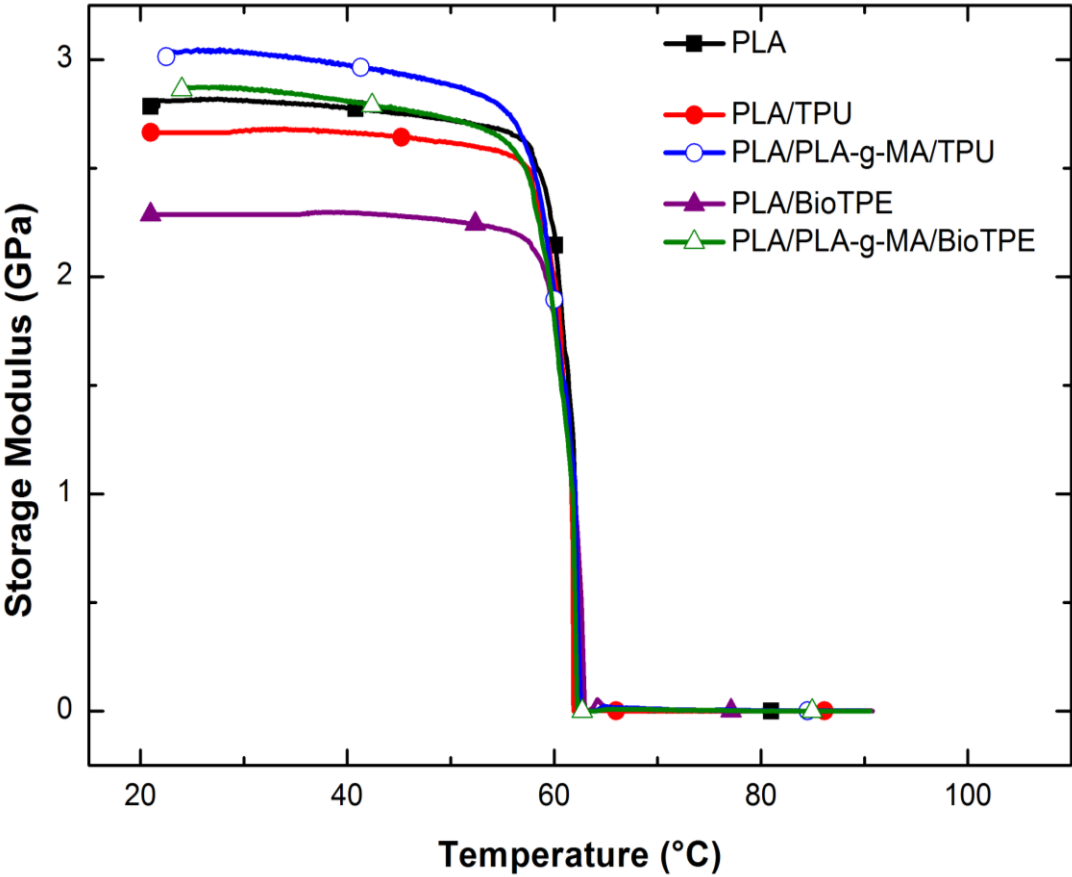


Figure 3.31 Storage Modulus Curves of the Blends with and without Compatibilization Obtained by DMA

CHAPTER 4

CONCLUSIONS

The main conclusions drawn from the three different parts of this thesis can be summarized as follows:

(i) Effects of Ethylene Copolymers

- SEM images indicated that smooth and brittle fracture surface of neat PLA transformed into rough and ductile surface when blended with ethylene copolymers. Immiscibility of PLA with ethylene copolymers was revealed by the observation of finely and uniformly phase-separated round domains of EVA, EMA and EBA-GMA.
- Due to the elastomeric nature of ethylene copolymers; stiffness, strength and hardness of PLA decreased. Depending on the type and content of the ethylene copolymers, the highest reductions e.g. in Young's modulus, tensile strength and hardness values of PLA were as much as 33%, 26% and 20%, respectively.
- Due to the effective rubber toughening mechanisms of shear yielding, cavitation, debonding, pull-out and crack deflection; ductility and toughness of PLA improved significantly. Depending on the type and content of the ethylene copolymers, the highest increases in % elongation at break, Charpy impact toughness and G_{IC} fracture toughness values of PLA were as much as 160%, 320% and 158%, respectively.
- Thermal analyses (DSC, TGA, DMA) indicated that there was no detrimental effects of EVA, EMA and EBA-GMA on the thermal transition and degradation temperatures including storage modulus values of PLA.

(ii) Effects of Thermoplastic Elastomers

- SEM studies again revealed that smooth and brittle fracture surface of neat PLA became very rough and ductile when blended with thermoplastic elastomers. Immiscibility of PLA with both thermoplastic elastomers was apparent as the formation of finely and uniformly phase-separated round domains of TPU and BioTPE.
- Due to the plasticizing effects of the soft segments of the thermoplastic elastomers, melt flow index and ductility of PLA improved significantly. For example, percent elongation at break increased 3 times. Consequently, due to the increased flexibility, elastic modulus (tensile and flexural) and hardness values decreased, but not more than 20% and 10%, respectively.
- Due to the hard segments of thermoplastic elastomers acting as fillers or physical crosslinks, there was almost no decrease in the flexural strength and slightly decreases in the tensile strength of PLA only at higher thermoplastic elastomer contents.
- Rubber toughening mechanisms; shear yielding, cavitation, debonding, pull-out and crack deflection were very significantly effective on the improved toughness of PLA. For instance, using only 10 phr TPU or BioTPE increased Charpy impact toughness more than 300%, while increases in K_{IC} and G_{IC} fracture toughness values were as much as 35% and 130%, respectively.
- Thermal analyses (DSC, TGA, DMA) again indicated that there was no significant detrimental effects of TPU and BioTPE on the thermal transition and degradation temperatures including storage modulus values of PLA.

(iii) Effects of Maleic Anhydride Compatibilization

- Titration method showed that sufficient degree of MA grafting on the PLA backbone could be obtained by melt blending of PLA with only 2 wt% MA via reactive extrusion.
- IR spectroscopy revealed that MA graft of the PLA-g-MA might interact with the functional groups present in the hard segments of TPU and BioTPE domains via primary chemical interactions, so that higher level of compatibilization could be obtained.
- When PLA-g-MA was not used, only secondary chemical interactions might take place between the carboxyl, hydroxyl end groups and the carbonyl groups of PLA with the functional groups of the hard segments of TPU and BioTPE.
- SEM studies indicated that PLA-g-MA compatibilization reduced not only the degree of debonding between the PLA matrix and domains of TPU and BioTPE, but also the number of pull-out sites of domains from the matrix. Moreover, MA compatibilization decreased the size of these round-shaped domains leading to higher level of surface area for more interfacial interactions.
- MFI values determined revealed that PLA-g-MA compatibilization could decrease the melt flow index of the blends owing to the higher chemical interactions that could increase the viscosities.
- Tensile and bending tests indicated that blending with TPU and BioTPE decreased elastic modulus and strength of PLA due to their elastomeric nature. When blends were compatibilized with PLA-g-MA, no further reductions of these mechanical properties were observed.

- Toughness tests revealed that Charpy impact toughness and fracture toughness (K_{IC} and G_{IC}) of inherently brittle PLA increased significantly by blending with thermoplastic elastomers. When these blends were compatibilized with PLA-g-MA, increases in all toughness values were much more significant due to the higher efficiency of rubber toughening mechanisms. For instance, G_{IC} fracture toughness of PLA increased by 80% and 128% with 10 phr TPU and BioTPE, respectively; after compatibilizing these blends, G_{IC} increases reached up to 110% and 166%, respectively.
- Thermal analyses (DSC, TGA, DMA) again indicated that when PLA-g-MA compatibilization was used, incorporation of TPU or BioTPE had no detrimental effects on the thermal properties of PLA.

Conclusive Remarks

This thesis indicated that “rubber toughening” approach can be used successively to improve toughness of inherently brittle PLA so that it can be used in many engineering applications. It was revealed that Charpy impact toughness and fracture toughness (K_{IC} and G_{IC}) values of PLA when blended with 20 phr ethylene copolymers or thermoplastic elastomers are comparable to the values of typical engineering thermoplastics such as polyamide. Moreover, it was observed that these toughness levels of polyamide can be obtained by blending with 10 phr MA compatibilized TPU or even by 5 phr BioTPE without any compatibilization. It was also seen that MA compatibilization of TPU and BioTPE resulted in strength and modulus values comparable to the values of polyamide.

REFERENCES

- [1] Lim L-T., Auras R., Rubino M., Processing technologies for poly(lactic acid), *Progress in Polymer Science*, 33(8): 820-852, 2008.
- [2] Garlotta D., A Literature Review of Poly(lactic Acid), *Journal of Polymers and the Environment*, 9(2): 63-83, 2002.
- [3] Lunt J., Large-scale production, properties and commercial applications of Polylactic acid polymers, *Polymer Degradation and Stability*, 59(1-3): 145-152, 1998.
- [4] Gupta B., Revagade N., Hilborn J., Poly(lactic acid) fiber: An overview, *Progress in Polymer Science*, 32(4): 455-482, 2007.
- [5] Guest M. J., Cheung Y. W., Wu Y., McBride E., Ethylene Copolymers, Ethylene-Acrylic Elastomers, *Encyclopedia of Polymer Science and Technology*, John Wiley and Sons, Vol. 2, 6, 162-489, 1964.
- [6] Bates F.S., Fredrickson G. H., Block Copolymers-Designer Soft Materials, *Physics Today*, 52(2): 32-38, 1999.
- [7] DeLassus P. T., Whiteman N. F., Physical and Mechanical Properties of Some Important Polymers, *Polymer Handbook*, John Wiley and Sons, 4th Edition, 160-169, 1999.
- [8] Bolgar M., Hubball J., Groeger J., Meronek S., *Handbook for the Chemical Analysis of Plastic and Polymer Additives*, Taylor and Francis Group, New York, 1-19, 2008.

- [9] Cella R. J., Morphology of Segmented Polyester Thermoplastic Elastomers, *Journal of Polymer Science: Polymer Symposia*, 42(2): 727-740, 1973.
- [10] Shollenberger C. S., *Handbook of Elastomers*, Chapter 14, 2nd Edition, CRC Press, 360-394, 2000.
- [11] Liu N. C., Huang H., Chapter 2: Types of Reactive Polymers Used in Blending, *Reactive Polymer Blending*, Hanser, Cincinnati, 15-20, 2001.
- [12] Phruksaphithak N., Noomhorm C., Polylactic Acid/Impact Modifier Blends, *Advanced Materials Research*, 486: 406-411, 2012.
- [13] Jiang J., Su L., Zhang K., Wu G., Rubber-Toughened PLA Blends with Low Thermal Expansion, *Journal of Applied Polymer Science*, 128(6): 3993-4000, 2012.
- [14] Odent J., Raquez J., Duquesne E., Dubois P., Random aliphatic copolyesters as new biodegradable impact modifiers for polylactide materials, *European Polymer Journal*, 48(2): 331-340, 2012.
- [15] Yokohara T., Yamaguchi M., Structure and properties for biomass-based polyester blends of PLA and PBS, *European Polymer Journal*, 44(3): 677-685, 2008.
- [16] He Y., Masuda T., Cao A., Yoshie N., Doi Y., Inoue Y., Thermal, Crystallization, and Biodegradation Behavior of Poly(3-hydroxybutyrate) Blends with Poly(butylene succinate-co-butylene adipate) and Poly(butylene succinate-co- ϵ -caprolactone), *Polymer Journal*, 31(2): 184-192, 1999.
- [17] Li Y., Shimizu H., Improvement in toughness of poly(L-lactide) (PLLA) through reactive blending with acrylonitrile-butadiene-styrene copolymer (ABS): Morphology and properties, *European Polymer Journal*, 45(2): 738-746, 2009.

- [18] Jiang L., Wolcott M. P., Zhang J., Study of Biodegradable Polylactide/Poly(butylene adipate-co-terephthalate) Blends, *Biomacromolecules*, 7(1): 199-207, 2006.
- [19] Noda I., Satkowski M. M., Dowrey A. E., Marcott C., Polymer Alloys of Nodax Copolymers and Poly(lactic acid), *Macromolecular Bioscience*, 4(3): 269-275, 2004.
- [20] Zhang W., Chen L., Zhang Y., Surprising shape-memory effect of polylactide resulted from toughening by polyamide elastomer, *Polymer*, 50(5): 1311-1315, 2009.
- [21] Ho C., Wang C., Lin C., Lee Y., Synthesis and characterization of TPO-PLA copolymer and its behavior as compatibilizer for PLA/TPO blends, *Polymer*, 49(18): 3902-3910, 2008.
- [22] Li Y., Liu L., Shi Y., Xiang F., Huang T., Wang Y., Zhou Z., Morphology, Rheological, Crystallization Behavior, and Mechanical Properties of Poly(L-lactide)/Ethylene-co-Vinyl Acetate Blends with Different VA Contents, *Journal of Applied Polymer Science*, 121(5): 2688-2698, 2011.
- [23] Ma P., Hristova D. G., Goossens J. G. P., Spoelstra A. B., Zhang Y., Lemstra P. J., Toughening of poly(lactic acid) by ethylene-co-vinyl acetate copolymer with different vinyl acetate contents, *European Polymer Journal*, 48(1): 146-154, 2012.
- [24] Cong D. V., Hoang T., Giang N. V., Ha N. T., Lam T. D., Sumita M., A novel enzymatic biodegradable route for PLA/EVA blends under agricultural soil of Vietnam, *Materials Science Engineering C*, 32(3): 558-563, 2012.
- [25] Yoon J., Oh S., Kim M., Chin I., Kim Y., Thermal and mechanical properties of poly(L-lactic acid)-poly(ethylene-co-vinyl acetate) blends, *Polymer*, 40(9): 2303-2312, 1999.

[26] Pluta M., Murariu M., Dechief A., Bonnaud L., Galeski A., Dubois P., Impact-Modified Polylactide-Calcium Sulfate Composites: Structure and Properties, *Journal of Applied Polymer Science*, 125(6): 4302-4315, 2012.

[27] Liu H., Song W., Chen F., Guo L., Zhang J., Interaction of Microstructure and Interfacial Adhesion on Impact Performance of Polylactide (PLA) Ternary Blends, *Macromolecules*, 44(6): 1513-1522, 2011.

[28] Yeh J., Tsou C., Li Y., Xiao H., Wu C., Chai W., Lai Y., Wang C., The compatible and mechanical properties of biodegradable poly(Lactic Acid)/ethylene glycidyl methacrylate copolymer blends, *Journal of Polymer Research*, 19(2): 9766-9780, 2012.

[29] Oyama H. T., Super-tough poly(lactic acid) materials: Reactive blending with ethylene copolymer, *Polymer*, 50(3): 747-751, 2009.

[30] Baouz T., Rezgui F., Yilmazer U., Ethylene-Methyl-Glycidyl Methacrylate Toughened Poly(lactic acid) Nanocomposites, *Journal of Applied Polymer Science*, 128(5): 3193-3204, 2012.

[31] Zhang X., Li Y., Han L., Han C., Xu K., Zhou C., Zhang M., Dong L., Improvement in Toughness and Crystallization of Poly(L-lactic acid) by Melt Blending with Ethylene/Methyl Acrylate/Glycidyl Methacrylate Terpolymer, *Polymer Engineering Science*, 53(12): 2498-2508, 2013.

[32] Feng F., Ye L., Morphologies and Mechanical Properties of Polylactide/Thermoplastic Polyurethane Elastomer Blends, *Journal of Applied Polymer Science*, 119(5): 2778-2783, 2011.

- [33] Han J., Huang H., Preparation and Characterization of Biodegradable Polylactide/Thermoplastic Polyurethane Elastomer Blends, *Journal of Applied Polymer Science*, 120(6): 3217-3223, 2011.
- [34] Hong H., Wei J., Yuan Y., Chen F., Wang J., Qu X., Liu C., A novel Composite Coupled Hardness with Flexibility-Polylactic Acid Toughen with Thermoplastic Polyurethane, *Journal of Applied Polymer Science*, 121(2): 855-861, 2011.
- [35] Zaman H. U., Song J. C., Park L., Kang I., Park S., Kwak G., Park B., Yoon K., Poly(lactic acid) blends with desired end use properties by addition of thermoplastic polyester elastomer and MDI, *Polymer Bulletin*, 67(1): 187-198, 2011.
- [36] Zhu R., Liu H., Zhang J., Compatibilizing Effects of Maleated Poly(lactic acid) (PLA) on Properties of PLA/Soy Protein Composites, *Industrial and Engineering Chemistry Research*, 51(22): 7786-7792, 2012.
- [37] Hwang S. W., Shim J. K., Selke S., Soto-Valdez H., Rubino M., Auras R., Effect of Maleic-Anhydride Grafting on the Physical and Mechanical Properties of Poly(L-lactic acid)/Starch Blends, *Macromolecular Materials and Engineering*, 298(6): 624-633, 2012.
- [38] Zhang J., Sun X., Mechanical Properties of Poly(lactic acid)/Starch Composites Compatibilized by Maleic Anhydride, *Biomacromolecules*, 5(4): 1446-1451, 2004.
- [39] Orozco V. H., Brostow W., Chonkaew W., Lopez B. L., Preparation and Characterization of Poly(Lactic Acid)-g-Maleic Anhydride + Starch Blends, *Macromolecular Symposia*, 277(1): 69-80, 2009.
- [40] Jandas P. J., Mohanty S., Nayak S. K., Morphology and Thermal Properties of Renewable Resource-Based Polymer Blend Nanocomposites Influenced by a

Reactive Compatibilizer, *Sustainable Chemistry and Engineering*, 2(3): 377-386, 2014.

[41] Jandas P. J., Mohanty S., Nayak S. K., Sustainability, Compostability, and Specific Microbial Activity on Agricultural Mulch Films Prepared from Poly(lactic acid), *Industrial and Engineering Chemistry Research*, 52(50): 17714-17724, 2013.

[42] Teamsinsungvon A., Ruksakulpiwat Y., Jarukumjom K., Preparation and Characterization of Poly(lactic acid)/Poly(butylene adipate-co-terephthalate) Blends and Their Composite, *Polymer-Plastics Technology and Engineering*, 52(13): 1362-1367, 2013.

[43] Teamsinsungvon A., Ruksakulpiwat Y., Jarukumjom K., Mechanical and Morphological Properties of Poly (Lactic Acid)/Poly (Butylene Adipate-co-Terephthalate)/Calcium Carbonate Composite, *18th International Conference on Composite Materials*, 2011.

[44] Yuan H., Liu Z., Ren J., Preparation, Characterization, and Foaming Behavior of Poly(lactic acid)/Poly(butylene adipate-co-butylene terephthalate) Blend, *Polymer Engineering and Science*, 49(5): 1004-1012, 2009.

[45] Nabar Y., Raquez J. M., Dubois P., Narayan R., Production of Starch Foams by Twin-Screw Extrusion: Effect of Maleated Poly(butylene adipate-co-terephthalate) as a Compatibilizer, *Biomacromolecules*, 6(2): 807-817, 2005.

[46] Fischer E.W., Sterzel H.J., Wegner G., Investigation of Structure of Solution Grown Crystals of Lactide Copolymers by Means of Chemical Reactions, *Colloid Polymer Science*, 251(11): 980-990, 1973.

- [47] Muenprasat D., Suttireungwong S., Tongpin C., Functionalization of Poly(Lactic Acid) with Maleic Anhydride for Biomedical Application, *Journal of Metals, Materials and Minerals*, 20(3): 189-192, 2010.
- [48] Pan J., Wang Y., Qin S., Zhang B., Luo Y., Grafting Reaction of Poly(D,L)lactic acid with Maleic Anhydride and Hexanediamine to Introduce More Reactive Groups in Its Bulk, *Journal of Biomedical Materials Research Part B: Applied Biomaterials*, 74B: 476-480, 2005.
- [49] Carlson D., Nie L., Narayan R., Dubois P., Maleation of Polylactide (PLA) by Reactive Extrusion, *Journal of Applied Polymer Science*, 72(4): 477-485, 1999.
- [50] Hwang S. W., Lee S. B., Lee C. K., Lee J. Y., Shim J. K., Selke S. E. M., Valdez H., Matuana L., Rubino M., Auras R., Grafting of maleic anhydride on poly(L-lactic acid). Effects on physical and mechanical properties, *Polymer Testing*, 31(2): 333-344, 2012.
- [51] Neuman R. C., Organic Chemistry, Carbonyl Compounds: Esters, Amides, and Related Molecules, 2013.
- [52] Jing X., Mi H., Salick M. R., Cordie T., Crone W. C., Peng X., Turng L., Morphology, mechanical properties, and shape memory effects of poly(lactic acid)/thermoplastic polyurethane blend scaffolds prepared by thermally induced phase separation, *Journal of Cellular Plastics*, 50(4): 361-379, 2014.
- [53] Lu Q., Macosko C. W., Promoting Adhesion to Thermoplastic Polyurethane (TPU) by Amine Functional Polypropylenes, *Polymeric Materials: Science & Engineering*, 89: 844-847, 2003.
- [54] Nishikava Y., Nakano T., Noda I., Two-Dimensional Correlation Analysis of Polyimide Films using Attenuated Total Reflection-Based Dynamic Compression

Modulation Step-Scan Fourier Transform Infrared Spectroscopy, *Applied Spectroscopy*, 61(8): 873-881, 2007.

[55] Kim S., Kang C., Chowdhury S. R., Cho W., Ha C., Reactive Compatibilization of the Poly(butylene terephthalate)-EVA Blend by Maleic Anhydride. II. Correlations Among Gel Contents, Grafting Yields, and Mechanical Properties, *Journal of Applied Polymer Science*, 89(5): 1305-1310, 2003.

[56] John J., Bhattacharya M., Synthesis and properties of reactivity compatibilized polyester and polyamide blends, *Polymer International*, 49(8): 860-866, 2000.

[57] Liang C. Y., Krimm S., Infrared Spectra of High Polymers Part IX. Polyethylene Terephthalate, *Journal of Molecular Spectroscopy*, 3(1-6): 554-574, 1959.

[58] Ochoa C., Vaidya U. K., Mechanisms of interfacial adhesion in metal-polymer composites - Effect of chemical treatment, *Composites: Part A*, 42(8): 906-915, 2011